

Benchmark Report on the use of Satellite Radar Imagery for Monitoring Fuel Moisture in Alaska

September 2006

NASA SENH Project NAS5-03113

*“Remotely Monitoring Plant and Soil Fuel
Moisture for Wildfire Danger Assessment using
Satellite Radar Data”*

PI: Laura Bourgeau-Chavez
Kevin Riordan & Gordon Garwood
Field Crew: James Slawski, Michael Medvecz, Seth Ames, and Timothy Walters

*Michigan Research and Development Center
General Dynamics Advanced Information Systems (formerly Veridian Systems)
1200 Joe Hall Dr. Ypsilanti, MI 48197*

Co-Investigators: William (Brad) Cella[±], Sharon Alden^{*}, Mary Kwart^F,
Karen Murphy[£], and Sue Ferguson[§]

[±] National Park
Service, Regional Fire
Management Officer
240 W.5th Ave. Rm 117
Anchorage AK 99501
brad_cella@nps.gov

^{*} National Park Service
stationed at Alaska Fire
Service BLM
Bin 311 P.O. Box 350
Ft. Wainwright, AK
99703-0005
sharon_alden@ak.blm.gov

^F U.S Fish & Wildlife
Service, Regional Fuels
Specialist
1011 East Tudor Road,
Mail Stop 221
Anchorage, Alaska
99503
mary_kwart@fws.gov

[£] U.S. Fish and Wildlife
Service, Regional Fire
Ecologist
1011 E. Tudor Road
Anchorage, AK 99503
Karen_A_Murphy@fws.gov

[§] U.S.D.A. Forest
Service
4043 Roosevelt Way NE
Seattle WA 98105-6497

TABLE OF CONTENTS

1. PURPOSE	3
2. WHY BURNED FORESTS ARE USED IN THE ASSESSMENT OF WILDFIRE POTENTIAL	4
3. APPROACHES.....	5
4. ORGANIZATION OF BENCHMARK REPORT	8
5. BENCHMARK OF PREVIOUS RESEARCH.....	9
5.1 FIRE SCAR DETECTION.....	9
5.2 SOIL MOISTURE AND SAR CORRELATIONS	10
5.3 FIRE WEATHER INDEX CODES AND SAR CORRELATIONS	10
6. BACKGROUND ON FIRE WEATHER INDEX SUBSYSTEM OF THE CANADIAN FOREST FIRE DANGER RATING SYSTEM.....	10
7. INITIALIZATION AND PROGRESSIVE CALIBRATION OF THE FWI SYSTEM DROUGHT CODE WITH SAR IMAGERY.....	11
7.1 DEVELOPMENT OF SAR-DC ALGORITHM.....	12
7.2 DESCRIPTION OF TECHNIQUE.....	14
7.3 APPLICATION OF SAR ALGORITHM	16
7.3.1 <i>Donnelly Flats 1999 Fire</i>	17
7.3.2 <i>Anderson Alaska Fires</i>	25
7.3.3 <i>Survey Line Alaska 2001 Fire</i>	26
7.4 DROUGHT CODE INITIALIZATION SUMMARY	27
7.4.1 <i>Analysis of Moisture Dynamics in Burned and Unburned Sites</i>	28
7.4.2 <i>2000 and 2005 Burned/ Unburned Soil Moisture Data Comparison at Permafrost and Non-Permafrost sites</i>	31
8. SOIL MOISTURE MAPPING IN BURNED BOREAL FORESTS	38
8.1 WHY USE BURN SEVERITY TO SEGMENT THE TEST SITES?.....	38
8.2 SOIL MOISTURE MAPPING PROCEDURE.....	40
8.3 ALGORITHM DEVELOPMENT OF SOIL MOISTURE CONDITION BASED ON ERS-2 SAR BACKSCATTER	44
8.3.1 <i>Moderate Burn Severity Moisture Model Development</i>	45
8.3.2 <i>Severe Burn Severity Moisture Model Development</i>	46
8.3.3 <i>Low Burn Severity Moisture Model Development</i>	48
8.4 BURNED BOREAL FOREST SOIL MOISTURE MAPPING SUMMARY	49
9. TIME SERIES ANALYSIS APPROACH FOR MAPPING FUEL MOISTURE ACROSS THE LANDSCAPE.....	50
9.1 SUMMER 2000-4 PCA OF DONNELLY FLATS.....	51
9.1.1 <i>Summary of PCA at Donnelly Burned Test Site</i>	60
9.2 UNBURNED SITE PCA OF DELTA JUNCTION	61

9.3	PRINCIPAL COMPONENT ANALYSIS AT SURVEY LINE BURN, ALASKA.....	65
9.3.1	<i>Summary of PCA Results at Survey Line Burned Site</i>	69
9.4	PRINCIPAL COMPONENT ANALYSIS (PCA) WITH RADARSAT IMAGERY OVER DELTA JUNCTION	70
9.5	PCA OF UNBURNED SITES AT SURVEY LINE	72
9.6	<i>IN SITU</i> VERSUS FWI CODES AT UNBURNED SITES	75
9.7	MODELING OF SOIL MOISTURE IN UNBURNED ALASKAN FORESTS	77
9.7.1	<i>Summary of Unburned Site PCA Results</i>	80
10.	INITIAL STAGES OF MODELING FOR TIME SERIES ANALYSIS	81
10.1	IMAGE SEGMENTATION	83
10.2	SUMMARY OF INITIAL NEURAL NETWORK ANALYSIS.....	84
11.	RECOMMENDATIONS.....	88
12.	PRESENTATIONS AND PUBLICATIONS	90
12.1.1	<i>International Boreal Forest Research Association Conference</i>	90
12.1.2	<i>Alaska Collaborator Meetings</i>	90
12.1.3	<i>North American Boreal Forest Carbon Emissions Collaboration Meeting</i> 91	
12.1.4	<i>Second North American Boreal Forest Carbon Emissions Collaboration Meeting</i> 92	
12.1.5	<i>2005 Fall AGU Conference</i>	92
12.1.6	<i>Alaska Satellite Facility (ASF) Newsletter Article</i>	92
12.1.7	<i>Circumpolar Remote Sensing Symposium</i>	92
12.1.8	<i>International Journal of Remote Sensing Manuscript</i>	93
12.1.9	<i>JGR Water Resources Research Manuscript</i>	93
12.1.10	<i>Polar Record Manuscript</i>	94
13.	LITERATURE CITED.....	95
Appendix A. Normalization of ERS-2 SAR Imagery.....		
Appendix B. Study Area, Site Description, and Field Collection Methods.....		
Appendix C. Comparison of Burn Severity Mapping Techniques.....		
Appendix D. Campbell Scientific Water Content Reflectometer Probe Calibration Manuscript for JGR Water Resources.....		
Appendix E. Manuscript Accepted for Publication in International Journal of Remote Sensing.....		
Appendix F. Manuscript Submitted for Peer Review in Polar Record on Improving the Prediction of Wildfire Potential with SAR.....		

1. Purpose

This document benchmarks the results of a three year NASA sponsored research project (2003-6) on **developing and demonstrating techniques for using single channel C-band Synthetic Aperture Radar (SAR) satellite imagery for assessing the potential for wildfire in Boreal Alaska**. Preliminary research conducted in boreal Alaska in 1999-2000 revealed relationships between C-band backscatter in burned boreal forests and Fire Weather Index (FWI) system codes as well as *in situ* moisture (Bourgeau-Chavez et al. 2000). From 2003-6, under the NASA Solid Earth and Natural Hazards program, continued research was conducted to develop SAR techniques for the application of improving or augmenting the FWI system in boreal Alaska to aid resource managers (National Park Service, U.S. Fish and Wildlife Service and Forest Service) directly involved in wildfire danger assessment. Interaction with Alaskan project co-investigators (natural resource managers) was essential to understanding their needs, interpreting the data, and developing methods to improve the shortcomings of the current weather-based system. Although the focus of this research was in Alaska, the methods are transferable to boreal Canada, and potentially boreal Russia. Both Alaska and Canada use the Fire Weather Index System (FWI), a subsystem of the Canadian Forest Fire Danger Rating System (CFFDRS).

In recent research that was comparable to our preliminary analysis in Alaska (Bourgeau-Chavez et al. 2000), investigators at University of New Brunswick demonstrated relationships between C-band backscatter in burned boreal forests of northwest Canada and FWI system codes (Abbott et. al. 2006).

2. Why Burned Forests are used in the Assessment of Wildfire Potential

The approaches used for assessing the potential for wildfire involve the use of recently (1-10 years since fire) **burned** areas. Although these areas are not in danger of burning, they allow for the evaluation of the ground surface moisture directly and they are indicative of the moisture in the surrounding **unburned** forests. Research shows that

they provide a direct comparison to fire danger codes, in relation to both *in situ* moisture and SAR backscatter. Further, research has demonstrated that there is a correlation between patterns of moisture in the **burned** and neighboring **unburned** forests, making the monitoring of burned areas useful for understanding the potential for wildfire in the surrounding unburned boreal forests.

3. Approaches

Three approaches have been under investigation for measuring and monitoring fuel moisture to assist fire resource managers in assessing the potential for wildfire; the first two have been fully demonstrated, while the third remains under development:

- 1) Improving the fire weather index system's Drought Code (DC) through algorithm development relating SAR backscatter to DC values (see section 6 below for detailed description of DC);
- 2) Directly predicting soil moisture in burned boreal forests using a combination of Landsat and SAR; and
- 3) Using time-series analysis of SAR imagery to spatially monitor fuel moisture.

These approaches are briefly described here with more detailed information provided in the succeeding sections. The first of these three methods is the simplest in that it allows the imagery to be used "off the shelf"¹ without georeferencing, as long as the location of the image, existing burned areas within the image and nearby weather stations are known. This approach involves averaging of all image pixels within a large area inside the burn (hundreds to thousands of pixels). By averaging over a large area, differences in backscatter across a burned landscape due to variations in surface roughness and vegetative regrowth are statistically reduced, and comparison between recent burns becomes feasible (Bourgeau-Chavez et al. 2006a,b). An algorithm specific to ERS-2 and recent black spruce burned forests of Alaska has been developed. This is

¹ note that calibration algorithms which are available from the processing facility may need to be applied to the imagery.

the most common forest type in Alaska. It has not been tested on other ecosystem types or in black spruce outside of Alaska. The averaged pixel values in dB are input to the developed algorithm and the Drought Code (DC) is estimated. Since DC is one of the fire weather index system codes that resource managers have the most difficulty initializing and since it has a lag time of 52 days, using SAR to initialize this code in spring will provide a great improvement in the FWI system. Although not created under this project, similar algorithms for Radarsat or Envisat can easily be developed using existing data.

The second SAR technique that was developed allows for direct prediction of volumetric soil moisture within the boundaries of a burned study site. Maps of soil moisture to 90 m resolution have been created using this method. This technique is also specific to black spruce ecosystem types of Alaska and has not been tested in other ecosystem types or in Canada. This method requires the categorization of the area within a burn into burn severity types, as defined by burn to the ground surface. Most of the biomass that burns in boreal ecosystems is located below ground. A method developed by Michalek et al. 2001 using Landsat data was used to categorize sites into burn severity types and then SAR algorithms that were developed to estimate soil moisture for each of three burn severity classes were applied to the ERS-2 imagery. The burn classes are based on those defined by Dyrness and Norum (1983) which range from 1 to 5 and are described as:

- (1) unburned moss
- (2) singed moss
- (3) light burn, moss layer burned down to humus with no moss regrowth
- (4) moderate burn, surface burned almost to mineral soil with some moss regrowth
- (5) severe burn, mineral soil exposed

We combine 2 and 3 as light burn and use 4 as moderate and 5 as severe. Using this method, areas within the Donnelly Flats burn scar were mapped for moisture condition on a variety of dates with 3.6 rms error. Note that current methods of using dNBR to estimate burn severity do not assess the burn to the ground surface and therefore are not applicable here (see Appendix C for comparison of dNBR to Michalek et al (2001) burn severity results).

The third method evaluated involves the use of time series analysis and the potential for mapping fuel moisture across the landscape. By using time series analysis each location within an image is compared to itself through time to determine change. This reduces errors due to variation in surface roughness and biomass and plant architecture, and allows the detection of changes in soil moisture without loss of resolution (30 m). While this works quite well at C-band in recent burns, open fields, and agricultural areas, an added complexity comes into play in unburned forests with scattering from the plant canopies and trunks. Although relationships exist between c-band backscatter from unburned forests and *in situ* moisture, the time-series analysis results are variable in unburned areas. A longer wavelength such as L-band SAR would likely work much better in the unburned forests for monitoring fuel moisture, and with the recent launch of ALOS PALSAR this approach is feasible. We present the research conducted on this approach using C-band in section 9. First we demonstrated the relationship between the loadings of new principal component images and soil moisture or FWI codes. Next we show the application of neural networks to extract the moisture information from a new image date after training with a time series of SAR data. We also reviewed methods of segmenting the image for landscape-scale mapping.

The ultimate goal of this project was to develop approaches for using SAR to improve fire danger prediction through assessment of fuel moisture conditions. Although, we originally had planned to focus more on developing principal component analysis or another form of time-series analysis for landscape scale monitoring, we shifted our focus to the first two approaches described above after review with end-user resource managers of both Alaska and Canada. The resource managers expressed that efforts to improve the existing FWI codes and documenting relationships between FWI codes and *in situ* moisture would help them more in the near-term than landscape level maps, and it would introduce the application of SAR in fire danger monitoring, making more complex uses of SAR in the future more feasible.

To overcome the hurdle of end-users adopting a new data type (SAR), the technique really needs to start out simple and it is helpful if the data have multiple uses. Recent communication with Alaska Fire Service (AFS) on this and related topics has developed

into an effort to assess the use of C-band SAR data for mapping extent and perimeters of burned boreal forests operationally in fall 2006. This is a technique that we developed under previous NASA grants (Bourgeau-Chavez et al. 1997, 2001) and we are actively consulting on the current “operational” project. See section 5.1 for more details. AFS will also preliminarily assess the utility of C-band SAR for fuel moisture assessment using the techniques developed under this NASA SENH project. We have provided AFS with all of our *in situ* moisture data collected under this project for their assessment of archival imagery.

4. Organization of Benchmark Report

This report is organized into sections on each of the approaches described above, including supplemental research comparing soil moisture in burned and unburned test sites, and presentations and publications. A series of appendices document: A) the need for normalization of ERS-2 data processed by ASF; B) detailed description of the study areas; C) comparison of dNBR to Michalek *et al.* 2000 method of mapping burn severity; D) water content reflectometer probe calibration manuscript in submission; E) IJRS manuscript accepted for publication in August 2006; F) Polar Record manuscript submitted in August 2006. But first we benchmark where the state of the art was prior to this current research. This will provide background information that is important to the application of SAR for fire resource management in boreal regions.

5. Benchmark of Previous Research

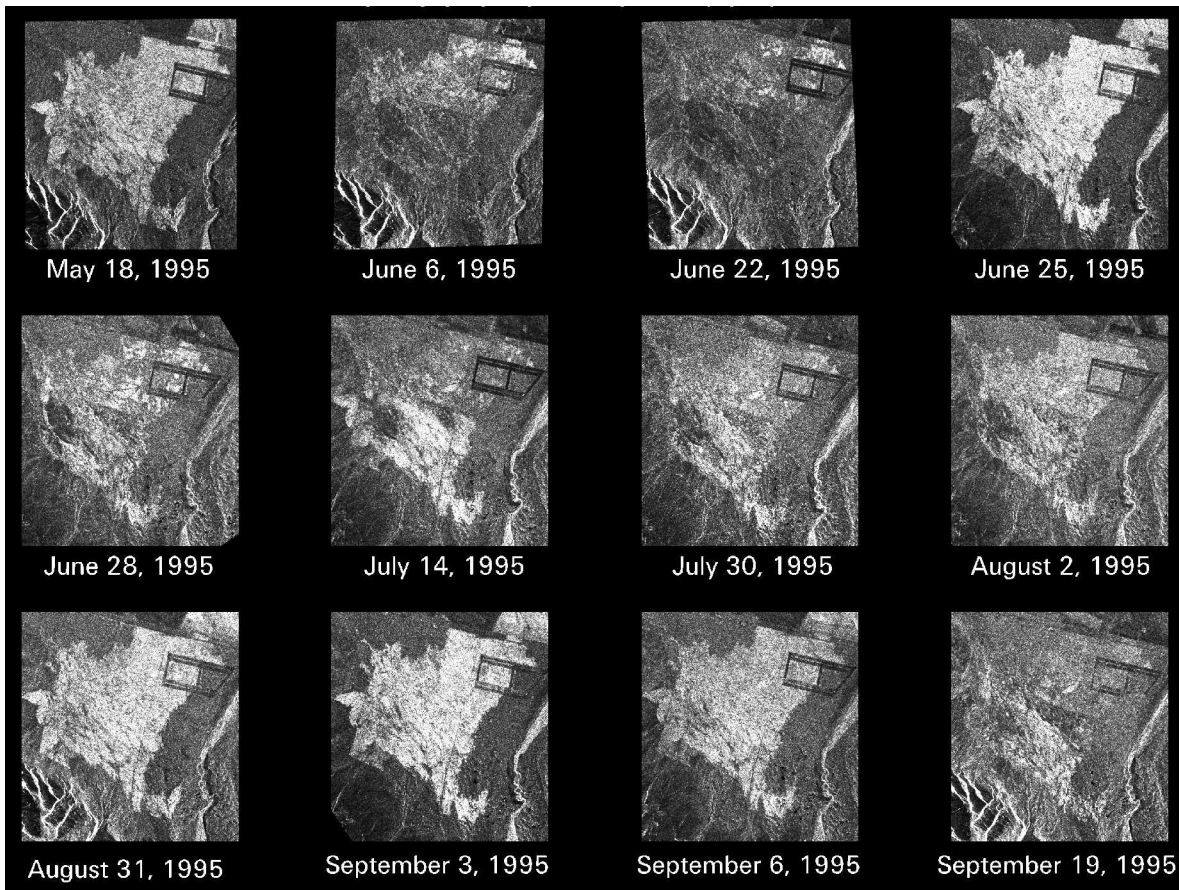


Figure 1. Seasonal ERS-1 images collected in 1995 over the 1994 Gerstle River burn (aka Hajdukovich Creek).

5.1 Fire Scar Detection

Previous research by the principal investigator and colleagues under past NASA grants demonstrated the utility of SAR imagery for detecting, mapping and monitoring fire scars in Alaska, Canada, and Russia (Bourgeau-Chavez et al. 1997, 2001). The fire scars are detectable because the canopy has been removed or killed (no longer living biomass), and the ground layer is exposed. The ground becomes very wet, in most cases, post-fire because of underlying permafrost layers melting or frozen ground thaw, and decreased evapotranspiration. This allows the sites to be detected and mapped. The moisture at these sites changes over the course of a growing season (Figure 1) and such changes are detectable in the SAR imagery, thus allowing the monitoring of soil moisture differences.

5.2 Soil Moisture and SAR Correlations

Previous NASA sponsored research by the PI and colleagues also established that relationships existed in moisture of burned black spruce test sites of Delta Junction and Tok Alaska and SAR backscatter. However, moisture measurements were either sparsely sampled gravimetric collections (French et al. 1997) or uncalibrated Campbell scientific water content reflectometer (CS-615, and CS-620 Hydrosense) probe measurements (Bourgeau-Chavez et al. 2000). Although data within a specific sampling location could be studied over time, between site analysis was impaired by lack of calibration.

5.3 Fire Weather Index Codes and SAR Correlations

Previous research also established that relationships existed between FWI codes and burned black spruce backscatter at Tok (Bourgeau-Chavez et al. 1999) and Delta (Bourgeau-Chavez et al. 2000), and that these relationships often had problems in spring and sometimes mid-summer. Note that during the current study we found that the problems with FWI codes and SAR backscatter were a feature of the FWI itself and not an issue related to the SAR imagery or environmental conditions within a burned region.

6. Background on Fire Weather Index Subsystem of the Canadian Forest Fire Danger Rating System

The FWI subsystem of the CFFDRS used in Alaska and Canada is a bookkeeping system based solely on meteorological data for the assessment of fire danger. Rain, temperature, relative humidity, and wind are used to predict the moisture status of forest litter and duff as well as drought conditions which are then used to determine fire danger. The FWI components are based on daily noontime measurements of dry-bulb temperature, relative humidity, ten meter open wind speed and 24 hour accumulated precipitation. The approach was developed using field experiments and extensive empirical analyses (Stocks *et al.* 1989).

There are six components of the FWI system which individually and collectively account for the effects of fuel moisture and wind on the potential for fire ignition (Alexander *et al.* 1996). Three of the codes are designed to estimate the moisture content in three distinct layers of soil, note that the exact depths will vary by site:

FFMC represents moisture in the litter material up to 2 cm in depth

DMC represents moisture in the upper duff material (~5-10 cm depth)

DC represents moisture in the lower duff layers, (~10-20 cm in depth)

These codes are based on the accounting of daily precipitation and drying. These three fuel-moisture codes are linked with wind to form two intermediate and one final index of fire potential, the FWI (Figure 2). Four codes (FFMC, DC, DMC and FWI) are used in tandem to estimate the potential for a fire to start.

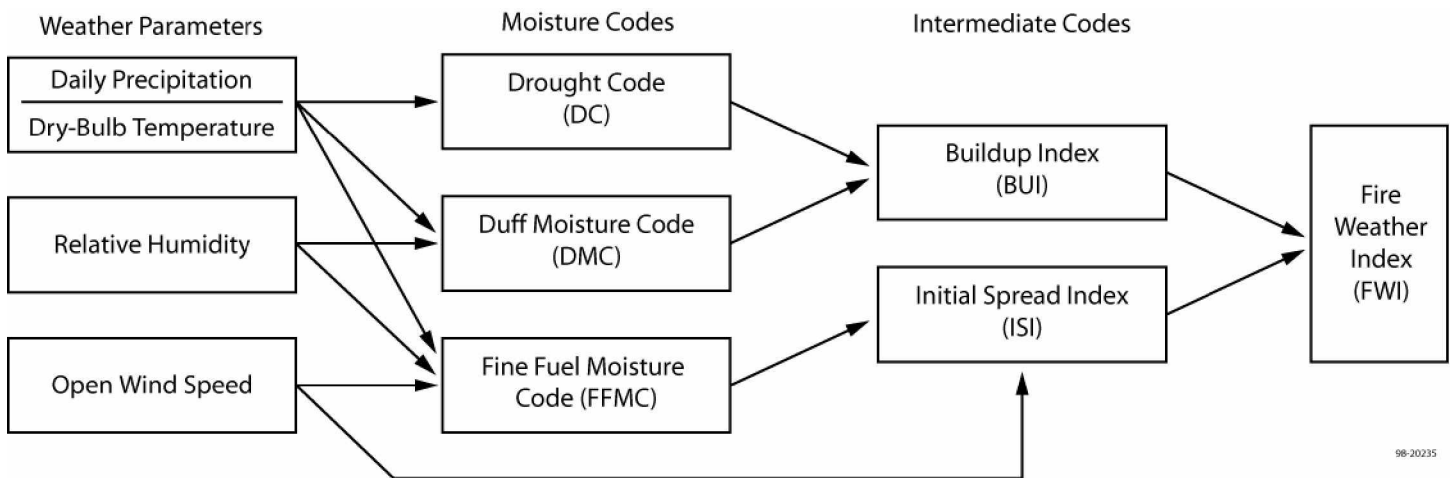


Figure 2. Diagram depicting the Canadian Forest Fire Danger Rating System’s Fire Weather Index System.

7. Initialization and Progressive Calibration of the FWI System Drought Code with SAR Imagery

The drought code (DC) is one of the indices of the Canadian Forest Fire Danger Prediction System’s Fire Weather Index System which is representative of moisture in the deeper (by definition, on average 18 cm below the surface) more compact organic soil layers of boreal forests, the lower duff layer. The Alaskan and Canadian resource managers have expressed issues with the DC in that the spring initialization of this code

is particularly difficult and with its 52 day lag, using the default spring value of 15 can cause the code to be off for about half of the fire season before it corrects itself. According to Stocks (1979) adjustments to spring start-up values are only occasionally required in eastern Canada, but are commonly needed in drier parts of western and northern Canada (Alexander 1983). When winter precipitation exceeds 200 mm, the DC default value of 15 works well because the duff layer has had a chance to saturate (Lawson and Dalrymple 1996). This is not the case for much of Alaska nor for western and northern Canada.

An additional problem with FWI is that while fuel types and drying conditions (day length, permafrost, decomposition rate, and soil type) vary across the North American boreal forest, the FWI moisture code calculations do not (Jandt et al 2005). In Alaska scientists and resource managers have noted that there are mid-summer variations in measured moisture values that are not accounted for in the FWI system. Melting of some of the frozen layers later in the summer in both continuous permafrost and discontinuous permafrost areas may be a cause of increased moisture not accounted for in the weather-based system. Yet this is a variable that cannot be easily measured as a weather parameter. A remote method to capture a snapshot of the current moisture condition at a particular location would assist fire danger prediction by determining when a departure from the default DC is appropriate and what that number should be.

Due to discussions with resource managers of Alaska and Canada concerning particular problems with DC in spring and with mid-summer frozen ground thaw, we developed techniques for predicting the DC based on backscatter from a recently burned boreal forest. This SAR-predicted DC-value may be used in spring to correct for errors in default start up values, but also to calibrate the FWI drought code periodically. We used our *in situ* to validate the results of these analyses.

7.1 Development of SAR-DC algorithm

We built the model to predict DC based on ERS-1 and ERS-2 SAR backscatter using data collected between 1992 and 2004 at the 1990 Tok burn, 2001 Survey Line

burn and 1994 Gerstle River burn (located near Delta) test sites (Figure 3).

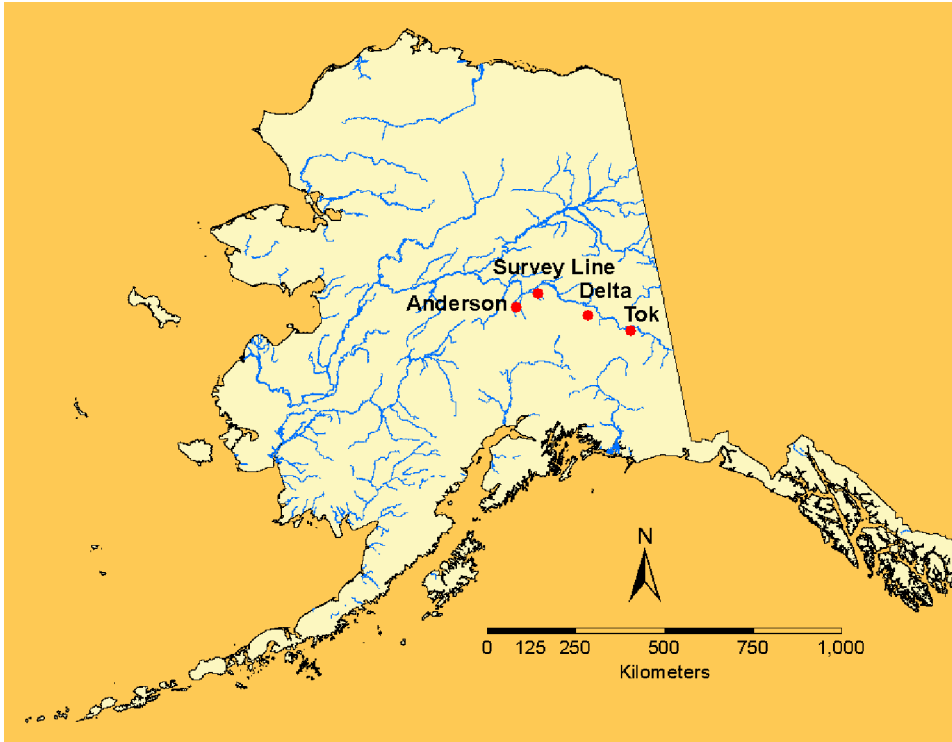


Figure 3. Study site locations in Interior Alaska. Delta sites include Gerstle River and Donnelly Flats burns.

The combined data from these three test sites are presented in Figure 4. The Gerstle River (GR) test site is underlain by discontinuous permafrost and, as other sites underlain by permafrost, exhibits a shift in the relationship between ERS backscatter and DC mid summer. This shift is hypothesized to be due to increased moisture mid-summer due to frozen ground thaw that is not taken into account in the weather-based DC but is apparent in the SAR imagery. Because of this shift the data displayed in Figure 4 are sorted by pre-30 July and post-30 July for GR and for Tok (which is not underlain by permafrost) as comparison. The green points are from the Survey Line Burn which, as Tok, is permafrost-free. In this plot we also differentiated night-time satellite overpass data for GR, but found no difference between night and daytime overpasses. Note that there is no shift in data collected pre-30 July (yellow triangles) and post-30 July (cyan X's) at Tok, as is expected.

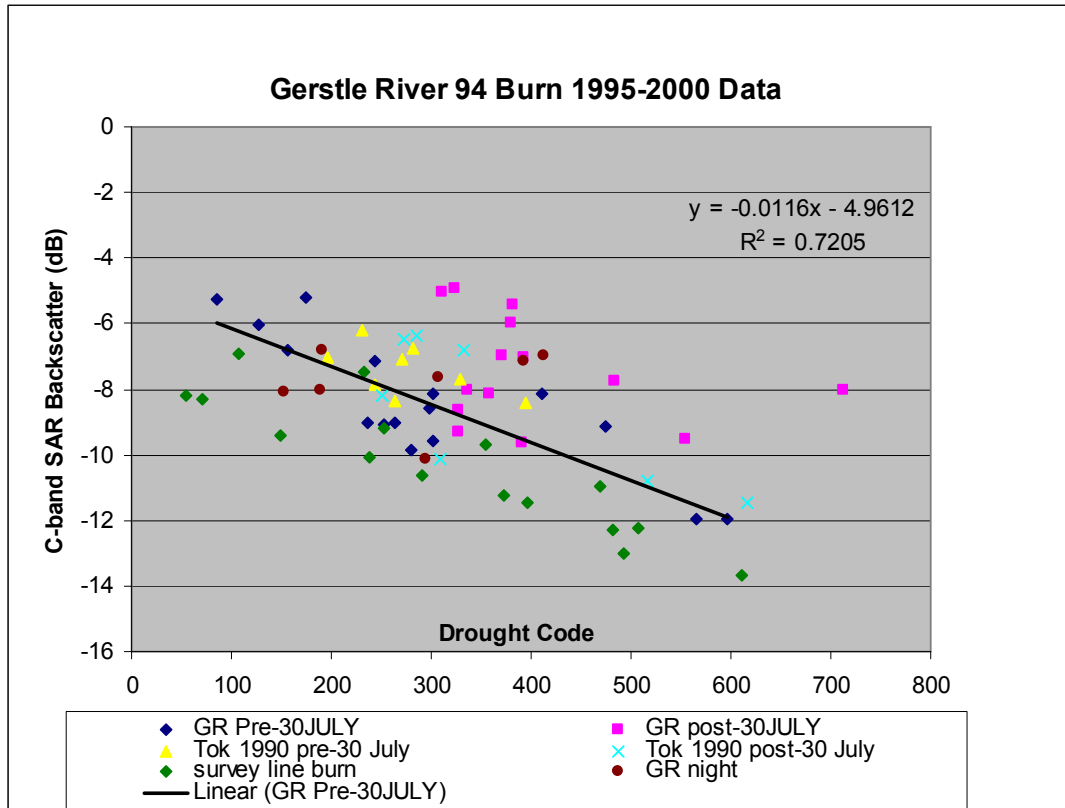


Figure 4. Plot of DC vs. ERS C-band Backscatter at the Gerstle River 1994 burn between 1995-2000, Tok 1990 burn between 1992-5, and the 2002 Survey Line Fire from 2003-4.

for ERS-2. Figure 5 shows the final DC prediction algorithm, for which we have eliminated all post-30 July data from the permafrost site GR (pink points of Figure 4). This model of Figure 5 has a coefficient of determination of 0.64, standard error of 64.68, and p-value $\ll 0.00001$. Since this model was built using multiple test sites and multiple years of data it is fairly robust. However, it has not been tested outside of interior Alaska.

7.2 Description of Technique

The algorithm developed is:

$$DC = -45.592 * (ERS-2 \text{ backscatter dB}) - 114.68 \quad (\text{eq 1})$$

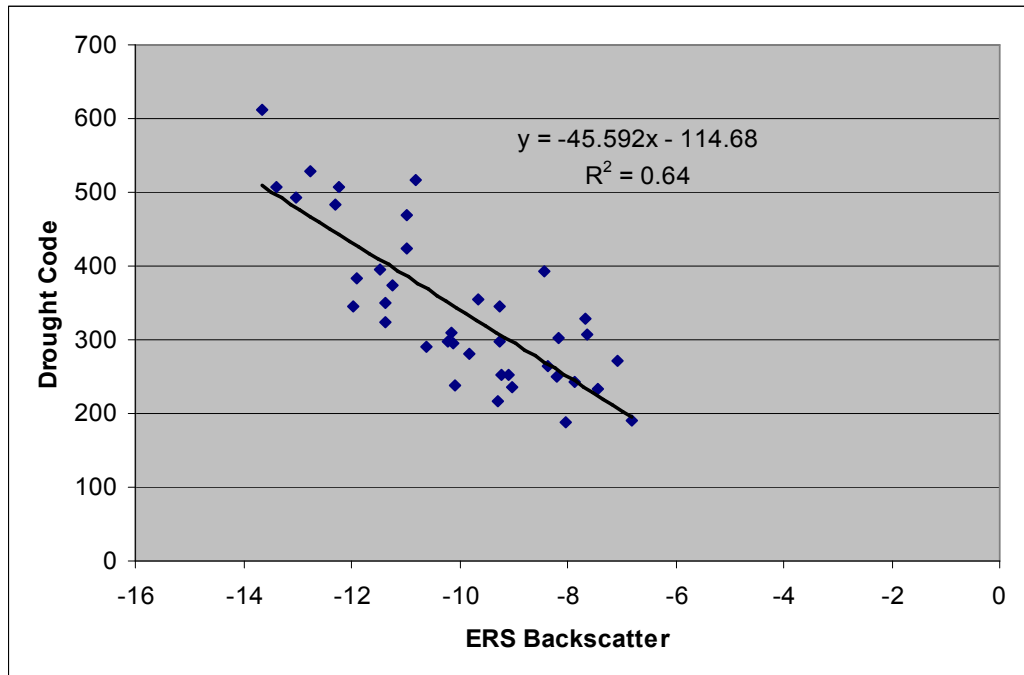


Figure 5. Final Prediction Algorithm of DC vs. ERS-Backscatter based on Tok, Gerstle River and Survey Line burn sites.

The technique involves obtaining a SAR image for the time-period or date of interest over the area of interest that includes a recently burned forest (0-10 years). Usually one or more spring scenes were available for initialization of the DC at Alaska test sites. This image does not need georeferencing for this technique to work. This image, “off the shelf” will most likely be in magnitude and must be converted to “intensity” via squaring, there may also be calibration that needs to be applied and that information/software is available from the processing facility. Next a large area within the burn is selected for averaging pixels. The averaged intensity pixel values are then converted to dB using equation 2 (Appendix A):

$$\text{Backscatter (in dB)} = 10 \cdot \log_{10}(\text{image intensity}) \quad (\text{eq 2})$$

For ASF ERS-2 data, the corresponding normalization factor (table 1 of Appendix A) must be applied. (Meadows et al. 2004). Finally, application of equation 1 to the averaged ERS-2 backscatter value in dB will provide a new drought code value.

This technique has been tested on fire scars as old as 10 years post-fire to test sites in interior Alaska, with high accuracy when compared to *in situ* data. These SAR-

derived DC values may be used: (1) to initialize DC in spring for weather stations near the fire scar being used; (2) to calibrate the DC throughout the summer for a particular weather station; or (3) to provide additional DC values for areas without weather stations. Daily updating of DC is not possible since data collection is bi-weekly for most SAR sensors. However, there are multiple satellites collecting data, and use of more than one satellite will make coverage much more frequent, although new algorithms will need to be developed for the different satellite sensors, especially for the HH-polarization and varying incidence angle data. This may easily be done using the techniques described in the “Development of SAR-DC algorithm” section.

7.3 Application of SAR Algorithm

Using the DC prediction algorithm, we then calculated DC-start values in spring for independent test sites using the Donnelly Flats burn (DF, located near Delta Junction) for Fort Greely Weather Station and the Anderson burns for the Nenana weather station. We also adjusted the 2005 data at Survey Line for the Fairbanks weather station. Using data over DF we adjusted the start values for DC at Ft. Greely for years 2000 to 2005. Analysis of this series of years allows for the evaluation of the trends and potential anomalies. It also allows for the determination of limitations on capability as the fire scars age from years 1 to 6 since burn.

Note that when *in situ* data are shown in the plots of this application section, the field measured volumetric moisture content has been converted to Drought Code for display purposes using the formula:

$$DC = \{ \ln (488.4 / GMC) \} \times 267.9 \quad (\text{eq.3})$$

This equation was developed by Lawson and Darlymple (1996) for white spruce-moss forests in White Horse, Yukon Canada to convert percent gravimetric moisture content (%GMC) to DC. A few equations have been developed for various sites across Canada to convert *in situ* moisture to DC. Since the White Horse location is most similar to interior Alaska spruce-moss forests, it was chosen for conversion in our research. To use equation 2 with our field measurements, which were collected as percent volumetric moisture content (VMC) using Campbell Scientific water content reflectometer probes

(Garwood et al. 2006), the VMC first needed to be converted to GMC using the bulk density (BD) of the soils. Unfortunately BD (grams of soil per unit volume) was calculated only for a subset of study locations, and all soil sample types were not represented. Therefore, we only present *in situ* here for locations where BD was measured. While, in most cases, our *in situ* moisture represents a mean of 50 sample locations over a 200 x 200 m area, only one or two BD samples were measured per site. Thus, caution must be exercised in interpreting the *in situ* displayed as DC in the plots which follow. The purpose of displaying the *in situ* is to demonstrate the trends in moisture over the fire season, and these are real trends, it is just the magnitude of the DC values may not be exact. Thus the plots of *in situ* may be, in reality, shifted slightly up or down.

7.3.1 Donnelly Flats 1999 Fire

The DF site is only partially underlain by permafrost, but it is subject to chinook winds in January and February, causing the site to be drier in springtime. Although field data show that the northern portion of this site is not underlain by permafrost, we did observe a mid-summer shift in the SAR vs. DC data indicating increased moisture at that time which is not associated with weather changes.

In 2000 and 2001, the default DC value of 15 was not used at Ft. Greely, instead AFS had used methods to predict the start values based on the previous fall's ending Drought Code (DC) value, over-winter precipitation, the nature of the area (Chinook prone) and the nature of spring break-up. In Delta Junction 'Chinook' winds often blow from the south, out of the Alaska Range, and can bring + 50 degree temperature readings in January- February. For comparative purposes we ran the FWI code with the default of 15 in spring as well as with the SAR-predicted start value and these are plotted together on the charts for 2000 and 2001.

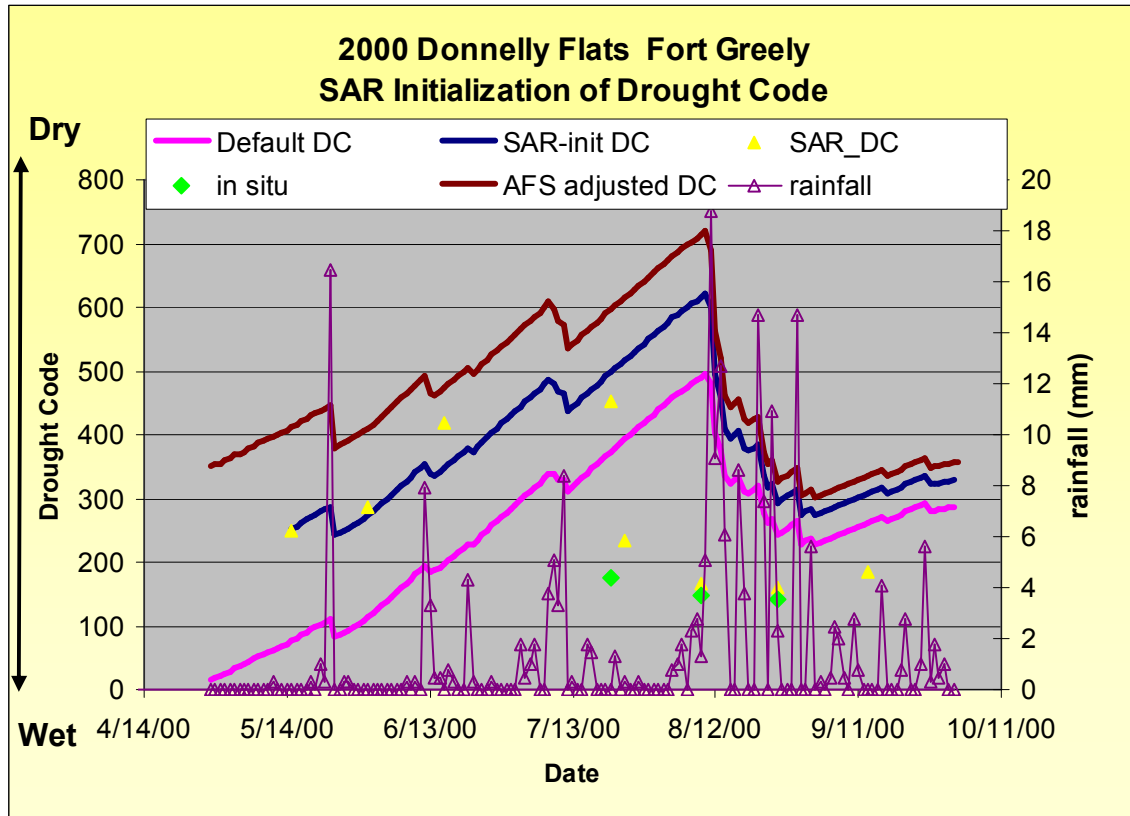


Figure 6. Plot of Seasonal Drought Code values for Fort Greely Weather Station, AK in 2000. Three DC lines are shown each having different spring initialization values: the Alaska Fire Service (AFS) over-wintered DC, the DC-15 default and the SAR-initialized DC. Also plotted are seasonal rainfall and *in situ* 6 cm moisture converted to DC.

The plot of 2000 Fort Greely Weather Station DC shows the SAR-initialized DC curve in blue (Figure 6). All available ERS-2 SAR images from this year were used to obtain SAR-derived DC values throughout the summer using the procedure described in 7.2 using equation 1. The SAR-derived DC values are shown as yellow triangles which overlay nicely on the SAR-initialized DC curve until mid-summer when the SAR and *in situ* (green diamonds) shows the DF site as getting wetter in late July. However, the weather-based DC curves continue to climb until mid-August when heavy rainfall causes the DC to drop. The pink curve on this and subsequent plots shows the default 15 initialization DC curve. Finally, the brown line shows the Alaska Fire Service (AFS) adjusted curve. The SAR-initiated DC curve falls between the default and AFS adjusted curves in 2000. However, in year 2001 they overlay almost exactly.

A similar plot for Fort Greely in 2001 (Figure 7) shows that in that year the AFS

adjusted curve is very close to the SAR-initialized DC curve with the default 15 initiated curve falling far below. This site is drier in the spring than the default implies, but according to SAR-predicted DC (yellow triangles), the site gets wetter mid-summer due to factors other than just rainfall. Note that *in situ* data collected in 2001 was very limited so it was not used for validation. However, rainfall overlaid on the plot shows that on the SAR collection dates of 6, 9, and 25 July there were 3.2, 0.3 and 5.8 mm of rainfall, respectively. And on the 12th of August, one day before the 13 August SAR collection 1.3 mm of rain fell, causing the SAR-predicted DC value to drop from over 400 to just over 200. Rain on the ground and vegetation surfaces can cause enhanced SAR backscatter that is not truly reflective of the actual soil condition, so caution should be used on rain dates, especially if the rainfall is a small amount but the effects on the backscatter are large. This may be the case on 13 August.

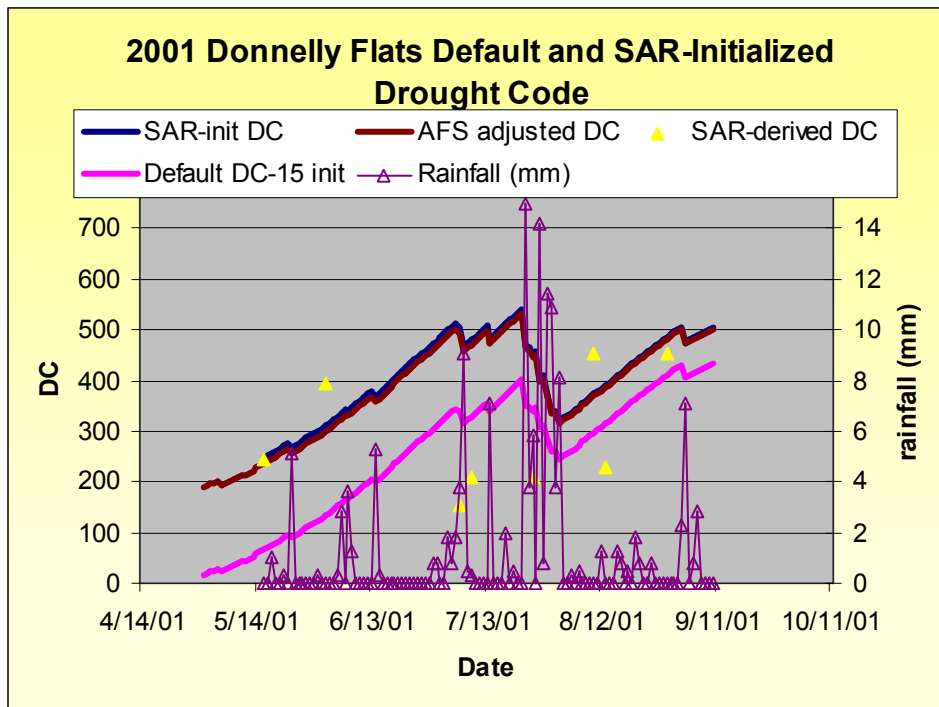


Figure 7. Plot of Seasonal Drought Code values for Fort Greely Weather Station, AK in 2001. Three DC lines are shown each having different spring initialization values: the Alaska Fire Service (AFS) over-wintered DC, the DC-15 default and the SAR-initialized DC. Also plotted are seasonal rainfall.

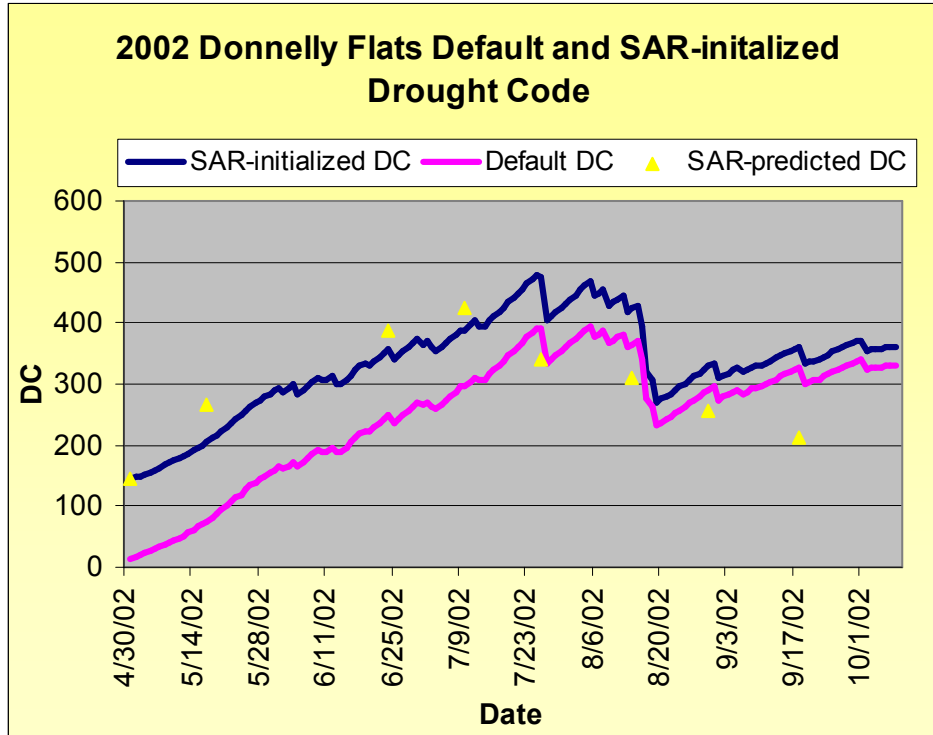


Figure 8. Plot of Seasonal Drought Code values for Fort Greely Weather Station, AK in 2002. Two DC lines are shown each having different spring initialization values: the DC-15 default and the SAR-initialized DC. Also plotted are SAR-predicted DC.

The test site was again analyzed in 2002, however in this year and subsequent years the AFS did not adjust the spring startup value (Figure 8). The SAR-predicted DC (yellow triangles) follow the spring SAR-initiated DC curve until mid-July when the moisture slowly increases at this site, but the weather-based DC has a lag in the drop and then begins to climb again, while SAR-predicted DC continues to drop in September.

ERS backscatter from the Donnelly Flats 1999 burn was also used to initiate DC in the spring of 2003 (Figure 9). Figure 9 shows the default DC curve (pink) for the summer of 2003 and the new SAR initiated DC (blue). The backscatter values from throughout the summer were used to predict DC and these values are shown as yellow triangles on the plot. The SAR-initiated code appears to work with respect to SAR-predicted DC values until mid-summer when the weather-based DC curve increases but the SAR-DC points show the DC is decreasing. *In situ* data (green circles) verifies this decrease in moisture mid-summer. Donnelly Flats is in a discontinuous permafrost area

and mid-summer melting of the frozen ground may be causing the actual moisture to increase not decrease (DC decreases not increases). The SAR-predicted DC values were then used to progressively readjust or calibrate the DC curve throughout the summer. While this was somewhat helpful, the DC has a tendency to increase (lower moisture) as time progresses and only large rainfall events will cause it to drop.

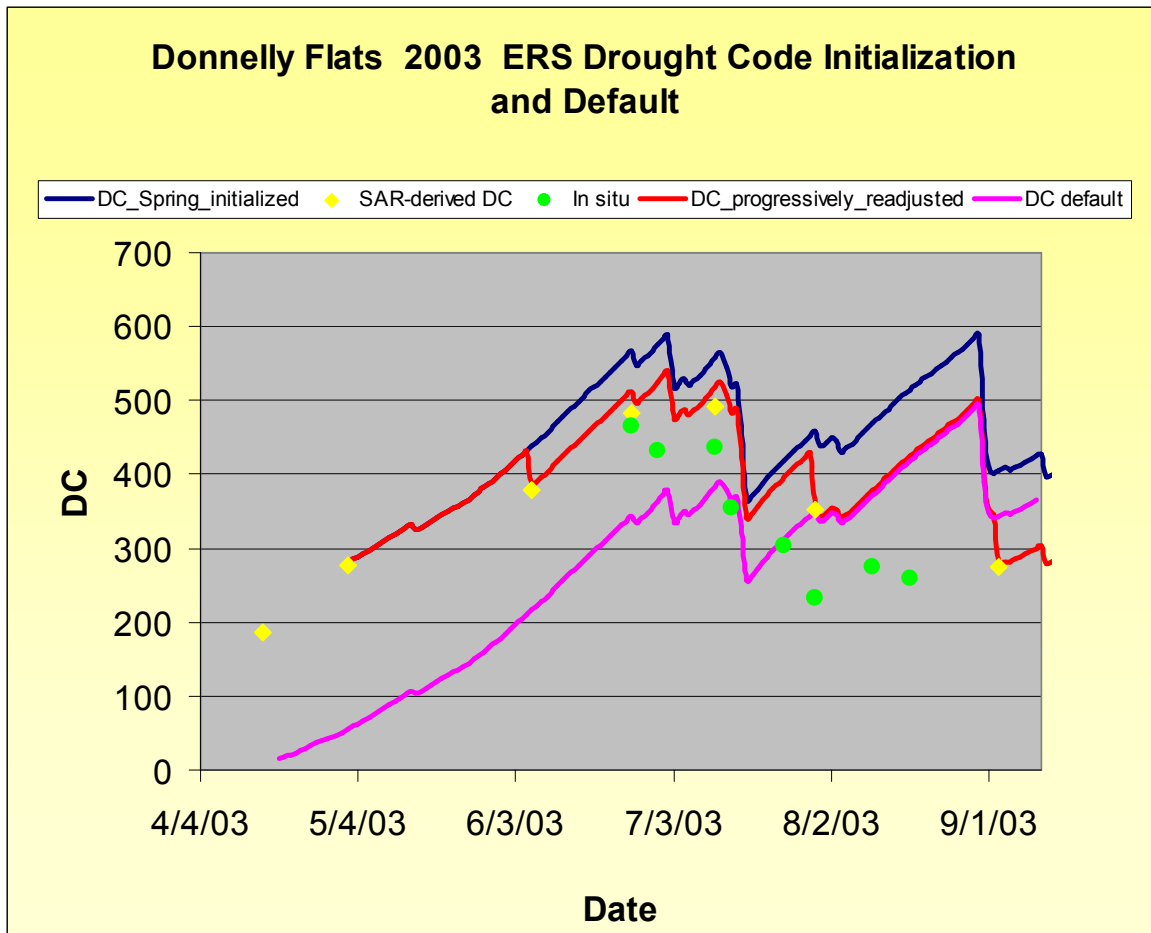


Figure 9. Plot of Seasonal Drought Code values for Fort Greely Weather Station, AK in 2003. Three DC lines are shown each having different spring initialization values; the DC-15 default, the SAR-initialized DC, and the progressively calibrated with SAR-DC. Also plotted are in situ 6 cm moisture converted to DC.

2003 was the first year we assessed since that is the year this project began, and we therefore tested to determine how much the DC-adjustments affected the final FWI calculation. In Figure 10, the 2003 fire season default FWI (yellow) is plotted against the FWI resulting from initializing the DC in spring with SAR (green), and the FWI resulting

from progressively adjusting the DC using SAR throughout the fire season (pink). At first the green and pink lines overlap, that is until another SAR image is used to adjust the DC on 5 June, at this point the adjusted curve goes from above the default to below, and the green (spring adjusted only) curve stays above the default yellow. The difference between the default and each of these SAR adjusted curves is presented in Figure 11, again the two curves overlap until 5 June. For the spring initialized DC (blue line), the percent difference in the final FWI code is high in the early season and gets lower as the season progresses. This difference is always positive. However, with the progressive SAR adjustment (pink line), the percent difference is highly variable throughout the season, with both positive and negative differences. This demonstrates what a huge effect using SAR to adjust the DC has on assessing the potential for wildfire.

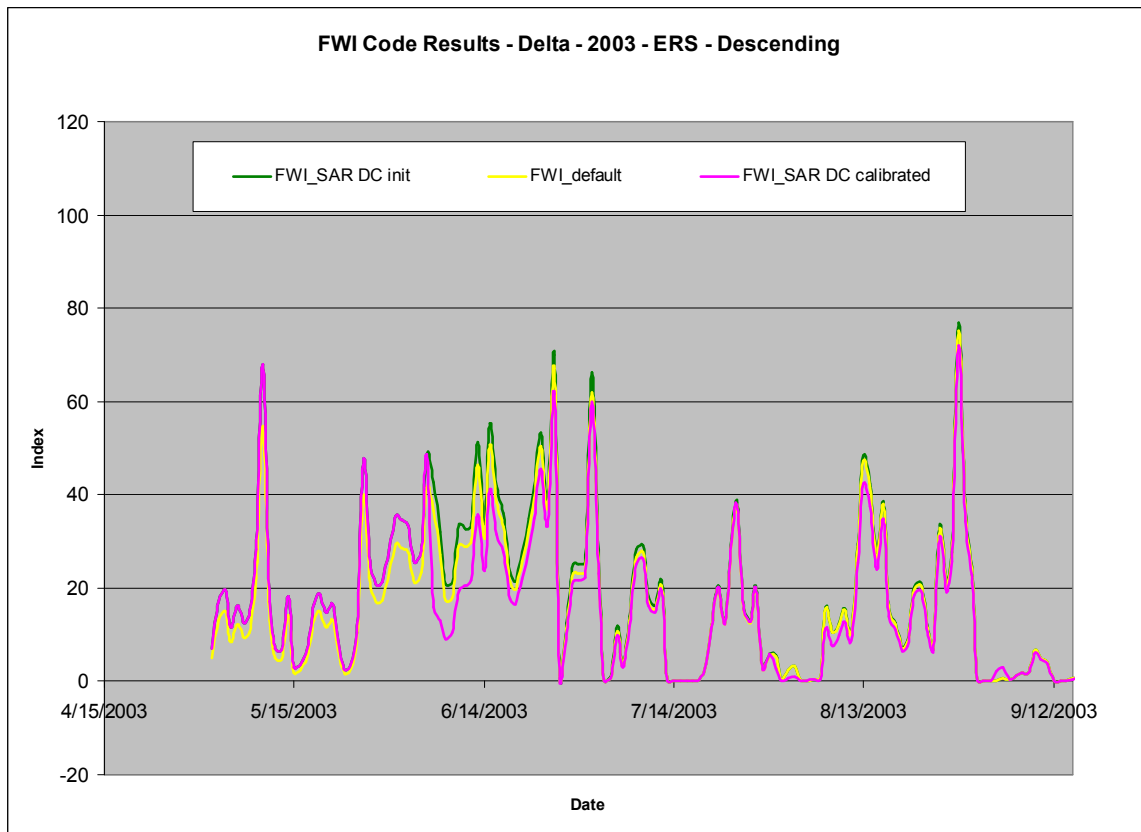


Figure 10. Plot of FWI codes with DC-initialized using SAR, DC-initialized using the spring default of 15, and DC-progressively calibrated throughout the summer with SAR.

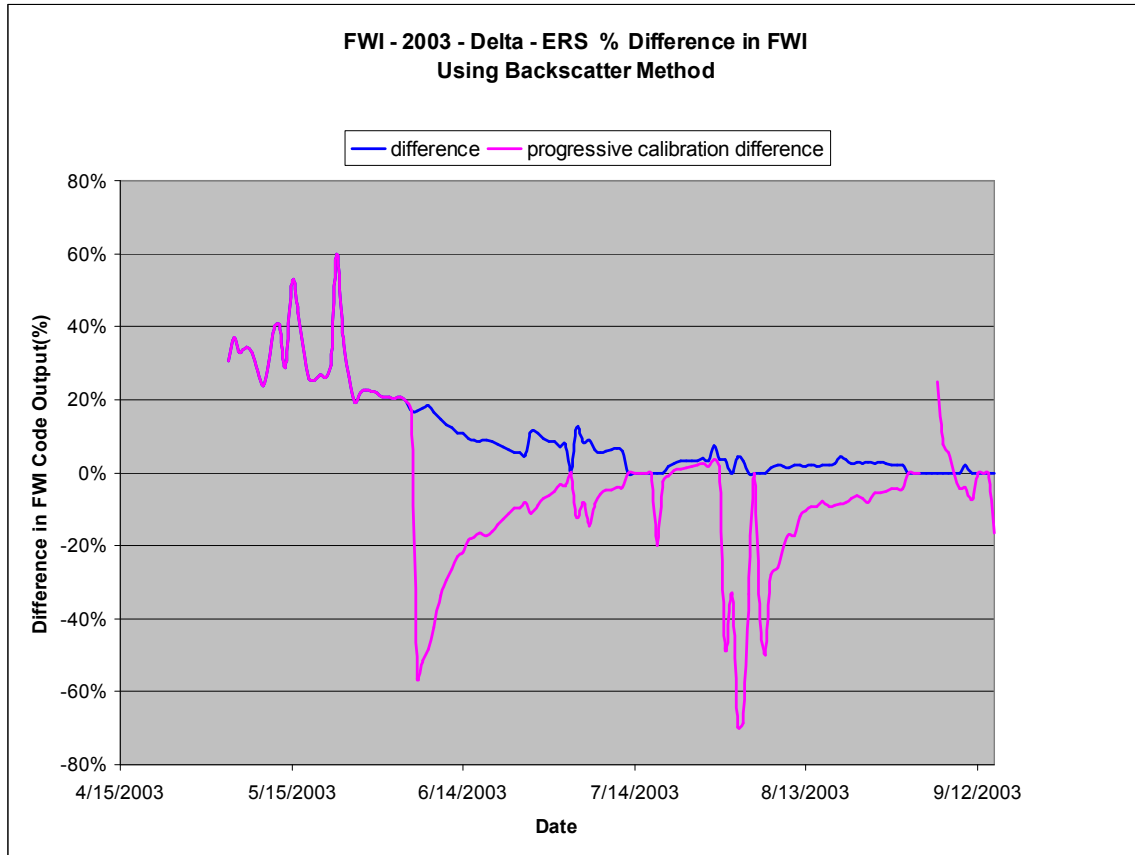


Figure 11. Plot of percent difference in FWI codes with DC-initialized using SAR and DC-progressively calibrated throughout the summer with SAR.

ERS-2 SAR was then used to initialize DC in spring of 2004 (Figure 12). This year was one of the driest on record for the state of Alaska, but for Delta Junction there were wet periods and dry periods, with a wet spring and dry June, wet July, dry August. This was a great field year for *in situ* moisture data, with field deployment beginning in mid-May and continuing into September. The SAR-predicted DC corresponds well to the *in situ* for most cases, with the exception of early July, and one day in early August. It should be noted that the *in situ* is representative of conditions within a 200 x 200 m area within the burn while the area used to predict DC from SAR was 3300 x 3300 m in size, however in this case even the backscatter from the smaller area reflects that the site is drier than *in situ* indicates. The discrepancy may be due to sampling error. The Envisat sensor also collected SAR data on 14 July 2004 with similar backscatter.

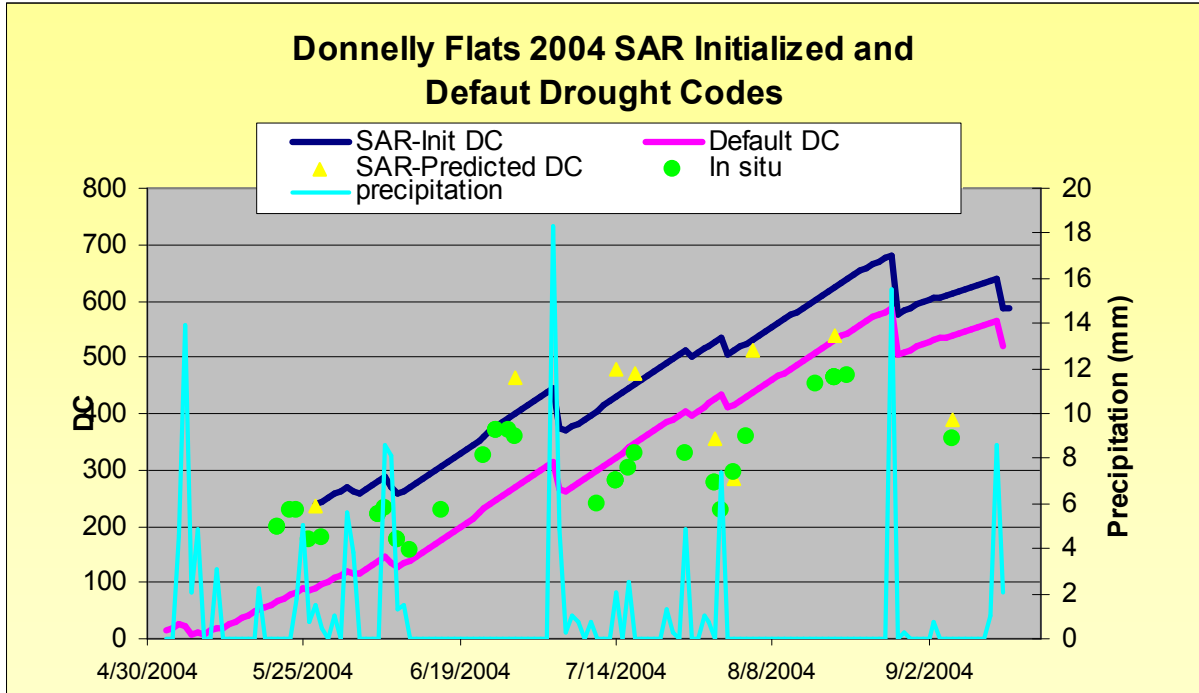


Figure 12. Plot of Seasonal Drought Code values for Fort Greely Weather Station, AK in 2004. Two DC lines are shown each having different spring initialization values: the DC-15 default and the SAR-initialized DC. Also plotted are SAR-predicted DC, rain data and 6 cm in situ.

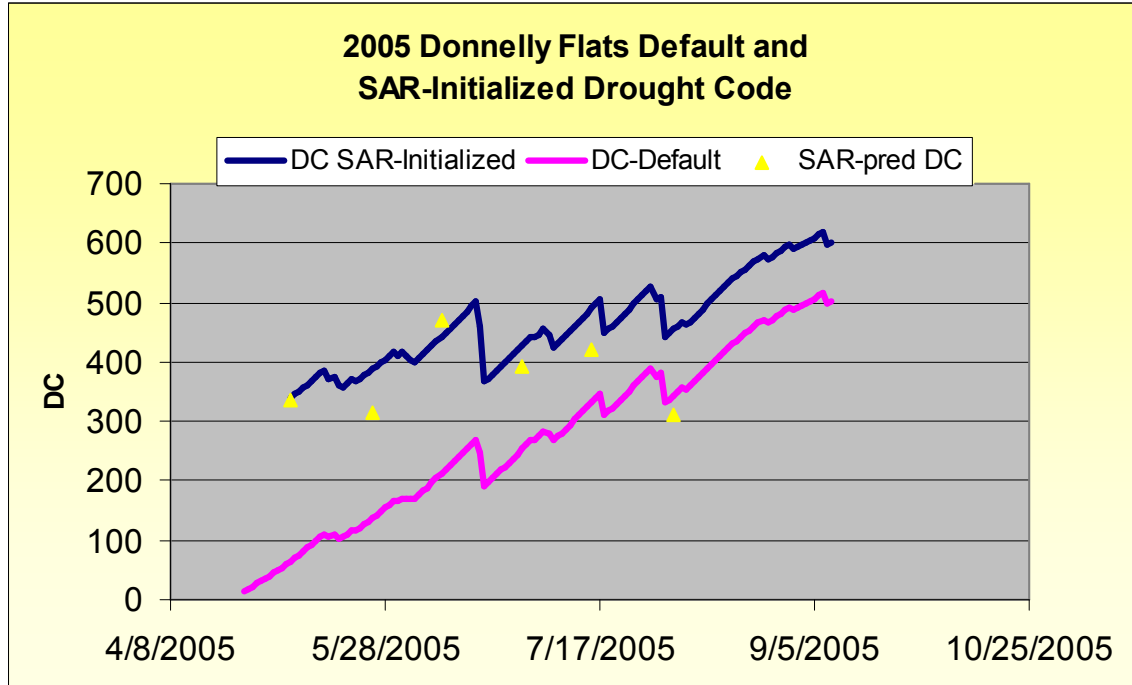


Figure 13. Plot of Seasonal Drought Code values for Fort Greely Weather Station, AK in 2005. Two DC lines are shown each having different spring initialization values: the DC-15 default and the SAR-initialized DC. Also plotted are SAR-predicted DC.

Finally, the SAR-initialization procedure was conducted in 2005 (Figure 13), again with SAR-predicted DC following the SAR-initialized DC-curve until mid-July when SAR-predicted DC drops but the weather-based DC continues to climb. Burned site *in situ* data were not collected in 2005, only unburned site, and sufficient bulk density data do not exist to convert the measured volumetric soil moisture of the unburned sites to gravimetric and thus DC.

7.3.2 Anderson Alaska Fires

This SAR-DC initiation procedure was repeated at the Anderson burn sites (Figure 14). Note that the weather station is located about 40 km away, so the correlation is likely lower than it was at DF. The 2003 Anderson Clear Fire (ACF) was used for initiation and *in situ* validation, and SAR-predicted DC values for the 1991 Anderson Burned Spruce (ABS) site are shown for comparison. Both test sites show comparable SAR results, and this permafrost site again shows the site as getting wetter mid summer rather than continuing along the weather based DC trend of increasing dryness (*in situ*

green points of Figure 14). This demonstrates that burn scars as old as 13 years post-fire can be used for this procedure. It depends on how quickly a site revegetates post-burn and the resulting level of biomass.

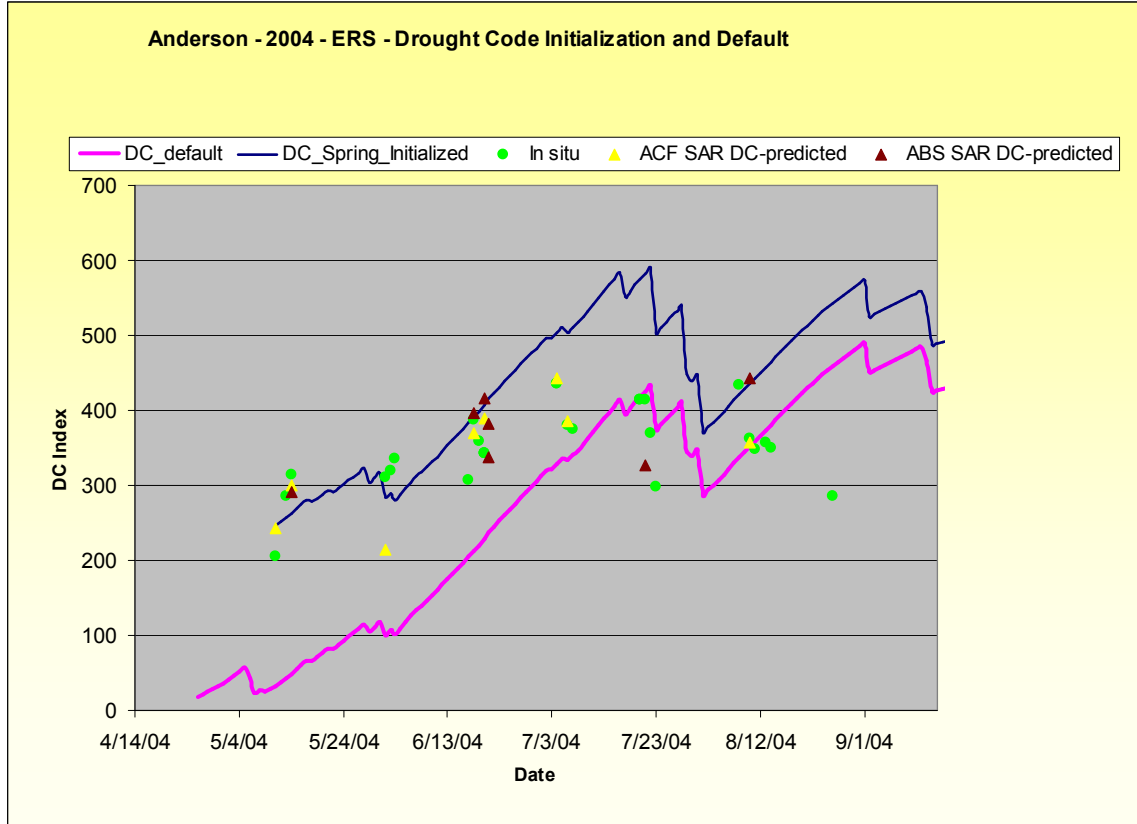


Figure 14. Plot of Seasonal Drought Code values for Nenana Weather Station, AK in 2004. Two DC lines are shown each having different spring initialization values: the DC-15 default and the SAR-initialized DC. Also plotted are in situ 6 cm moisture converted to DC and SAR predicted DC from two sites: 2003 ACF burn and 1991 ABS burn.

7.3.3 Survey Line Alaska 2001 Fire

The final site that we applied this algorithm was the 2005 Survey Line Burn. This site is permafrost free and the adjustment shows that initially the site is drier than the default DC of 15, but the site does not experience the mid-summer increased moisture that the permafrost zone fires do. This new plot follows the SAR-derived DC better than the default, and the two lines merge mid-summer (Figure 15). This is the point after the 52 day lag when DC should correct itself. Also plotted on this chart are the 7 cm *in situ*

data and rainfall. These show consistent trends between rainfall and drops in the *in situ* and SAR-derived DC points. Also note that based on the *in situ* and SAR, the conditions appear drier here in mid-summer (mid-July) than are predicted by the default DC or the spring initialized DC. This site may also benefit from progressive calibration of DC throughout the summer.

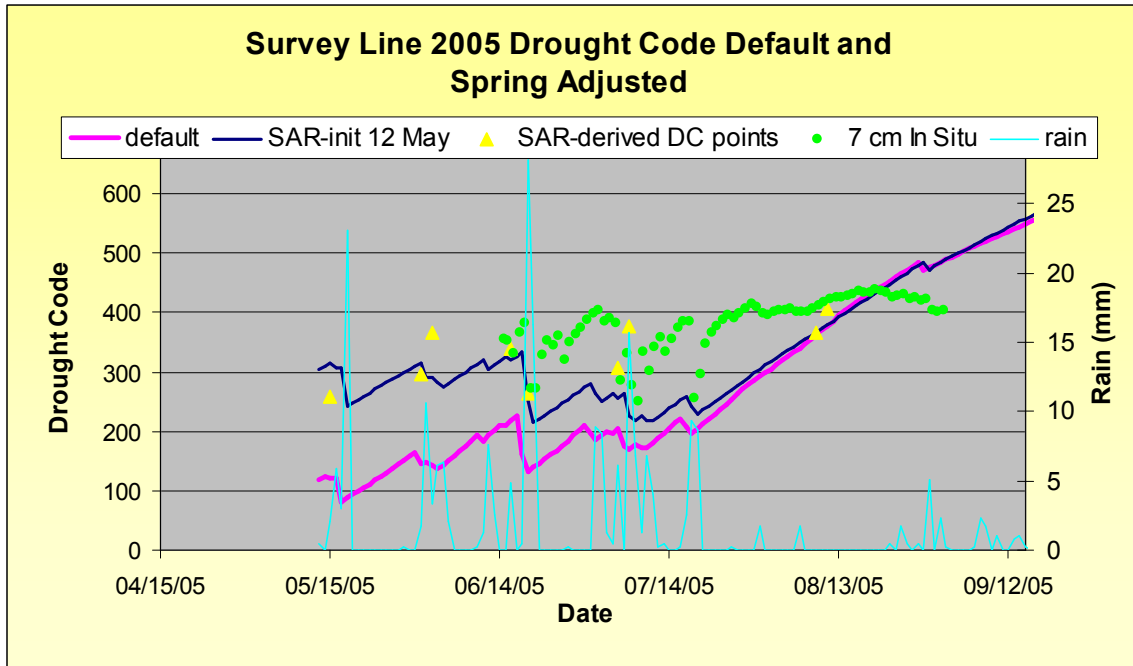


Figure 15. Plot of Seasonal Drought Code values for Fairbanks Weather Station, AK in 2005. Two DC lines are shown each having different spring initialization values: the DC-15 default and the SAR-initialized DC. Also plotted are seasonal rainfall and in situ 7 cm moisture converted to DC.

7.4 Drought Code Initialization Summary

SAR data represent an innovative tool to improve the current weather-based fire danger system by initializing the spring values of DC, calibrating the codes throughout the season and providing additional point-source data. **This approach has been deemed extremely useful for the near term in an operational sense.** Sharon Alden who works with the FWI daily says that “A satellite based method for determining when a departure from the default DC is appropriate and what that number should be would be a great help” in their fire danger assessment. Also, the method could be used to obtain additional

DC values considering the rather sparse network of weather stations that exist across the state of Alaska. Research demonstrated that SAR can be used for initializing and adjusting the DC throughout the fire season at test sites located in Interior Alaska. The methods were tested on independent test sites, with the exception of the Survey Line 2005 analysis for Fairbanks Airport Weather Station which represented one of the sites used in algorithm development, but the data were from a subsequent year. These methods, which have been assessed based on *in situ* and precipitation, are consistent across the test sites and years of data, showing that the SAR-prediction method of DC appears to be a reliable method for adjusting DC in spring and calibrating throughout the growing season, as well as adding additional DC points across the landscape. The only question that remains is how are the patterns of moisture observed in these burned sites related to patterns of moisture in neighboring unburned test sites. An *in situ* investigation was conducted and is presented in the next section.

7.4.1 Analysis of Moisture Dynamics in Burned and Unburned Sites

Since we are using burned sites in conjunction with unburned sites to develop our fuel moisture monitoring methods, and since fires only occur in the unburned sites, our collaborators have expressed concern about potentially different drying dynamics occurring between the unburned and burned study sites. If there were a difference then one could not be used as a surrogate for the other. To investigate this, the moisture dynamics for a burned site (DF-1) and a nearby unburned site (DF-2) were directly compared over the summer of 2004. Site DF-1 had similar pre-burn conditions to DF-2 so it makes a good comparison. Results show high coefficients of determination for 6 cm ($R^2 = 0.84$) and 12 cm ($R^2 = 0.93$) burned versus unburned moisture measurements. The results are displayed in the graphs below (Figures 16 and 17). Similar results were found for burned and unburned test sites at Gerstle River (Figure 18) and Anderson.

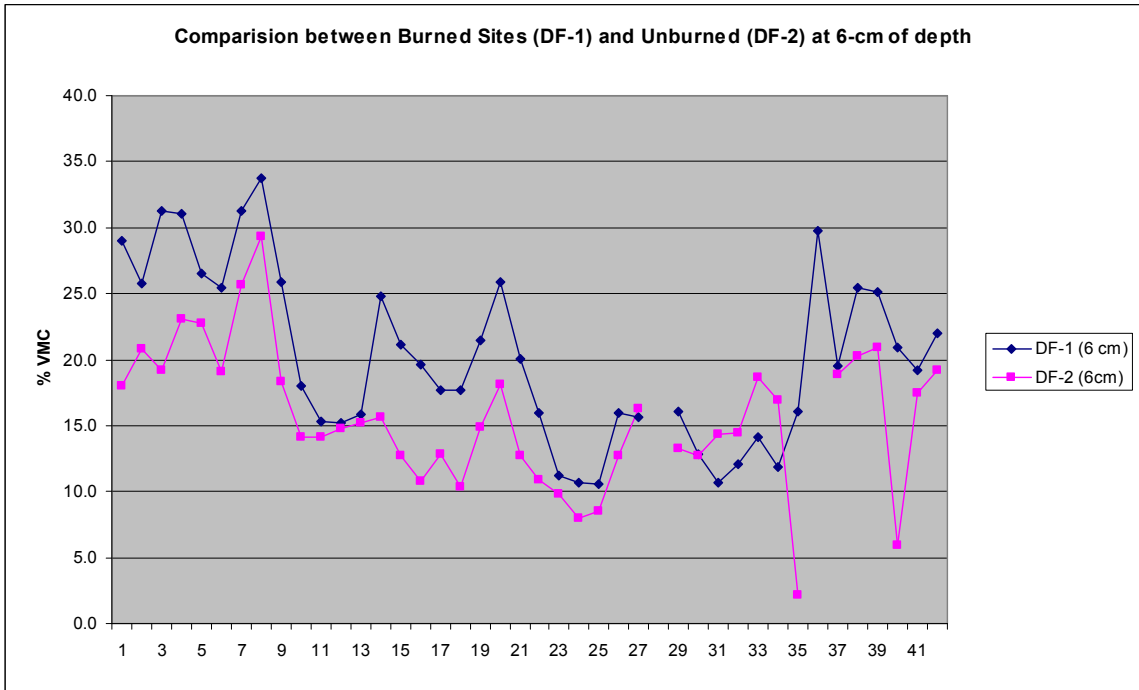


Figure 16: Comparison between 6-cm moisture dynamics in burned (DF-1) and unburned (DF-2) forests over time

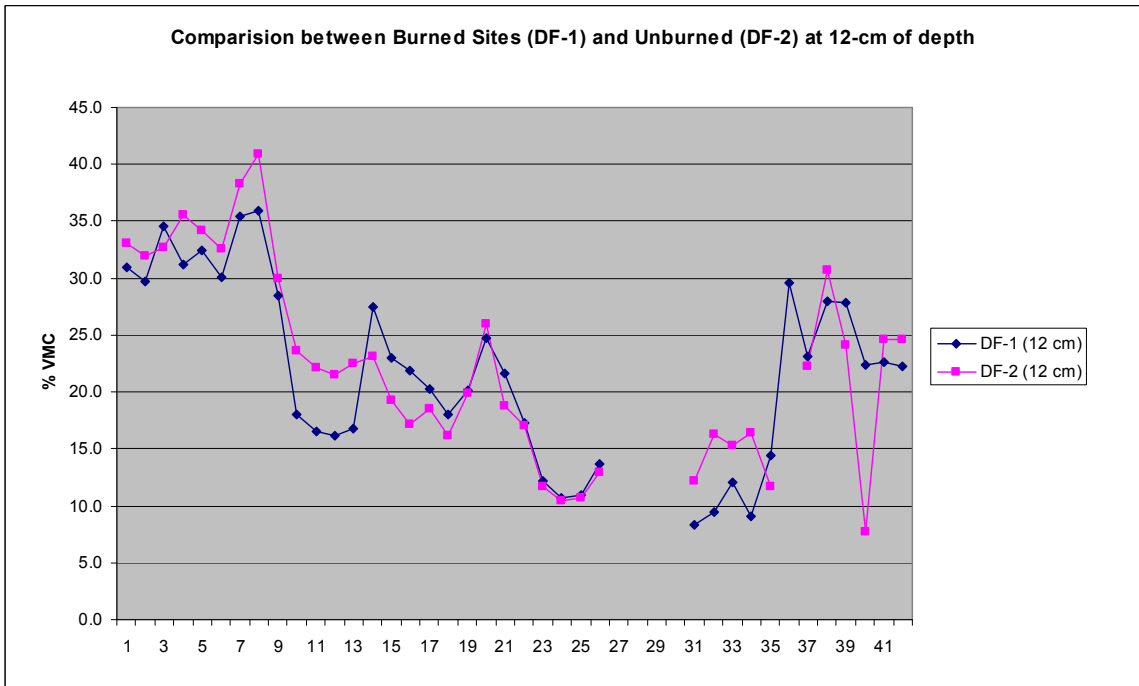
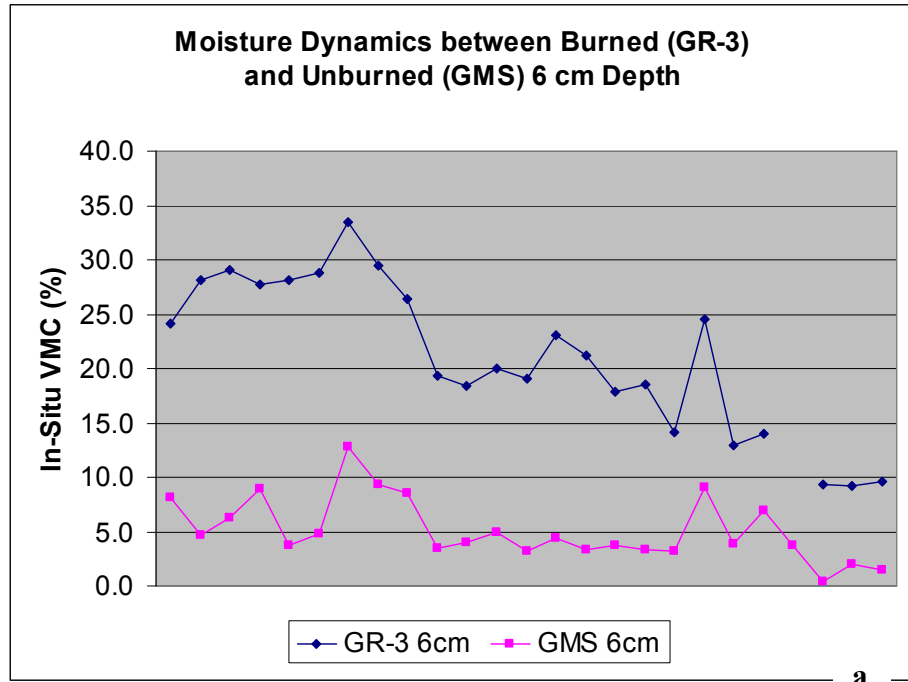


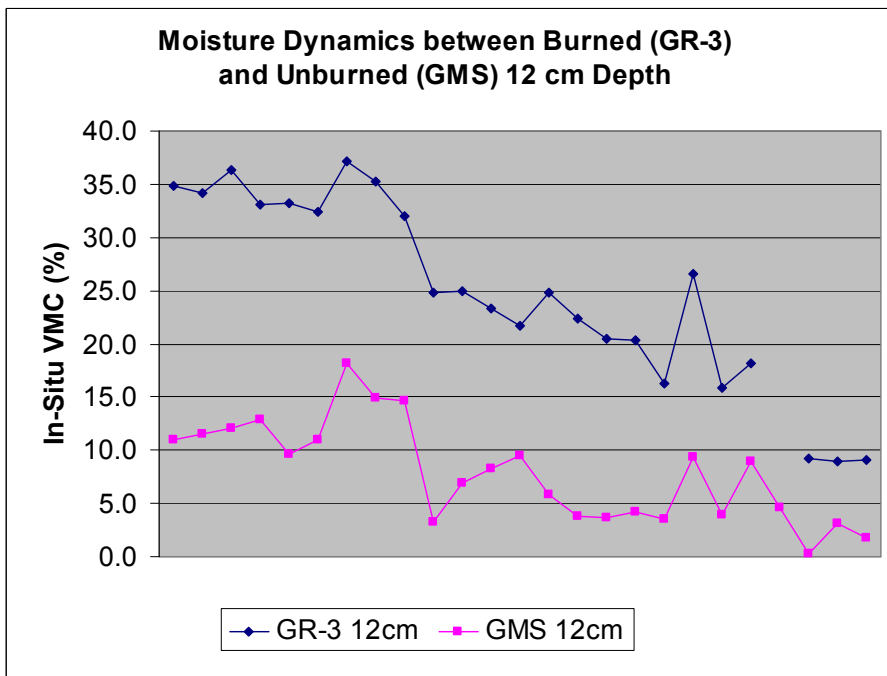
Figure 17: Comparison between 12-cm moisture dynamics (DF-1 and DF-2) over time

As depicted in Figures 16, 17, and 18 there is a clear relationship between the moisture dynamics of the burned and unburned sites for both 6-cm and 12-cm depths. For the most part, the two lines of each plot follow similar patterns. The 6 cm plot does show an offset between the burned and unburned sites at Donnelly Flats. It is expected that the offset seen in the 6-cm plot is the result of a much thicker mat of organic material on the unburned site with that material being removed with the fire at the burned location. This offset is also seen in both the 6 and 12 cm plots of Figure 18. What is important is that the patterns of changing moisture are similar between the burned and unburned sites, thus the patterns of drying and wetting are similar, although the absolute values are different.

There are a few dates where the volumetric moisture is significantly different between the burned and unburned sites. These dates are likely a result of sampling error.



a



b

Figure 18: Comparison between a) 6-cm and b) 12-cm moisture dynamics (GR-3 and GMS) over time

7.4.2 2000 and 2005 Burned/ Unburned Soil Moisture Data Comparison at Permafrost and Non-Permafrost sites

The comparisons above relate distributed sampled averaged *in situ* moisture

measurements over a 200 x 200 m test area using the Hydrosense probe (CS620) inserted vertically into the soil (12 cm) and at 60° (6 cm). In 2000 and 2005 point-source moisture monitoring instruments were deployed at several sites at multiple depths. In 2000 the CS615 instruments were used and inserted horizontally into the soil at a variety of depths. In 2005 CS625 probes (similar to CS616) were inserted vertically at various angles to obtain various depths. This section presents comparisons between paired burned and adjacent unburned point-location *in situ* moisture. Results reveal similarities in patterns of volumetric soil moisture, although the magnitude may be offset. These comparisons are made to show that burned sites can be used as surrogates for unburned sites. Data presented here are from 2005 at Survey Line (Non-Permafrost) and from 2000 and 2005 at Gerstle River and Donnelly Flats (Permafrost Sites). The recent calibration of the CS615 probes, allows us to work with the data collected over GR and DF in 2000 (Appendix D).

Comparisons of *in situ* moisture collected in 2005 at the two unburned sites at Delta Junction, Donnelly Flats 2 (DF-2) and Gerstle Moderate Spruce (GMS), show that these two sites vary in hydrologic moisture class with DF-2 being much wetter (Figure 19). However the patterns of increasing and decreasing moisture follow the same trend with an offset in the magnitude. Note that the *in situ* data have been calibrated for the organic soils. The drought code is plotted (inverted) on the graph of Figure 19 for comparison, although there is not a direct comparison between the DC of the y-2 axis and % volumetric moisture of the y-1 axis. However, it is noticeable that the DC is not capturing all of the peaks and troughs of the *in situ*. This plot shows that even between neighboring unburned black spruce sites, soil moisture conditions vary greatly.

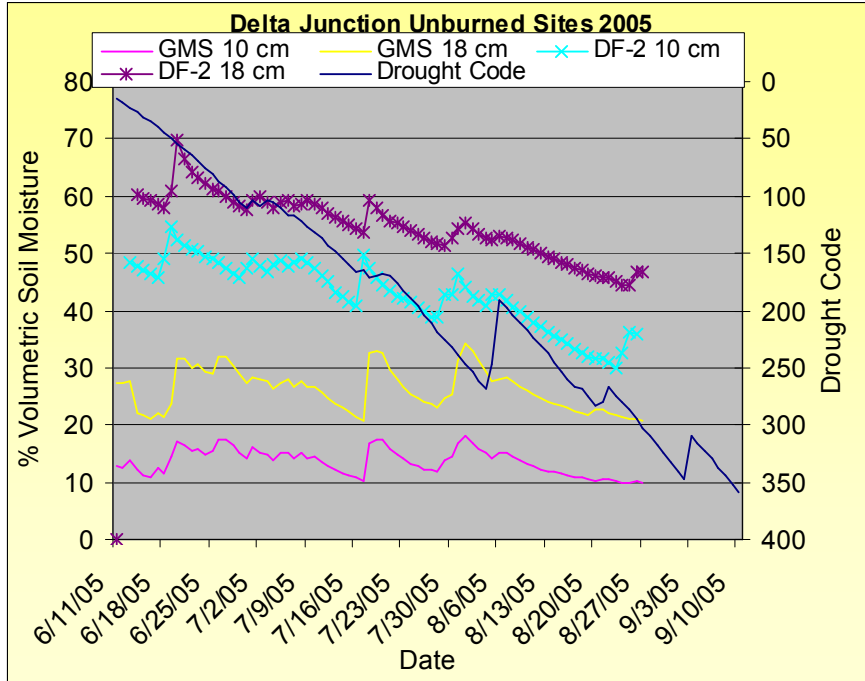


Figure 19. Plot of % Volumetric Soil moisture collected at 2 depths for GMS and DF-2 for the summer of 2005.

In Figure 20 below, 2005 data from Survey Line, paired burned and unburned sites, are compared against the Drought Code calculated from a nearby weather station in Fairbanks. The DC is inverted here for comparison to % volumetric soil moisture, note that the DC increases with drier conditions. Also note that there is not a direct comparison between the y-1 axis VMS

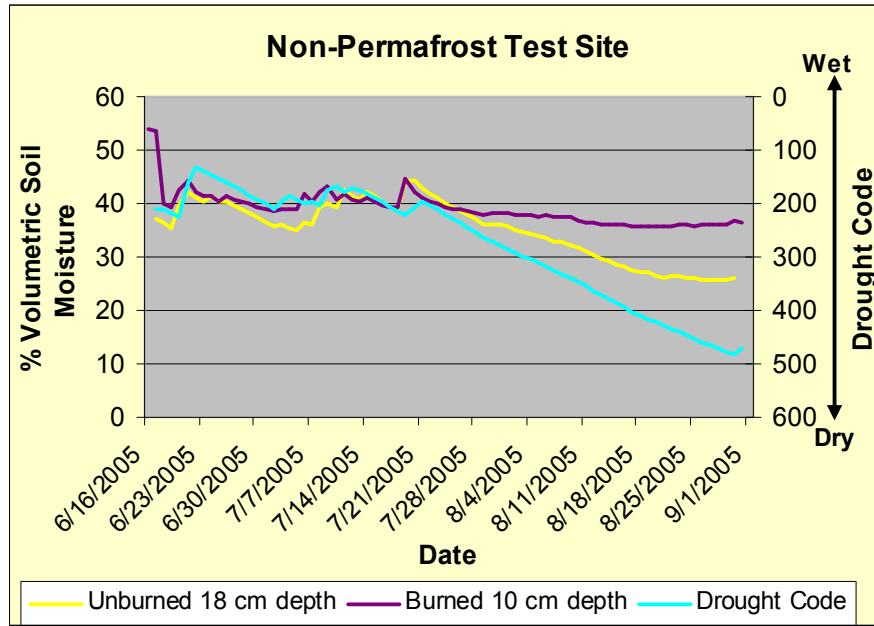


Figure 20. Survey Line Burned vs. Unburned soil moisture at comparable duff layer depths for the summer of 2005. Probes were inserted vertically and each line represents 3 or 4 probes from different locations within the test site (200x200 m area) averaged.

scale and the y-2 axis DC scale. A direct comparison can be made for gravimetric soil moisture and DC, however the former varies by bulk density. For the non-permafrost Survey Line test area, DC appears to become much drier in the later summer than either the 10 cm burned moisture or the 18 cm unburned.

Plots of *in situ* moisture from the CS615 probes collected in 2000 at Gerstle River Burned and Unburned sites near the buffalo field in the northeastern part of the burn, at 25 cm below the surface reveals that as the ground initially thaws in early spring, the burned site appears to thaw within days to 25 cm, while the burned site remains frozen at this depth until mid-June when it appears to melt. Meanwhile DC (from Ft. Greely) continues to increase in dryness. Although 25 cm is much deeper than what DC is representative of, the *in situ* lines of Figure 21 provide evidence of the increased soil moisture due to frozen ground thaw while DC continues to show decreasing moisture.

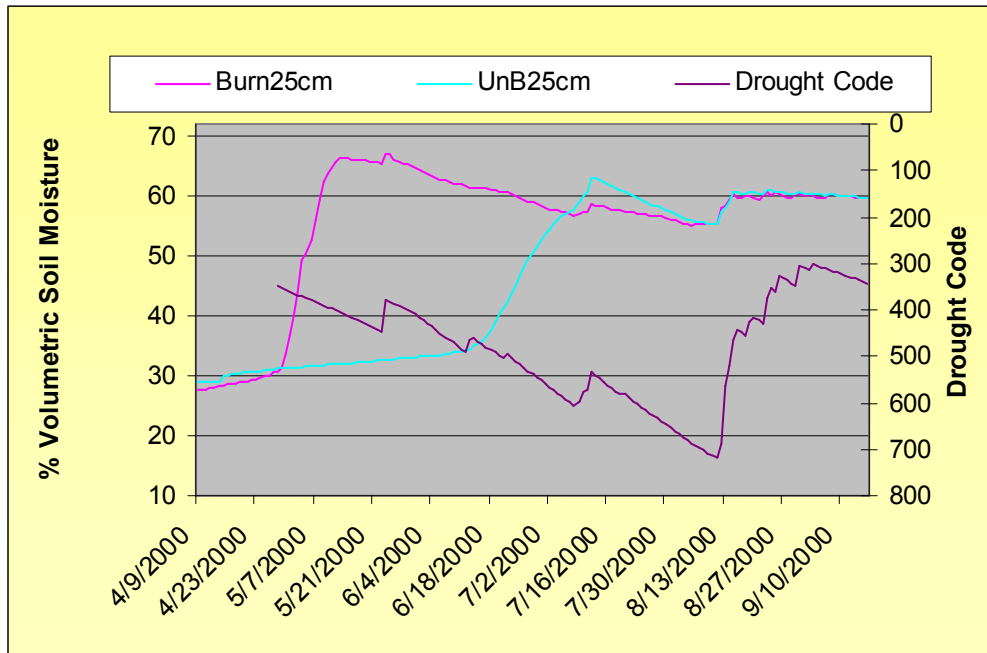


Figure 21. Plot of Burned and Unburned 25 cm depth soil moisture measured in 2000 at Gerstle River, AK. Probes were inserted horizontally, and each line represents a single probe.

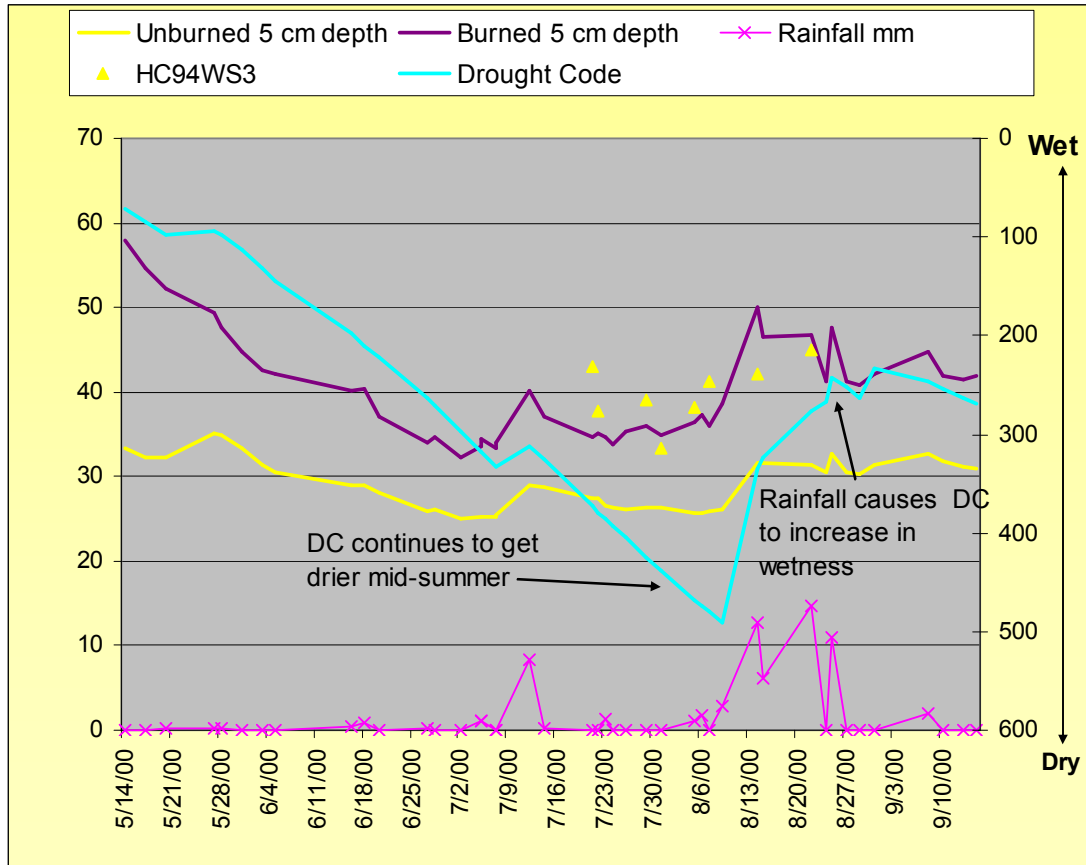


Figure 22. Plot of Burned and Unburned 5 cm depth soil moisture measured in 2000 at Gerstle River, AK. Probes were inserted horizontally, and each line represents a single probe.

Data from the same two Gerstle River test sites but at 5 cm depths for the burned and unburned sites reveal similar trends in moisture over the summer, while DC continues to get drier until mid-summer when high amounts of rainfall cause the DC to increase (Figure 22). These permafrost test sites are also likely affected by mid-summer frozen ground thaw. Data from the CS615 probe over the burned sites, shown as the solid purple line agrees with Hydrosense CS620 6 cm depth data (yellow triangles) from the same time period (although averaged over a distributed 200 x 200 m area rather than a single point, and from an adjacent but similar test site).

A comparison of 5 cm moisture in 2000 of an unburned site located to the west of the northern part of the 1994 Gerstle River burn and two moderately burned test sites, one in the Gerstle River Burn and the other in the Donnelly Flats burn also reveal similar

trends in moisture patterns (Figure 23).

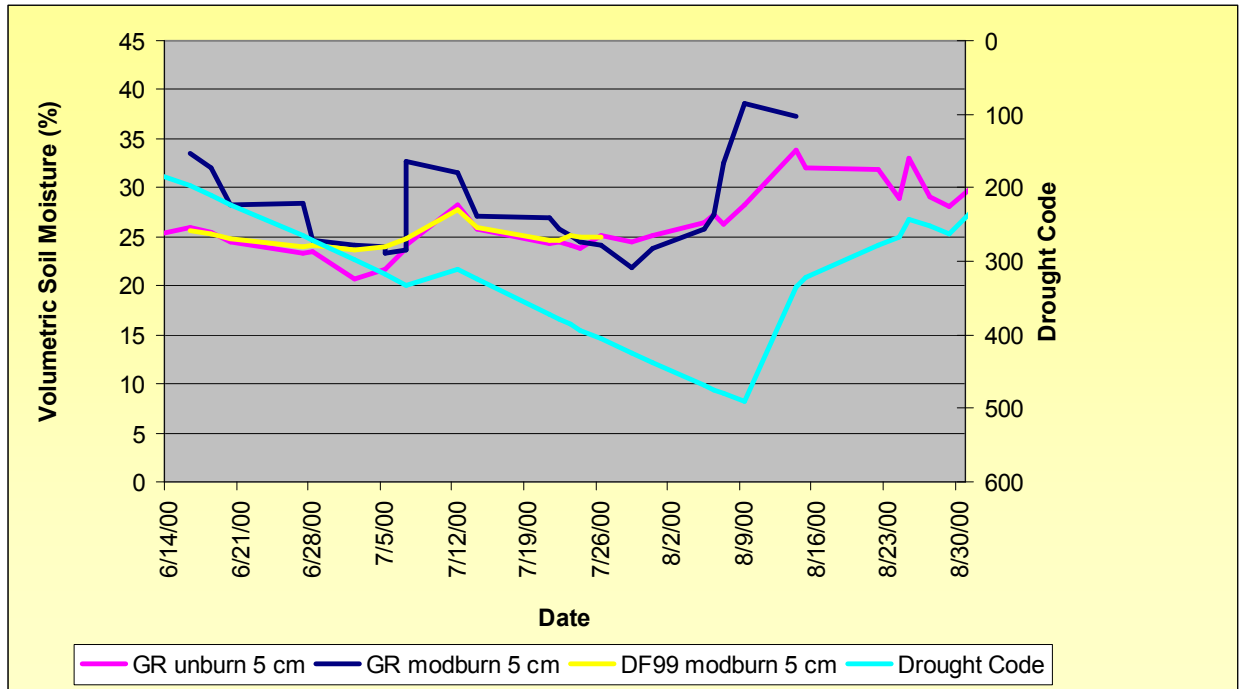


Figure 23. Plot of unburned GR moisture versus moderately burned GR and DF moisture in 2000. Each line represents a single probe.

8. Soil Moisture Mapping in Burned Boreal Forests

By combining data from this and past studies and conducting calibration of the probes used to measure *in situ* soil moisture for the organic soils (see appendix D, Garwood et al. 2006), we were able to develop a technique for segmenting a burn scar by burn severity, with the emphasis on the burn to the ground layer. And then use these burn severity classes to apply soil moisture predicting SAR algorithms developed for each burn severity class. This method provided accuracy of 3.6 rms error in volumetric soil moisture. For this method, the SAR data have to be smoothed to reduce speckle and thus the resolution is reduced from ~30 m to ~90 m. This method also requires Landsat data to categorize a burned site into burn severity classes and then apply developed algorithms for each class to the backscatter of an input SAR image. We had hoped that the Landsat derived differenced Normalized Burn Ratio (dNBR) being developed for much of Alaska under current government programs would be useful, eliminating our need to categorize new Landsat scenes. However, we found the method of creating dNBR does not use the TM bands needed to adequately measure burn severity to the ground surface. Areas with exposed mineral soil are classed “severe burn” using the Michalek method but exposed mineral soil is not used as a variable in the dNBR method (see appendix C for details on a comparison between these methods). While our approach is still feasible, as an application it requires start-up work with Landsat that differs from what the management community is currently focused on. However, the dNBR remains under evaluation by the management and scientific community and issues with belowground consumption are a concern.

8.1 Why use burn severity to segment the test sites?

In recently burned Alaskan boreal forests, biomass typically changes very little over a season and it is generally low enough in recent burns to have negligible effects on the attenuation of the SAR soil moisture signal. Surface roughness also changes very slowly at recently burned boreal sites, allowing a localized homogeneous burned forest site to be monitored for soil moisture over several seasons with fairly high accuracy. The problem arises when comparing different test sites across the burn which may vary in type of exposed soil, surface roughness, and revegetation; three parameters that affect C-band

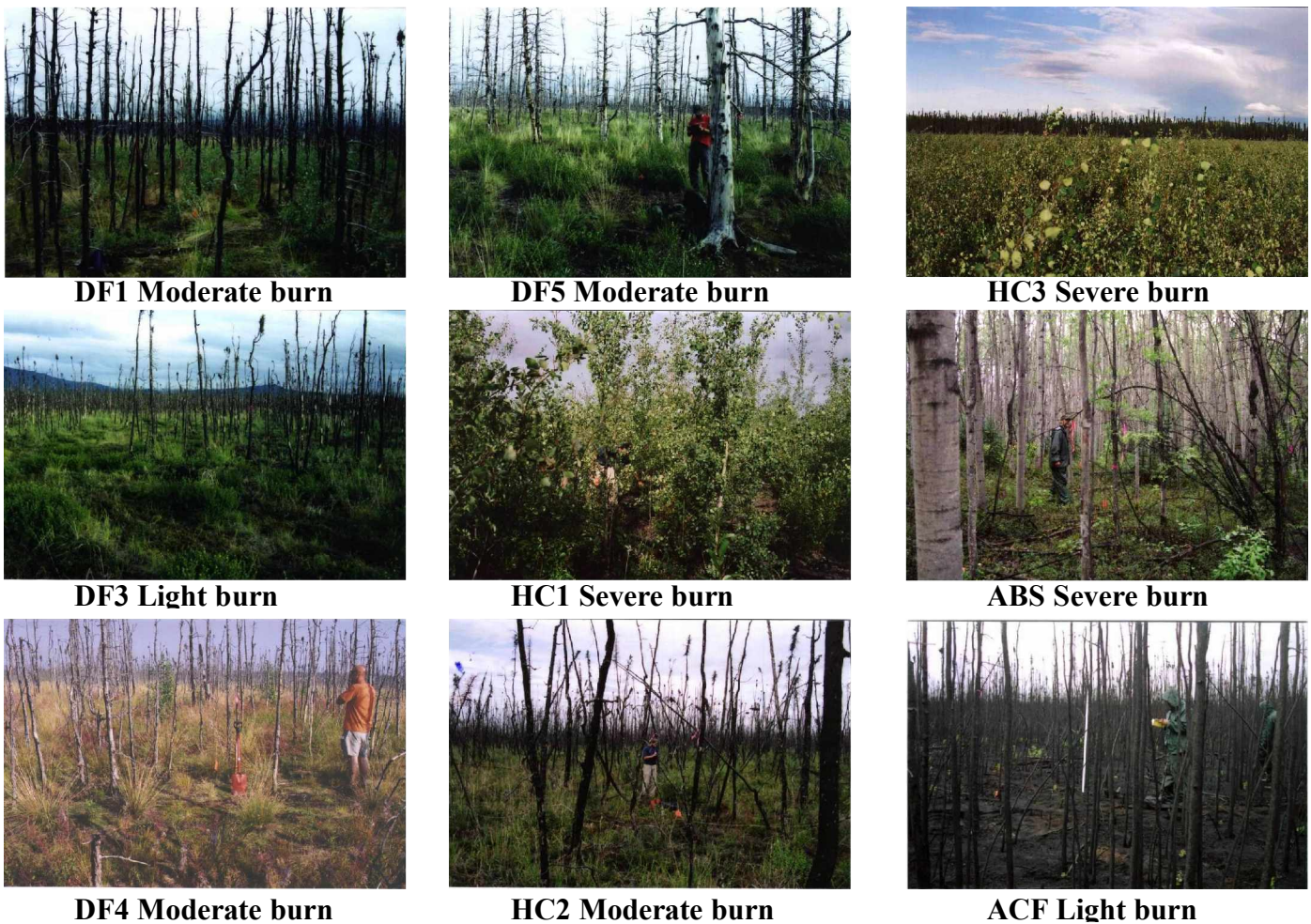


Figure 23.5. Photos of burned test sites and validation sites. Photos taken in 2003

microwave scattering. However, there is a single factor that influences the variability in all three of these biophysical parameters which can be estimated remotely, burn severity (Michalek *et al.* 2000, Key and Benson 2004). Fires burn the organic soils and influence the soil density and surface roughness that remains post-burn, as well as post-fire revegetation. By quantifying the severity of burn across the fire-disturbed landscape and then grouping test sites by this burn severity parameter in the analysis of SAR backscatter

versus soil moisture, we were able to develop models to predict spatial variation in soil moisture on an individual date (Figure 23.5).

8.2 Soil Moisture Mapping Procedure

Algorithms were developed to relate c-band burn backscatter to soil moisture collected coincident with satellite overpasses. The sites were assessed in the field for burn severity and sites with similar burn severity were grouped prior to producing the soil moisture algorithms. The final simple linear regression algorithms are presented in Table 1 and they provide the number of samples used to develop the equation, the p-value, standard error and coefficient of determination.

Table 1. Simple linear regression models for soil moisture prediction and statistics for the soil sampling sites, grouped by burn severity. R^2 = coefficient of determination, SE = standard error, m = slope, b = intercept. Note that rain dates have been removed.

Model	Sample size	<i>p</i> -value	R^2	SE	<i>m</i>	<i>b</i>
Severe burn 6 cm	28	<< 0.0005	0.59	9.25	6.4327	99.807
Severe burn 12 cm	31	<< 0.0005	0.56	9.128	5.9324	95.093
Mod-burn 6 cm	32	<< 0.0005	0.82	3.84	2.4724	49.344
Mod-burn 12 cm	38	<< 0.0005	0.69	4.9	2.3076	49.23
Low burn 6 cm	12	0.001	0.69	3.434	1.7854	39.461
Low burn 12 cm	14	0.0008	0.62	3.312	1.6244	39.843

To apply these algorithms across a burned landscape, the burn severity must be known and this can be mapped remotely using Landsat data. The Landsat data are acquired over the burned area of interest from dates soon after the fire to assess the burn severity using methods described by Michalek et al. 2001 (bands 1-6 are used in supervised classification) to create a burn severity map in a GIS (Figure 24). The burn severity categories are then used to segment a SAR scene of the study area. The SAR

data are first filtered to reduce speckle using a 5x5 averaging window. Next the image data are converted to dB. Finally the corresponding moisture prediction algorithms of Table 3 are applied to the SAR segmented data. Figure 25 shows four moisture prediction maps created through this method.

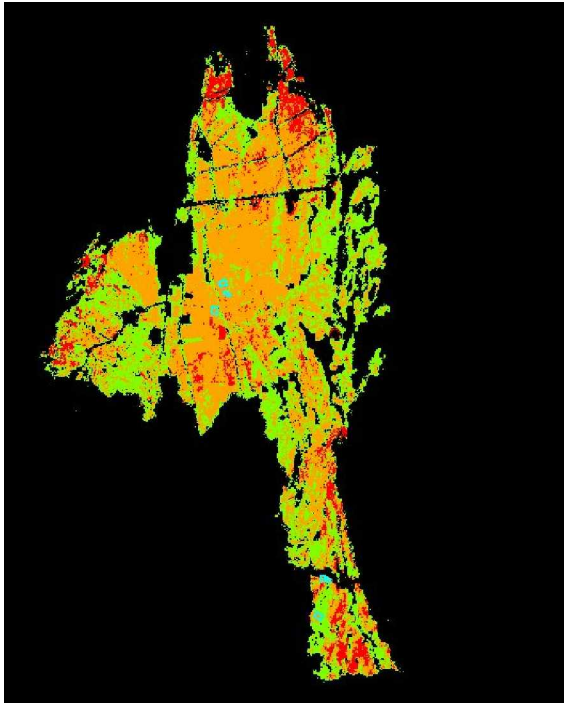


Figure 24. Landsat-derived burn severity map of the Donnelly Flats 1999 burn (from David Williams and Eric Kasischke UMD, 2001). Red = severe burn (> 80% mineral soil exposed); orange = moderate burn severity (>15 % < 80% mineral soil exposed); green = low burn severity (< = 15% mineral soil exposed). The cyan boxes are test sites.

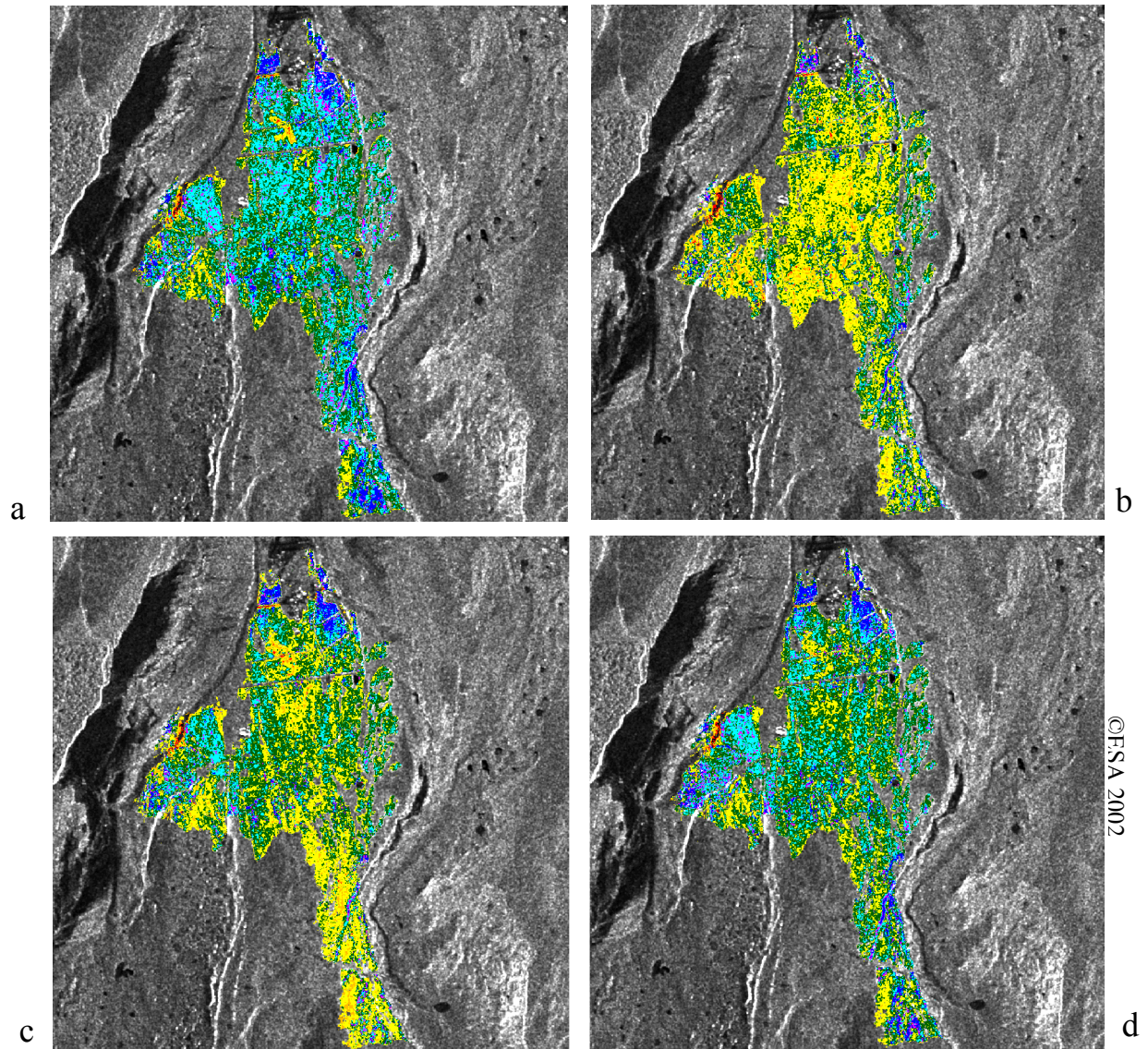


Figure 25. Individual date patterns of 12 cm soil moisture maps for the Donnelly Flats 1999 burn. Data are from 2002; a) 17 May; b) 24 June; c) 26 July; and d) 14 August.

Moisture Classes	
	4-14%
	15-19%
	20-24%
	25-29%
	30-34%
	35-39%
	40-65%

For validation of these maps, 12 cm *in situ* data collected on 24 June and 14 August 2002 were compared to map values of predicted moisture (Table 2). The difference between the predicted and *in situ* moisture ranges from +4.79 to -7.54, with a mean of -1.94. Overall the comparison to *in situ* data showed a fairly good agreement between predicted and actual measurements, with a low rms error of 3.61 volumetric soil moisture.

Table 2. Comparison of *in situ* data collected on 24 June and 14 August 2002 to predicted soil moisture at those sites in Figure 14.

Date	Site	Predicted moisture	<i>In situ</i> Moisture	Difference	Difference ²
24-Jun-02	DF 1	25.18	24.92	0.26	0.07
24-Jun-02	DF 2	21.57	25.22	-3.65	13.33
24-Jun-02	DF 3	23.04	22.90	0.14	0.02
24-Jun-02	DF 10	23.25	26.28	-3.03	9.18
24-Jun-02	DF 11	23.25	27.90	-4.65	21.65
24-Jun-02	DF 12	21.82	24.24	-2.42	5.84
24-Jun-02	DF 13	21.26	28.80	-7.54	56.91
14-Aug-02	DF 1	30.91	29.94	0.97	0.95
14-Aug-02	DF 2	28.48	32.92	-4.44	19.71
14-Aug-02	DF 3	28.10	23.31	4.79	22.97
14-Aug-02	DF 10	27.29	33.15	-5.86	34.34
14-Aug-02	DF 11	28.74	31.13	-2.39	5.70
14-Aug-02	DF 12	27.47	27.28	0.19	0.04
14-Aug-02	DF 13	27.23	29.29	-2.06	4.25
14-Aug-02	DF 14	26.31	25.77	0.54	0.29
			Mean	-1.94	13.02
			rms error		3.61
			%rms error		13.1%

This analysis and validation demonstrates the ability to remotely map soil moisture across a burned boreal forest on an individual date when the site is segmented by burn severity. This capability has many applications beyond monitoring moisture patterns for fire danger prediction (Bourgeau-Chavez *et al.* 2005ab), including post-fire succession, seedling recruitment, ecological and hydrological analysis and net primary productivity studies.

8.3 Algorithm Development of Soil Moisture Condition Based on ERS-2 SAR Backscatter

In situ data from two burn scars near Delta Junction were used for development of the SAR-soil moisture algorithms, the 1999 Donnelly Flats and 1994 Gerstle River (a.k.a Hajdukovich Creek) test sites, and independent data from test sites near Anderson Alaska were used for validation. Sites with similar field-measured burn severity categories were grouped for analysis. This resulted in four sites in the moderate burn category including 2 sites from Donnelly flats and 2 sites from Hajdukovich Creek; two sites in the severe burn category from the Hajdukovich Creek burn; and one site in the low burn severity category from Donnelly Flats. Examples of these burn severity class sites are presented in Figure 26. For detailed information on study sites see the Appendix B on study sites and for detailed information on specifics of this procedure see Appendix E (IJRS manuscript in press). Our soil moisture *in situ* data were then used to investigate the relationship between soil moisture and ERS-2 SAR backscatter within these groups. *In situ* moisture collected at the sites within each burn severity group on the various dates and years were analyzed together. All dates of data collection that had rainfall recorded, either by the local weather station or by the field crew, were not included in the model development, unless the moisture values were above 30% which would indicate that the sites were wet prior to the current rain event. This eliminated problems with backscatter being elevated due to moisture on the vegetation and litter layer which are not indicative of the soil moisture.

By segmenting the sites into burn severity groups and then analyzing the relationships between 6 and 12 cm *in situ* soil moisture within these groups and ERS backscatter, we developed fairly strong correlations (Table 2). All Pearson correlations were greater than 0.74. The 6 cm soil moisture correlations with SAR were better than 12 cm for all burn severity groups (Table 2). Also note that the 6 cm measurements were strongly correlated to the 12 cm for the severe and moderate burn categories ($r=0.87$ and 0.94 , respectively). This is probably because at the moderate and severely burned sites the vertically inserted probe is entering the mineral soil at both 6 and 12 cm depths, but

for the low burn severity sites, the 6 cm probe is entirely in organic soil while the 12 cm probe is crossing over the mineral soil layer boundary, in many cases.

8.3.1 Moderate Burn Severity Moisture Model Development

The simple linear regression model developed for 6 cm *in situ* moisture collected at the moderate burn sites of Hajdukovich Creek and Donnelly Flats versus ERS-2 backscatter (Figure 26) resulted in a strong relationship with a coefficient of determination of 0.82 and a significant sample size (n=36). Another moderately burned test site located in Donnelly Flats (DF4) and monitored in 2003-4 was used for validation (overlaid square points of Figure 26). These points fall within the bounds of the modeled data and present a tighter fit around the regression than the modeled data.

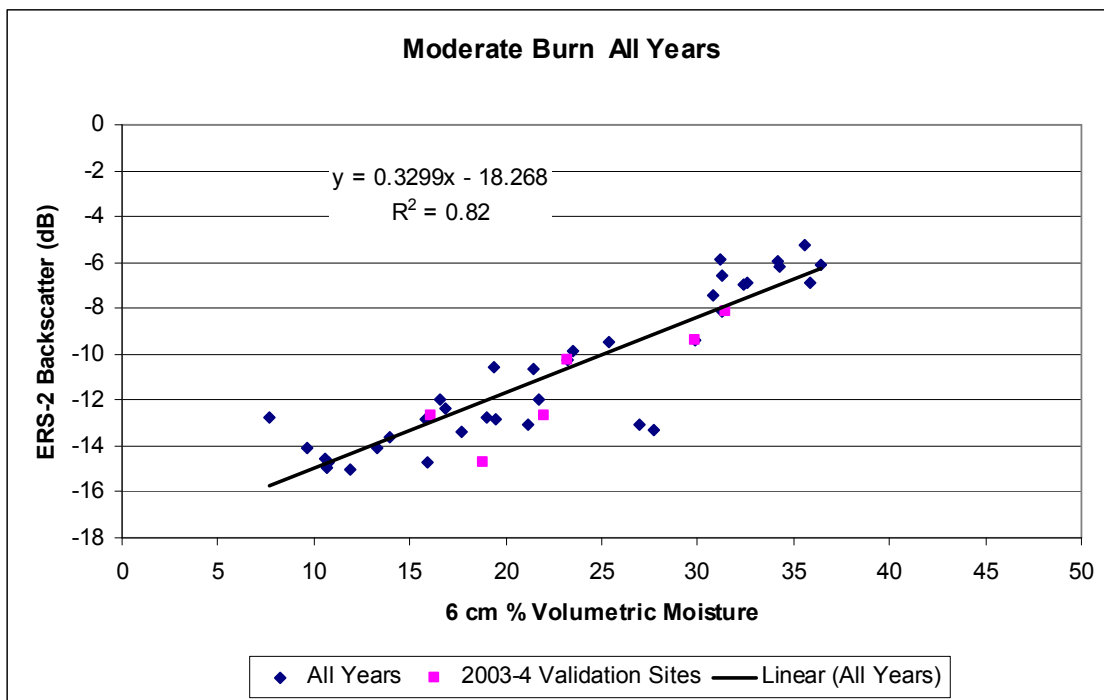


Figure 26. Plot of Moderate burn backscatter from Hajdukovich Creek and Donnelly Flats moderate burn sites for years 2000, 2001, 2003, and 2004 with linear fit. 2003-4 validation sites are overlaid for comparison.

8.3.2 Severe Burn Severity Moisture Model Development

For the severely burned HC sites (HC 1 & 3, Figure 27), a simple linear model was developed for SAR backscatter versus soil moisture with a coefficient of determination of 0.59 and a significant sample size ($n=32$). Data were collected between 2000-1 and 2003-4. No *in situ* data were collected for HC sites in 2002. Moisture at the severe burn sites in 2000-1 ranged from 22 to 62 % in the upper 6 cm. In 2003 it ranged from 15 to 26%, and in 2004, one of the driest summers on record, moisture ranged from 7 to 31% (with 31% occurring in May). Due to the cold climate and often permafrost conditions, boreal soils are often waterlogged beneath the surface. These moisture ranges are comparable to values reported by Jandt *et al.* (2005) and Ferguson *et al.* (2003). To validate the model, we have plotted data from another severely burned test site near Anderson Alaska (ABS). These data were collected in 2003-4, and ranged from 12 to 42% moisture. The validation data fall within the bounds of the modeled data. Also presented are the data from all severely burned test sites that were eliminated from the original plot due to recorded rain, either by the local weather station or by the field crew. The data collected on rain dates for the most part land within the bounds of the modeled data. However, the triangle that is an outlier is from 23 July 04 when 0.63 inches of rain were recorded at Anderson. The other dates had light rain which did not affect the backscatter at these sites. Note that the slope of the severe burn algorithm is much flatter than the moderate burn curve. The range in backscatter is also smaller (7dB) versus the moderate burn site (>9dB). The severely burned sites have greater revegetation post-burn which is likely attenuating more of the signal from the soil surface.

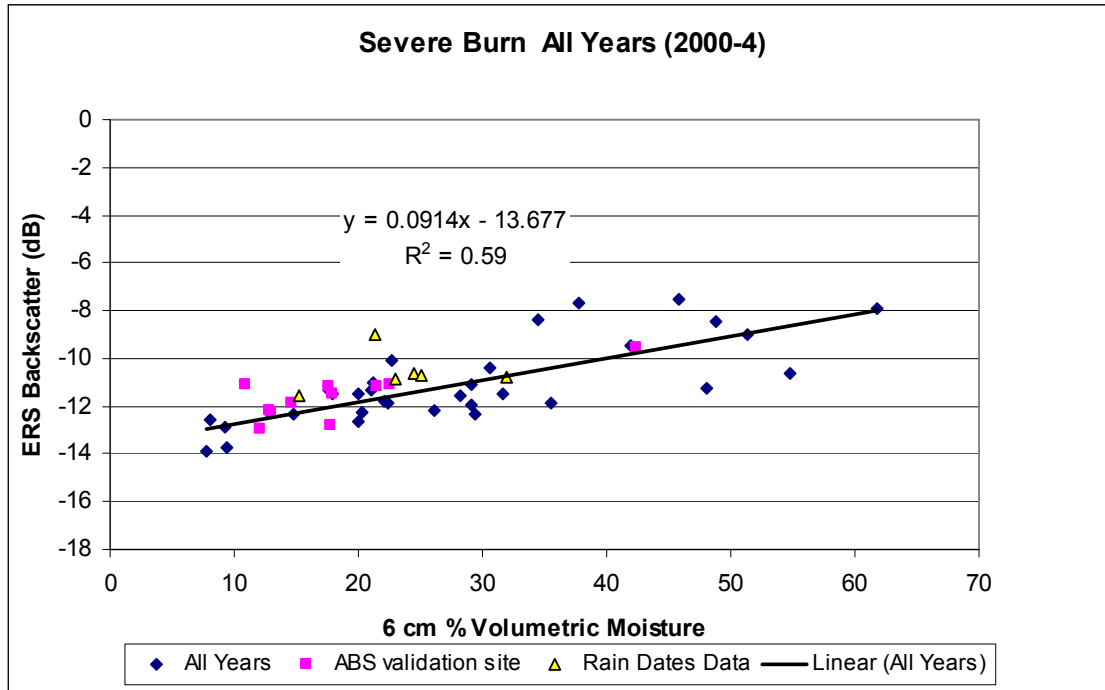


Figure 7. Plot of ERS-2 backscatter versus in situ moisture collected at the two severely burned sites of HC (HC1&3), with 2003-4 Anderson burned spruce (ABS) as validation. Data from rain dates are also overlaid.

8.3.3 Low Burn Severity Moisture Model Development

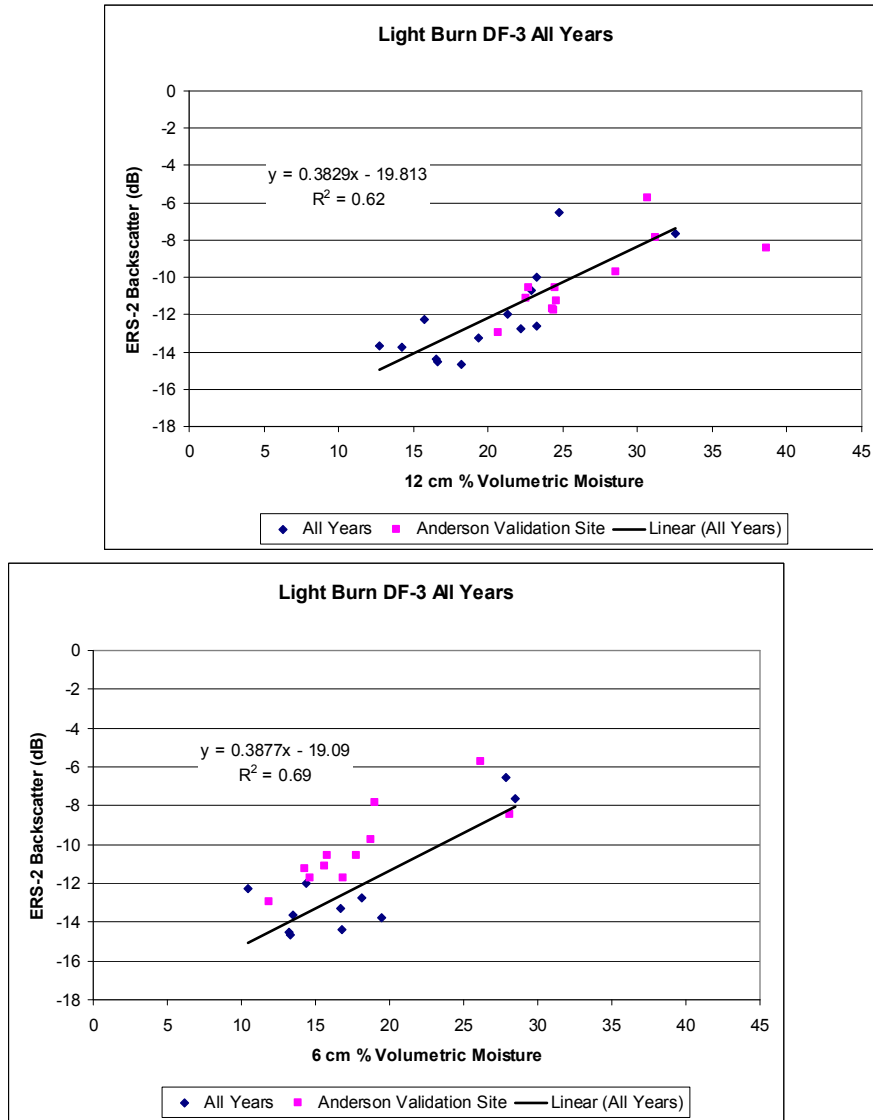


Figure 28. (a) Plot of six centimeter depth and (b) 12 cm depth volumetric soil moisture versus ERS SAR backscatter in dB at the low burn severity DF3 site. Data from the 2003-4 low burn severity Anderson site (ACF) was overlaid for validation.

For the low burn severity site (DF3) the sample size was smaller (12), but a simple linear regression fit the data well ($R^2 = 0.70$). A 2003-4 test site near Anderson (ACF) that was also lightly burned was used as a validation site (Figure 28a). The ACF site shows slightly higher backscatter for each 6 cm moisture level than DF3. This may be due to the thicker singed moss/upper duff layer at the Anderson site and thus deeper penetration by the SAR. Although, theoretically the penetration depth of a medium is a

single wavelength (5.7 cm for C-band), the moss is very light and airy and the SAR likely penetrates it more than a wavelength when it is dry. In fact we found SAR penetration of dry singed moss/upper duff to be greater than 12 cm in a laboratory experiment where we placed a 12 cm deep sample from DF3 in a chamber with perfect absorbers and illuminated it with C-band microwave energy (Bourgeau-Chavez *et al.* 2000). Therefore our 6 cm moisture samples at the Anderson ACF site would not be as well correlated to the SAR backscatter because the singed moss and upper duff is often deeper than 6 cm. When data from the 12 cm probes were related to ERS-2 SAR backscatter it resulted in a regression (Figure 28b) with a slightly lower coefficient of determination (0.62) than the 6 cm plot, but a smaller bias between the Donnelly Flats and Anderson data. This indicates that the SAR may be penetrating deeper than 6 cm into the low bulk density singed moss and upper duff of the ACF site.

8.4 Burned Boreal Forest Soil Moisture Mapping Summary

The results here demonstrate the utility of combining remote sensing capabilities (optical and microwave) to assess the moisture condition of a burned landscape. This technique applies to black spruce recently burned ecosystems of interior Alaska, however the technique should be transferable to black spruce feather moss ecosystems of Canada as well. We developed these techniques specifically for ERS, however, similar algorithms may be produced for other SAR systems (Radarsat and Envisat). We did not investigate the utility of these methods on other boreal landscape types.

We did try applying the dNBR Landsat method of categorizing the test sites into burn severity, but this method does not depict the burn severity to the ground well. This is due to the bands used for analysis. Since most of the biomass consumed in boreal forests lies beneath the forest floor, the dNBR method is not as useful for belowground burn severity in Alaska or Canada. However, its utility continues to be pursued by the NPS and other agencies and researchers of Alaska and Canada for aboveground burn severity. We continue to be involved in assessments of the dNBR studies and working groups assessing this and CBI methods. See Appendix C for details on our comparison.

9. Time Series Analysis Approach for Mapping Fuel Moisture across the Landscape

The last of the SAR approaches, time-series analysis, has shown much promise. This approach is based on comparing each location on the landscape to itself through time. This time-series analysis approach reduces the influences of time-invariant features such as surface roughness and biomass, while leaving the time-variant moisture feature for extraction. We have demonstrated the applicability at several study sites and for several years worth of data, for both Radarsat and ERS. Because of the multi-year analysis we had some glitches that were discovered mid-way through the project that we needed to deal with and were forced to repeat or adjust much of the analysis. These glitches included: (1) problems with the ERS-2 data calibration of Alaska Satellite Facility (ASF) not accounting for a loss of system gain over the years (see Appendix A); (2) problems with the DC start values in spring not being representative of actual ground conditions (see section 7.0); and (3) problems with our main test sites (Delta Junction) being underlain by permafrost which is hypothesized to cause mid-summer frozen ground thaw, and thus increased moisture not accounted for in the weather-based FWI system, but which is sensed by the SAR.

Despite these glitches we have made much progress on this approach and investigated methods of using the time series to predict the conditions on a new image date, including neural networks. Much of the research investigating the *in situ* was necessary before this approach could be fully developed, and the approach developed in section 7.0 may be necessary to calibrate the FWI from year to year since we are using it as “truth”. There were not enough *in situ* data from any single year, except 2004 and 2005, to validate the principal component analysis results, but we were able to use data from multiple years. Presented here are multi-year and seasonal analysis results of the PCA performed on the normalized (Appendix A) SAR data, to investigate the relationships between radar backscatter and FWI codes. First we present the PCA

performed over the Donnelly Flats (DF) site and adjacent unburned areas. There is a weather station located at the north end of the Donnelly Flats site. Then we present results over the unburned areas near DF and GR which were sampled continuously in 2005 for *in situ* moisture. Next we move to the Survey Line fire and present the results from this non-permafrost test site and nearby unburned forests. The weather station used for this site is located at the Fairbanks airport. Lastly we demonstrate the utility of Radarsat for PC analysis.

9.1 Summer 2000-4 PCA of Donnelly Flats

A series of thirty six ERS-2 images over Donnelly Flats from the summer seasons May-September of 2000 to 2004 were used in PC analyses. The first three output PC images from the analysis of all 36 input dates are presented in Figure 25. The first PC image shows stable scene elements such as the airport runway, the extent of the burn scar, rivers, etc. The PC-2 and 3 images show changing scene elements and we found good correlations primarily between PC-2 or 3 loadings and fire weather codes, depending on the year(s) of analysis.

PC loadings are defined as the correlation between each input image and the resulting new PC image. The loading of each input image with each principal component was calculated after Jensen (1996) using the formula:

$$R_{kp} = \frac{a_{kp} * \sqrt{\lambda_p}}{\sqrt{Var_k}}, \text{ where} \quad 5$$

a_{kp} = eigenvector for image date k and component p,

λ_p = eigenvalue for component p, and

Var_k = variance of image date k in the covariance matrix

The five year analysis of PC Loadings versus Fire Weather Index codes overall resulted in individual years having the highest correlations with PC2 loadings and FFMC, with the exception of year 2001 which was PC3 loadings versus FFMC, and year 2002

which only had a strong correlation with DC (Table 4). When observing multiple years, PC2 consistently showed better results than PC3, and FFMC showed consistently higher correlations (>0.50) than any other fire weather code (Table 4). It should be noted that in some cases PC1 showed high correlations, often equal to PC2. The Fine Fuel Moisture Code (FFMC) is a measure of the top few cm of organic soil and litter and it is strongly influenced by changes in the relative humidity and a lag time of only 12 hours, which may be why it was found to be correlated to our PCA at Donnelly Flats, and in particular our multi-date analyses. Since the DC is so affected by spring start up values and has such a long lag time, combined with mid-summer thaw not accounted for in the weather-based DC, multi-year analysis was found to have problems in correlation of DC to the PC-loadings at Delta Junction sites.

For the relationship between PC-2 loadings and FFMC for all 36 input images, the Pearson correlation coefficient ($r=0.56$) was moderate (Figure 29). Figure 29 shows the FFMC as the pink line, and PC-2 as the blue line and they are plotted against date on the x-axis. The PC-2 to FFMC relationship change with seasons is demonstrated in this graph (Figure 29) which shows the two plots (FFMC and PC-2 loading) deviating from each other in spring (start of plot 5/15/00) then they start to follow the same pattern (although with a difference in magnitude) starting in June 2000, then in September of 2000, the plots deviate again. This seasonal pattern is more or less repeated across the chart as you move through time from spring to summer to fall. We therefore reran the analysis using only the spring images (May), then using only the summer images (June to July) and finally using only the autumn images (August to September). This resulted in a much better correlation, although negative, of PC-2 loadings to FFMC in summer when theoretically the codes should work best (0.-87, Figure 32), but also better correlations in spring (-0.59, Figure 31) and fall (-0.64, Figure 33). Since the data are inversely correlated the y-2 axis of each plot has been inverted.

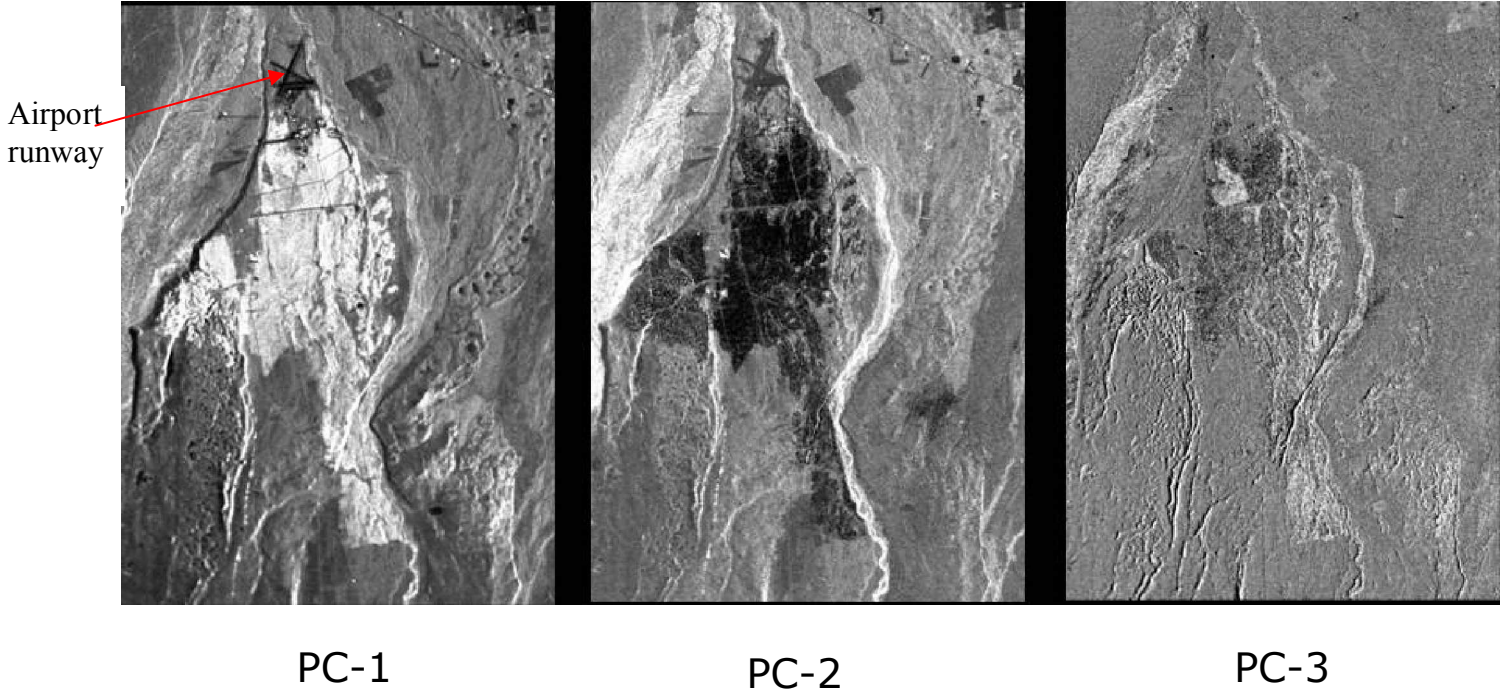
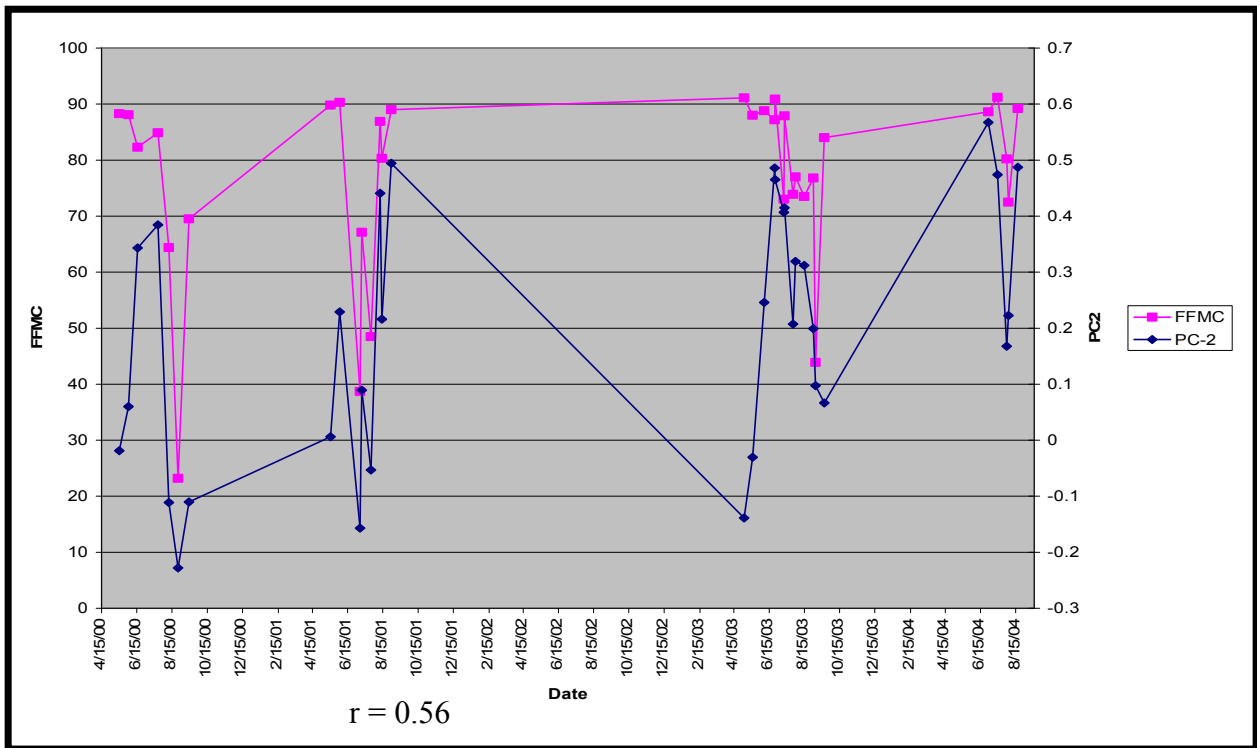


Figure 29. First three principal component images of Donnelly Flats based on 36 input summer scenes from 2000-4 ERS-2 data.



- Figure 30. Plot of FFMC and PC-2 loadings from 5/15/2000 to 9/1/2004. Note that only May to September data are displayed.

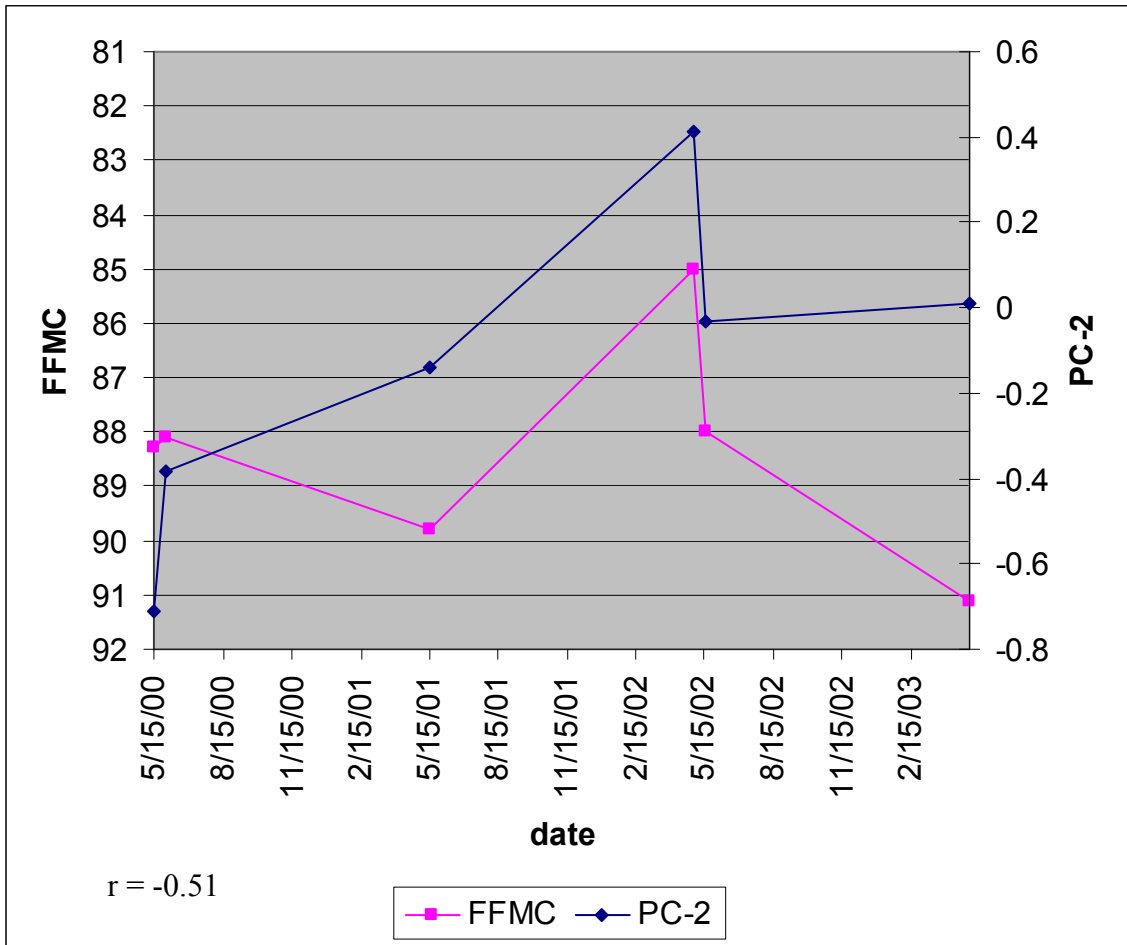


Figure 31. Plot of FFMC and PC-2 loadings from spring only (2000-4) at DF.

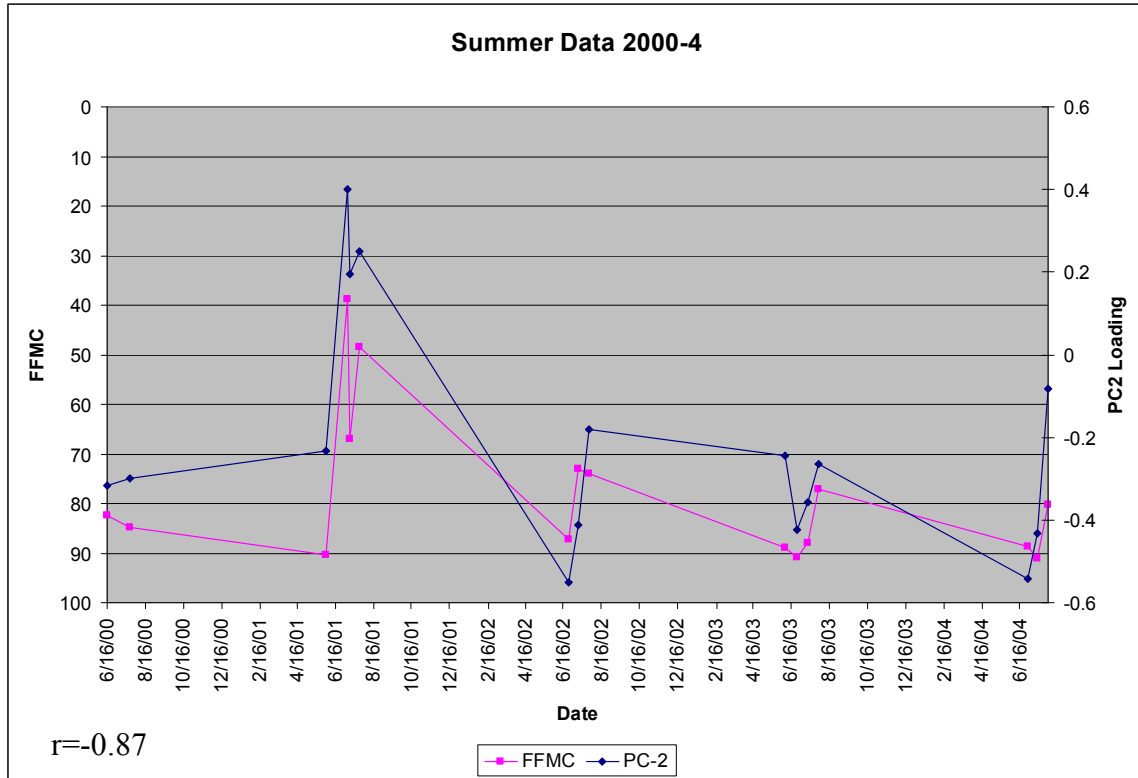


Figure 32. Plot of FFMC and PC-2 loadings from summer only (June-July 2000-4).

For the spring plot (Figure 31) we only had a few May scenes and FFMC was fairly constant through the years with a value around 80-90. A higher FFMC indicates drier conditions. More data are really needed to evaluate the relationship in spring. The fire managers of Alaska and Canada have indicated problems with initiating fire weather codes in the spring. However, the FFMC has a very short lag time, which should allow it to correct itself in a matter of a day or two. The FFMC varies much more in our summer (40 to 90) and autumn (20 to 90) analyses, however our sample sizes are also much larger during those time periods.

For the spring dataset the relationship of PC2 to DC (-0.91) is actually stronger than to FFMC ($r = -0.51$) as shown in Figure 34 (note y-2 axis is inverted). Also presented are the plots of DC vs. PC2 for summer and fall data of 2000-4 seasons at DF (Figures 35, 36). The relationship of PC2 to FFMC ($r = -0.87$) is stronger than that to DC ($r = 0.51$) in the summer. Note that this is the time when frozen ground thaw affects the DC at this Delta Junction test site. For the fall dataset the correlation is very low (0.03),

but the plot shows similar trends between DC and PC2 over time. Late in the season the DC tends to be high and not change much and this is likely affecting the correlation.

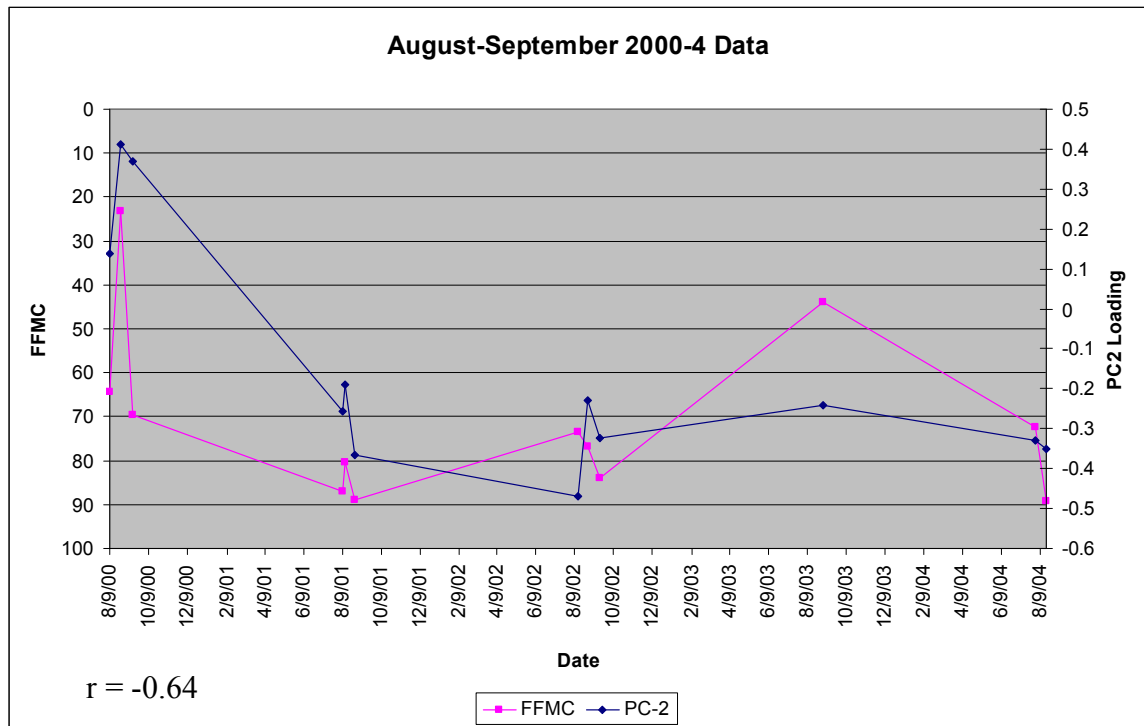


Figure 33. Plot of FFMC and PC-2 loadings from autumn only (August-September 2000-4).

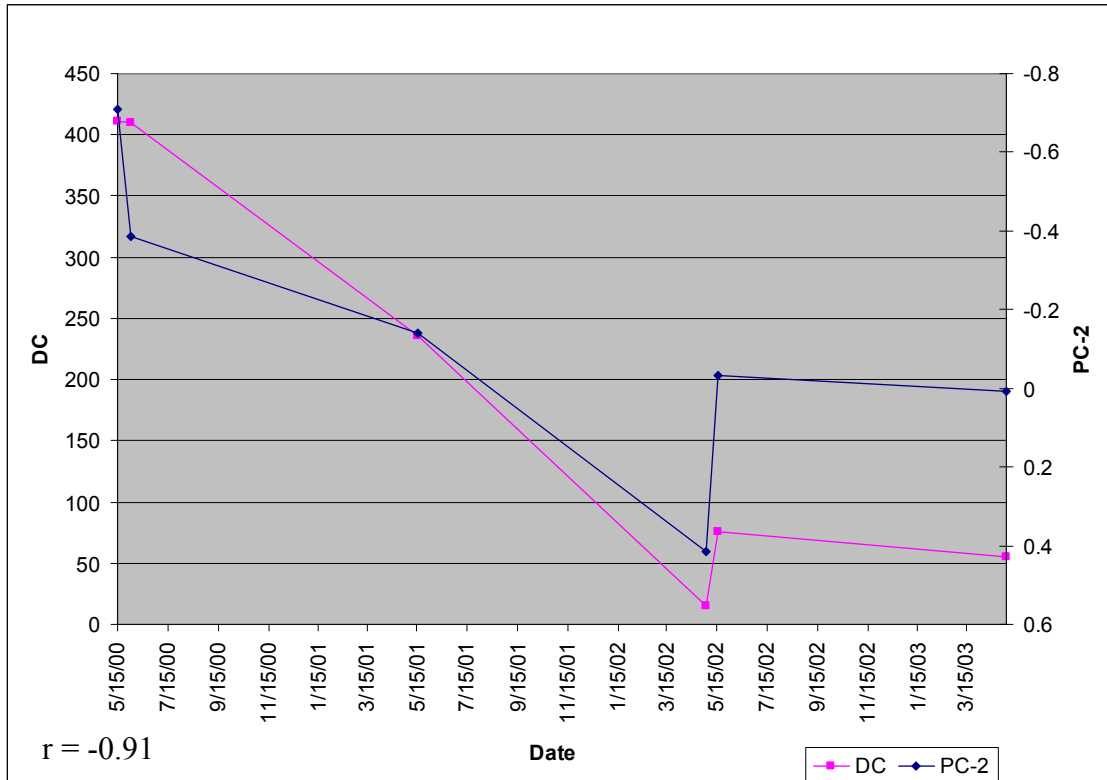


Figure 34. Plot of DC and PC-2 loadings from spring only (2000-4) at DF.

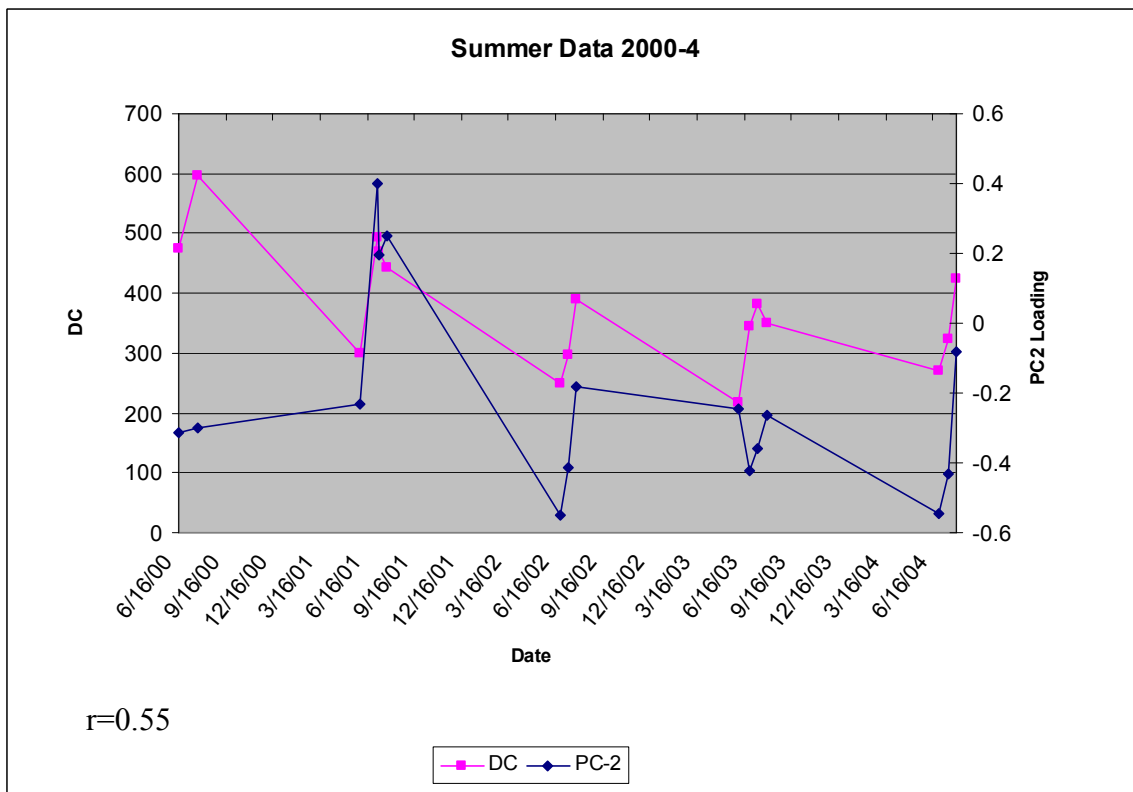


Figure 35. Plot of DC and PC-2 loadings from summer only (2000-4) at DF.

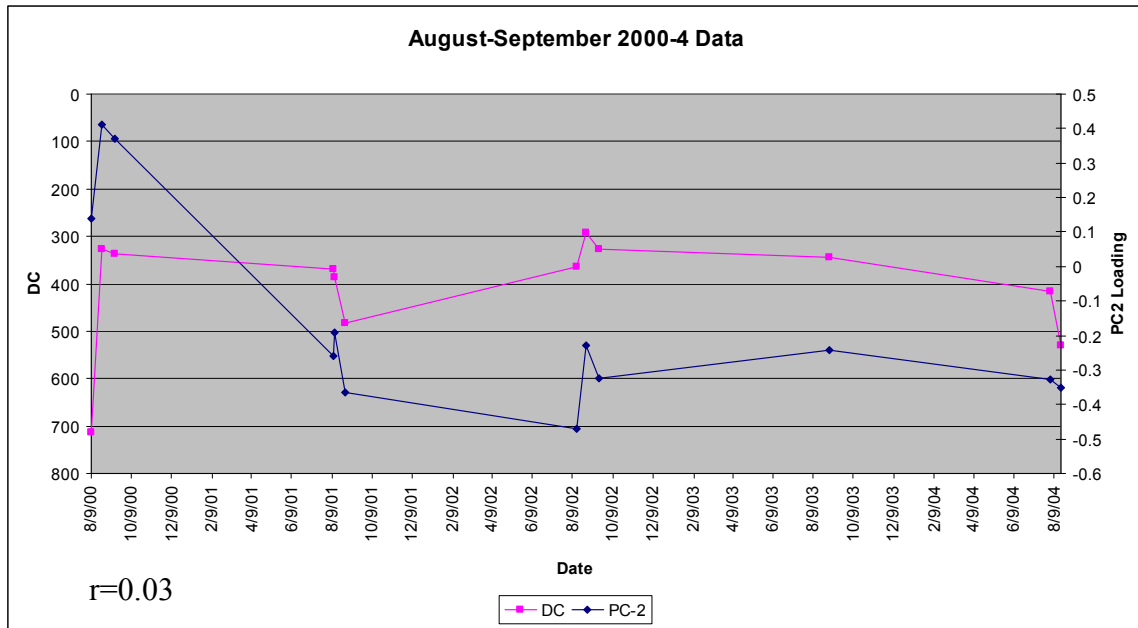


Figure 36. Plot of DC and PC-2 loadings from fall only (2000-4) at DF.

Finally, we present a direct comparison between PC-2 loadings and *in situ* soil moisture at DF (Figure 37). For this analysis we averaged all moisture values for each date across all sites within the DF study area (DF-1, 2, 3, etc). On some dates only one site was sampled while on other dates up to 8 study sites were sampled (2002). We had a total of 14 six cm sampling dates and 16 twelve cm sampling dates (only 12 cm depth were sampled in 2002). Note that there were few May and September *in situ* dates of collection, so caution must be taken in developing conclusions from this plot. This plot does show a strong correlation between *in situ* 6 cm moisture and PC-2 loadings ($r=-0.86$) for mostly summer and fall dates. This result is very encouraging, since several problems with the weather based system have been noted, and because the FWI codes are generalized, so they will not be representative of all sites within an area. Since *in situ* moisture measured directly at the DF site has strong correlations to the PC-loadings from the ERS dataset analysis, we therefore developed a regression algorithm based on these five years of data to predict surface soil moisture from PC-2 loadings (Figure 38). Using this algorithm, a new image date can be added to the dataset, PCA run, and the PC2 loading for the new date should be able to be used to predict *in situ* moisture.

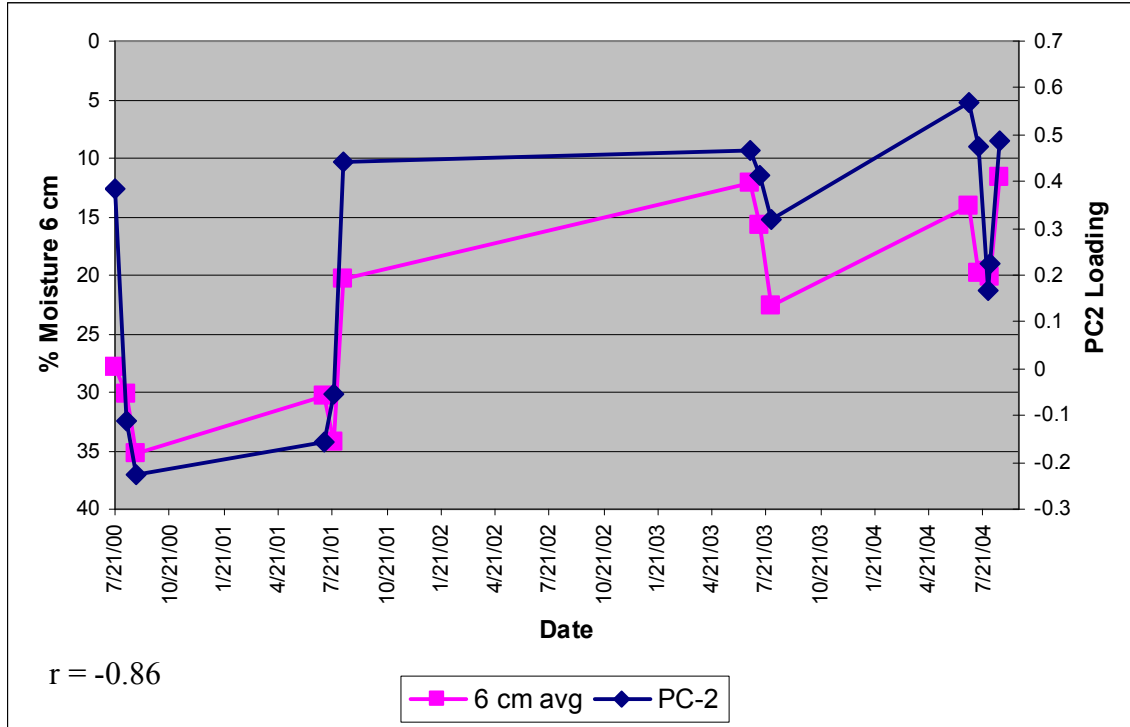


Figure 37. Plot of in situ soil moisture and PC-2 loadings from 2000-2004 field seasons at DF.

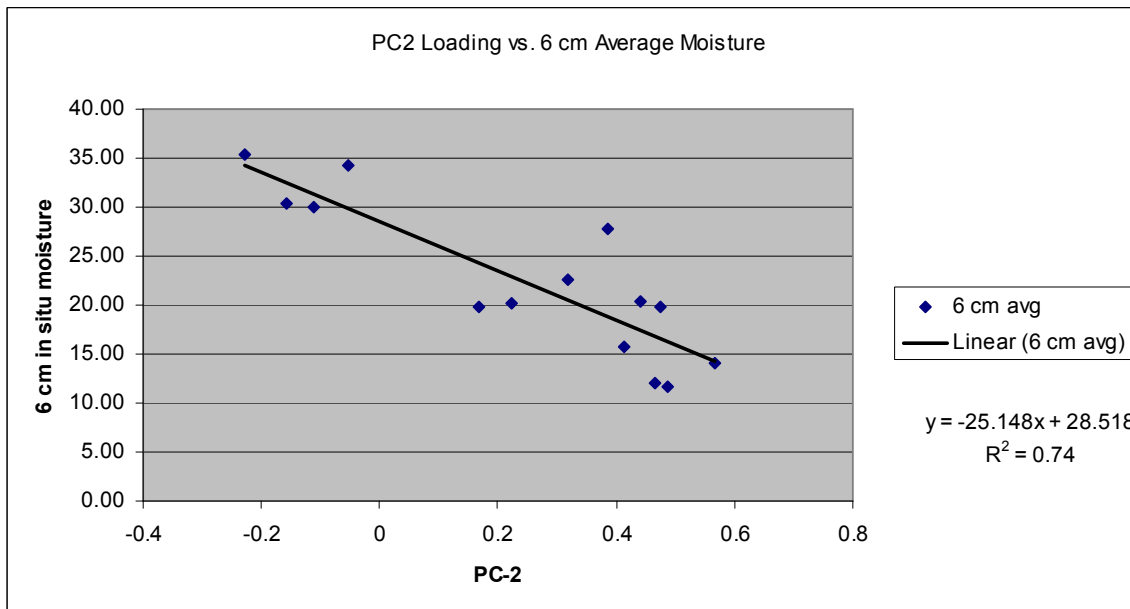


Figure 38. Prediction plot and regression for PC2 vs 6 cm in situ moisture.

9.1.1 Summary of PCA at Donnelly Burned Test Site

The *in situ* comparison to PCA (Figures 37-38) demonstrates the strong correlation of SAR to fuel moisture in burned landscapes. While analysis of *in situ* to all season ERS PC data showed this strong relationship, comparison of PC loadings to all-season FWI codes was less successful. In the latter case, analysis of the fire weather data versus PC loadings had better results when evaluated on a seasonal (i.e. spring, summer, fall) basis than observing all (2000-4) seasons over the five year period. The seasonal plots show that there are correlations between fuel moisture codes and time series analysis of ERS-2 SAR data. The problems with all-season data arise from issues with the FWI codes themselves and the fact that Delta Junction lies in a discontinuous permafrost zone.

The next steps were to evaluate unburned boreal forests, non-permafrost burned and unburned test sites (Survey Line), as well as review PCA of Radarsat data.

Table 4. List of Pearson correlations for PC loadings versus Fire Weather Codes for each single and multi-year combination. Some have no April passes, since April is often still frozen. Asc passes, means both ascending and descending passes were included in the analysis.

Year(s)	Strongest PC loading	FFMC	DC	FWI
2000	PC2	-0.61	0.32	-0.92
2001	PC3	-0.85	0.79	-0.30
2002	PC2	0.33	-0.71	
2003	PC2 &3	-0.74(-0.62)	0.82 (0.89)	-0.25
2004	PC2	-0.88	0.44	-0.78
2000-1	PC2	-0.64	0.40	-0.64
2000-2	PC2	-0.75	0.25	-0.38
2000-3	PC2	0.59		0.38
2000-4	PC2	0.56		0.40
2000-4 no april	PC2	0.56		0.37
2000-4 no april asc passes 04	PC2	0.47	.021	0.37
Spring	PC2	0.53	-0.90	-0.90
2000-4 no april asc passes 04 Spring	PC2	-0.59	-0.83	-0.92
Summer	PC2	-0.87	0.55	-0.43
2000-4 no april asc passes 04 Summer	PC2	0.81	-0.48	0.40
Fall	PC2	-0.63		-0.41
2000-4 no april asc passes 04 Fall	PC2	-0.63	.024	-0.42
2000-4	PC2	6 cm <i>in situ</i> -0.86	12 cm <i>in situ</i> -0.68	
2000-4 add 04 asc	PC2	-0.76 6 cm		

9.2 Unburned Site PCA of Delta Junction

Several unburned areas were analyzed within the Delta Junction and Survey Line SAR imagery. The unburned sites at DF and GR where *in situ* was monitored in 2005 were the focus of our initial research into PCA of unburned forests. Tables 5 and 6 show

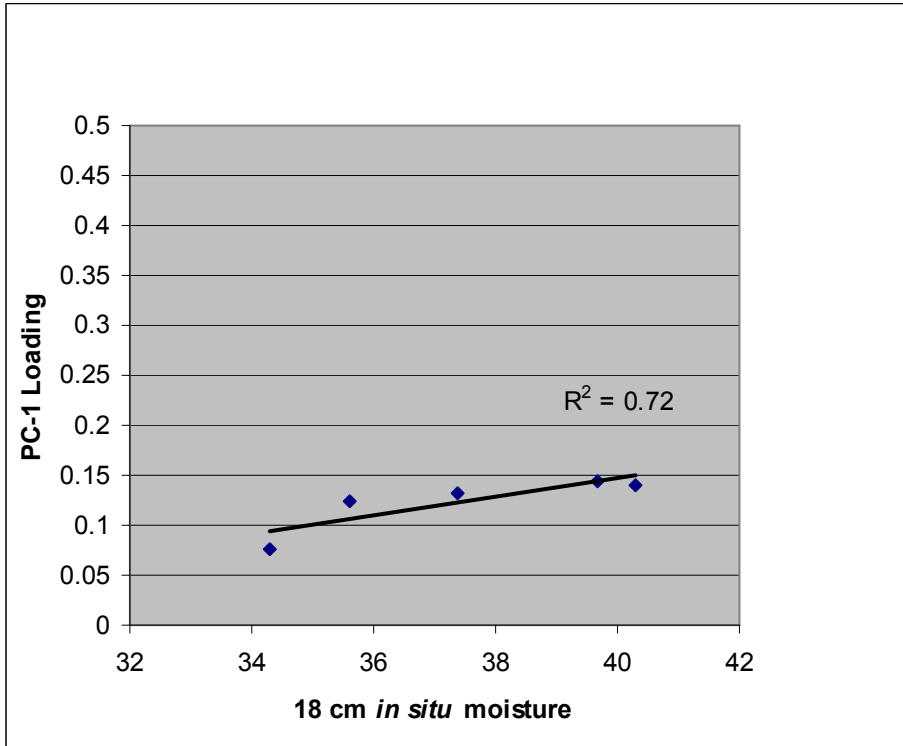
the Pearson correlations between the various FWI codes, *in situ* moisture and PC loadings. In each case the *in situ* moisture shows strong correlation to PC1 and 2, however, relationships between PC loadings and FWI codes are highly variable. Figure 39 shows plots of PC1 and 2 loadings vs. 18 cm *in situ* moisture with PC1 demonstrating the best results as far as tightness around the regression and greater coefficient of determination. In Figure 40 we plotted the same two PC loadings vs. DC, again with PC1 showing better results than PC2, but in this case second order polynomials were the best fit.

Table 5. List of Pearson correlation coefficients for the unburned site at DF 2005.

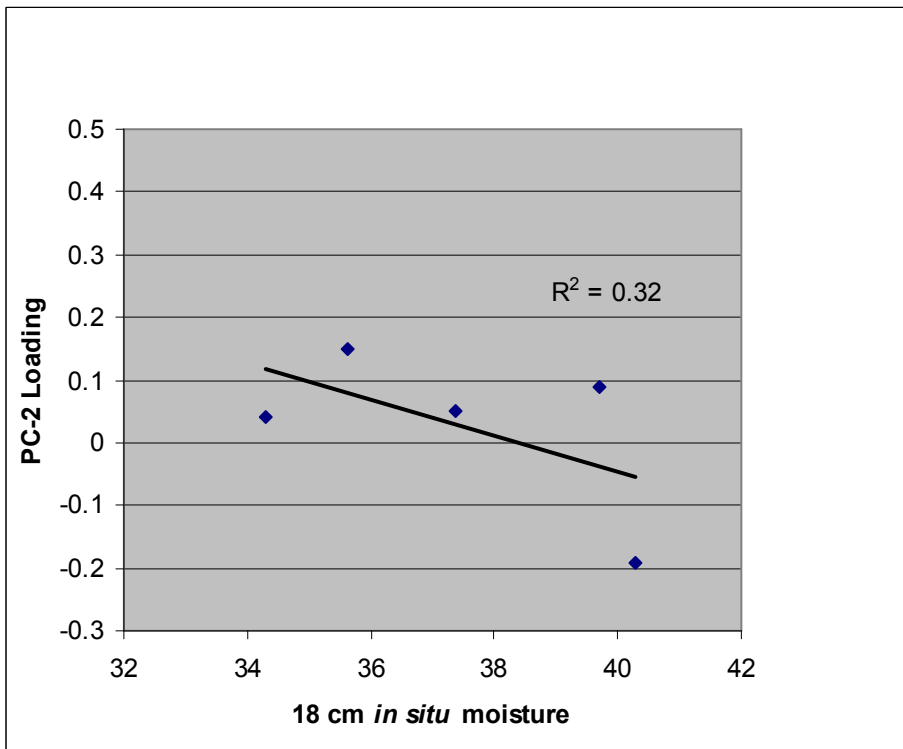
	pc1	pc2	pc3
ATF	0.30	-0.36	0.88
PREC	-0.20	0.89	-0.04
WSM	-0.32	0.42	-0.80
RHP	0.48	0.02	0.17
FFMC	-0.30	-0.26	0.21
DMC	-0.67	0.12	0.24
DC	0.03	-0.20	0.76
ISI	-0.51	0.17	-0.68
BUI	-0.50	0.04	0.49
FWI	-0.86	0.24	-0.17
dsr	-0.81	0.17	-0.18
DC	0.74	-0.46	-0.01
10 cm	0.96	-0.80	-0.45
18 cm	0.91	-0.70	-0.30
30 cm	0.85	-0.62	-0.20

Table 6. List of Pearson correlation coefficients for the unburned site at GR 2005

	pc1	pc2	pc3
DAY	-0.68	-0.60	0.81
ATF	-0.54	-0.63	0.43
PREC	-0.01	0.10	-0.10
WSM	0.73	0.77	-0.57
RHP	-0.47	-0.42	0.48
FFMC	0.04	-0.09	-0.06
DMC	-0.13	0.19	0.23
DC	-0.72	-0.54	0.78
ISI	0.59	0.46	-0.61
BUI	-0.38	-0.07	0.46
FWI	0.26	0.28	-0.27
dsr	0.34	0.37	-0.38
10 cm	0.80	-0.63	-0.24
18 cm	0.85	-0.57	-0.28
30 cm	0.85	-0.50	-0.36

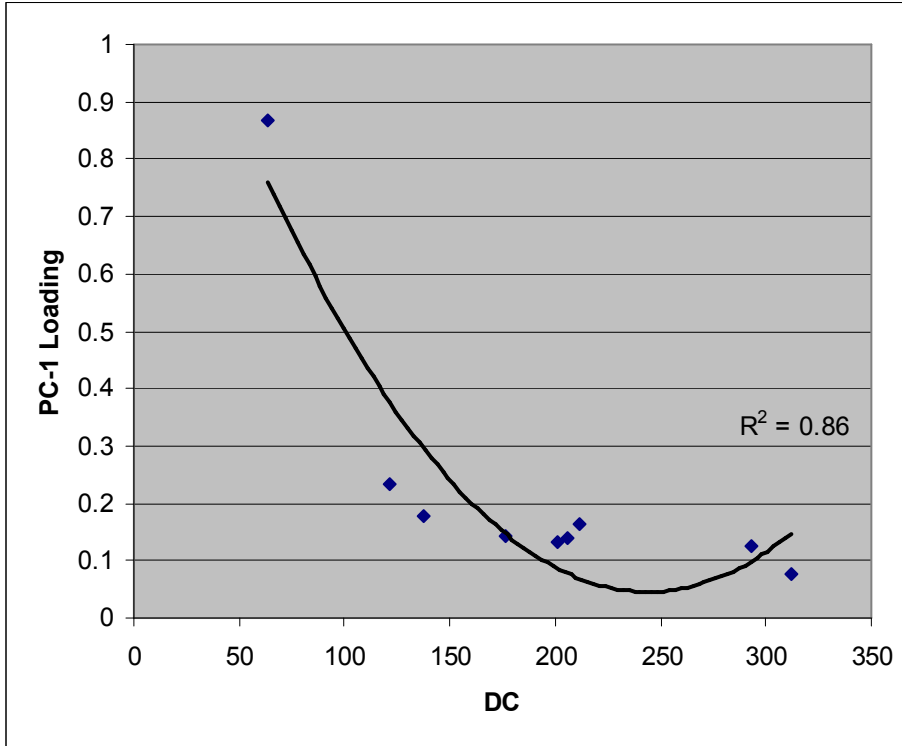


A

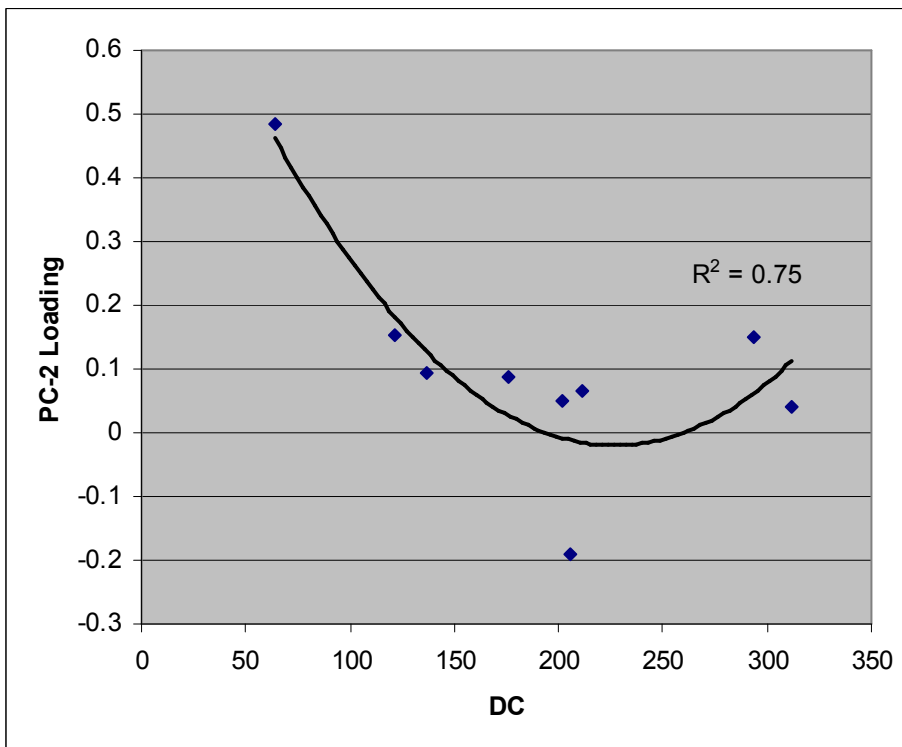


B

Figure 39. Plots of A) PC1 loading vs. 18 cm in situ moisture; and B) PC2 loading vs. 18 cm in situ moisture.



A



B

Figure 40. Plots of A) PC1 loading vs. DC; and B) PC2 loading vs. DC with polynomial fits.

9.3 Principal Component Analysis at Survey Line Burn, Alaska

In order to demonstrate the repeatability of earlier research with PCA at the Donnelly Flats burned study site, we turned to the Survey Line burn and adjacent unburned areas for investigation. Initial analysis of Survey Line Burn data resulted in good agreement between DC and ERS backscatter, based on 2003-4 data. In this report we added 2005 data to the earlier analysis and found 2005 to be consistent with the previous years' data (Figure 41). In addition, unlike the Delta Junction sites, a divergence of the data post-July was not seen in any of the years at Survey Line (see pink points of Figure 41). This would indicate that this site is likely unaffected by permafrost and resulting problems with DC.

2005 Survey Line was chosen because of the continuous *in situ* moisture monitoring conducted that summer, thus *in situ* could be used in lieu of problems with the FWI codes. However, the analysis of *in situ* backscatter vs. FWI shows that there do not appear to be problems with the DC late summer at this site (non- permafrost site). Therefore, the FWI were used in the post-analysis of the PCA loadings. A time series of 10 input ERS images were used for this analysis (Figure 42). The images were subsetted to include continuous areas in and around the 2002 Survey Line Burn. The area was adjusted to maximize the coverage on all 10 dates. Note that the burned boundary is not as clear for this particular fire as most are (see figure 1), but the PCA works just as well at this site as it does in more clearly defined burn scars.

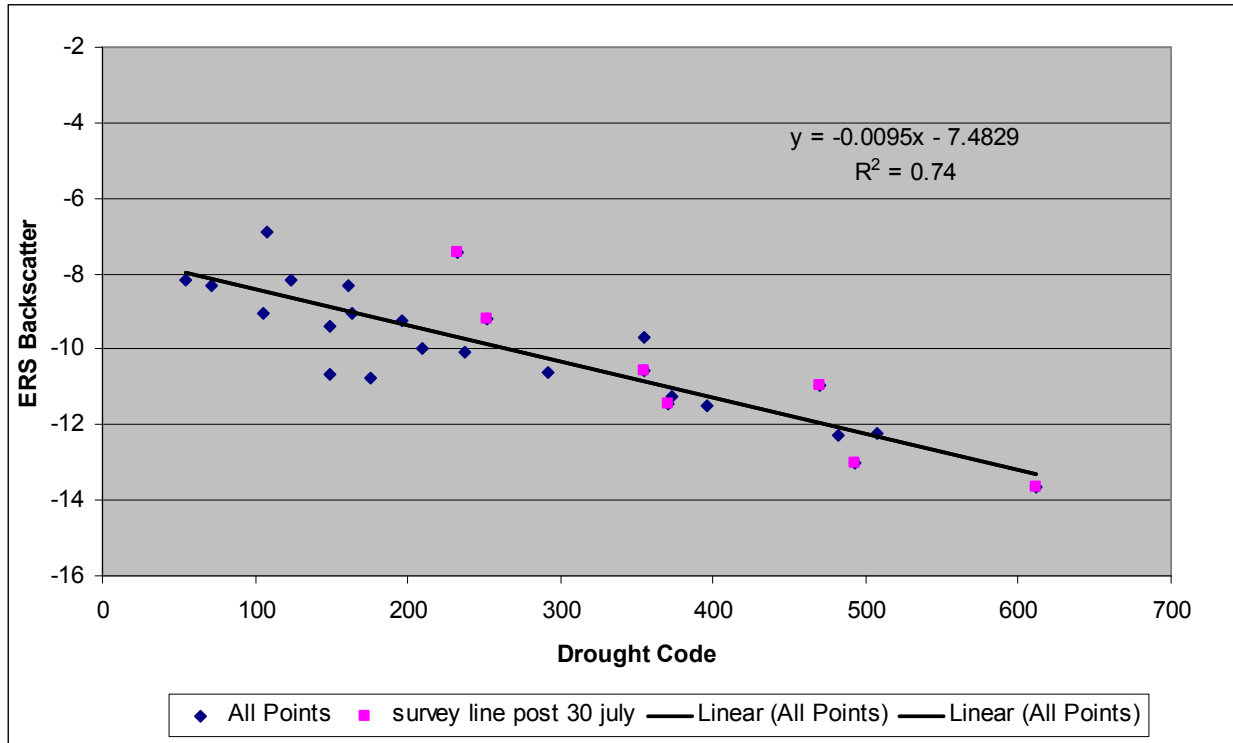


Figure 41. Plot of 2003-5 burn backscatter from the Survey Line 2002 fire versus ERS-2 backscatter. Data from post 30-July are highlighted as “pink” points.

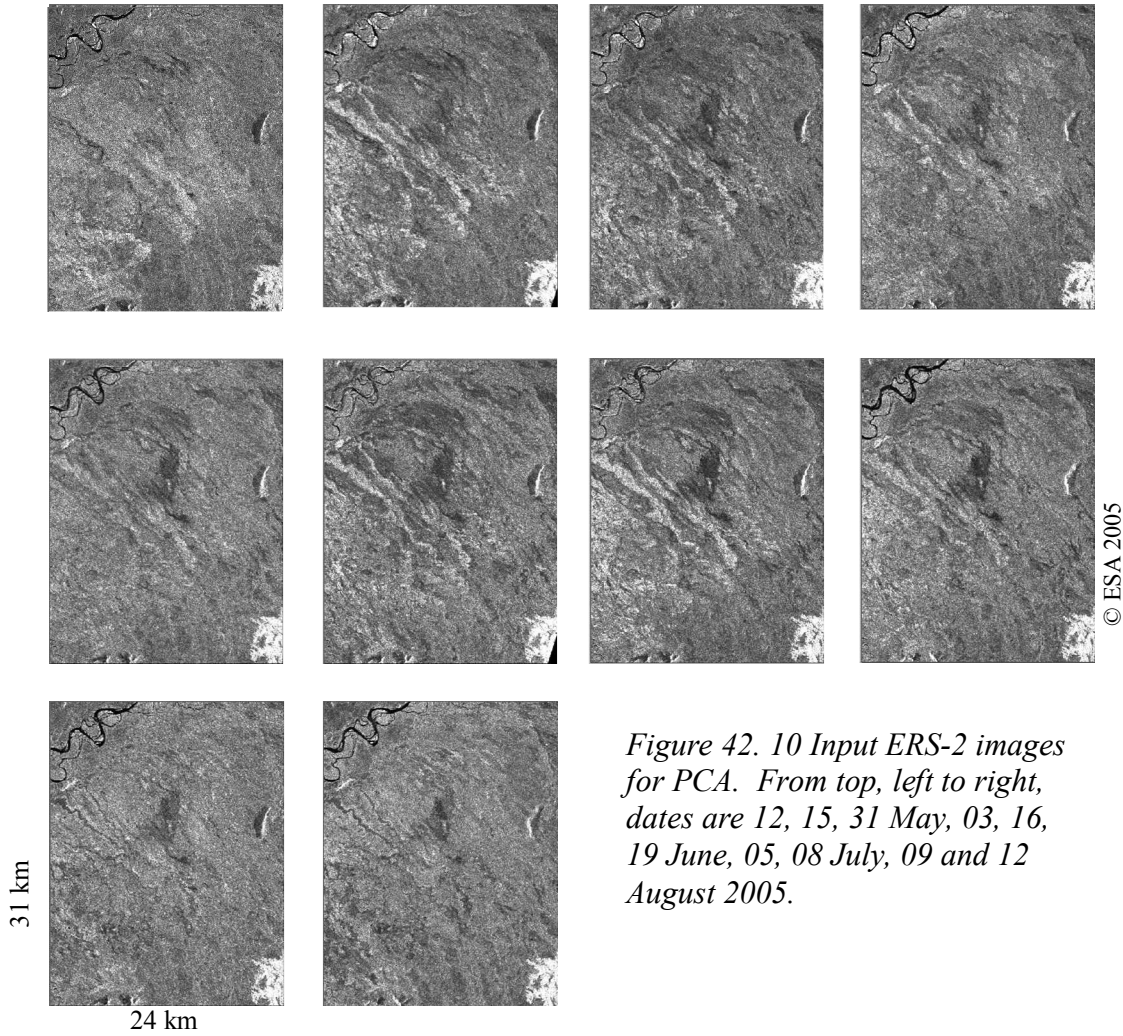


Figure 42. 10 Input ERS-2 images for PCA. From top, left to right, dates are 12, 15, 31 May, 03, 16, 19 June, 05, 08 July, 09 and 12 August 2005.

An analysis of the PC2 loadings for the Survey Line data versus DC from corresponding dates (Figure 43) shows an inverse relationship between the two variables by date (plotted with Y-2 axis inverted). Regression analysis shows a coefficient of determination of 0.85 for these variables, indicating that one may be used as a predictor of the other.

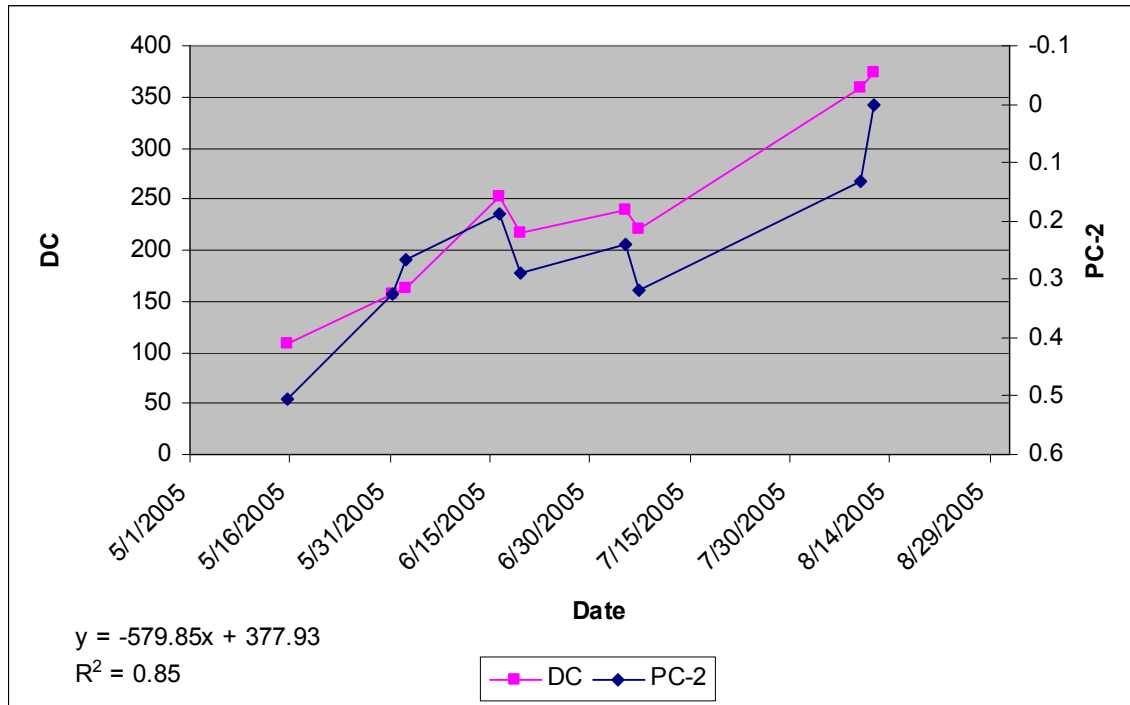
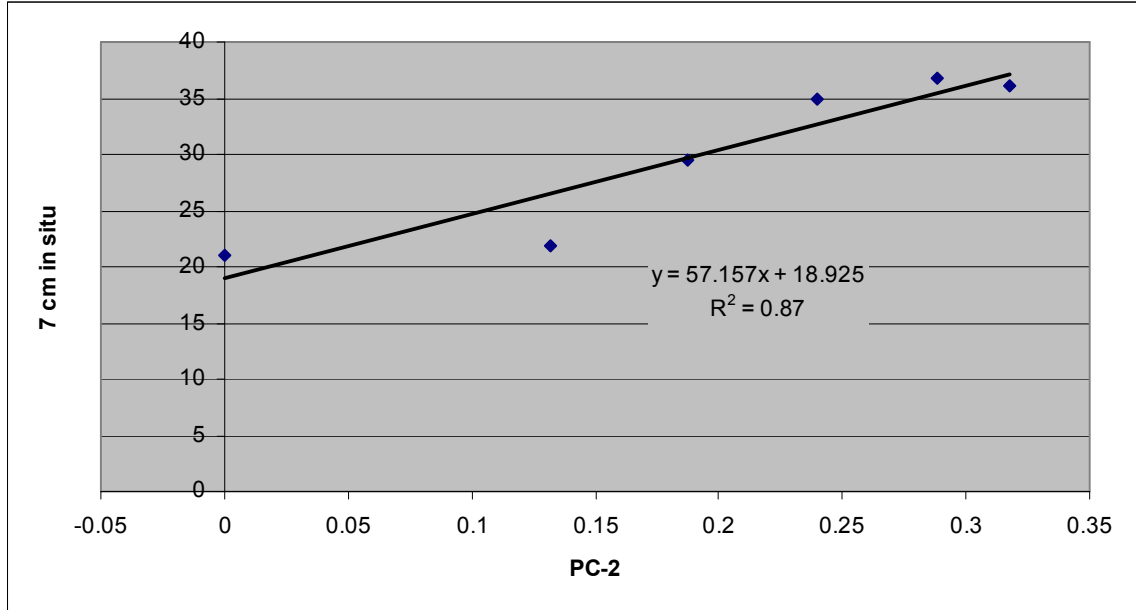


Figure 43. Plot of PC-2 loadings for summer 2005 and Drought Code (DC) from corresponding dates for the Survey Line Burn. Note that PC2 has been inverted on this plot.

Since this site is unaffected by mid-summer thaw, the relationship between backscatter and DC is clear in this case. The algorithm for PC analysis should be developed in areas unaffected by mid-summer thaw and then applied to the permafrost test sites. A direct comparison of PC2 to *in situ* moisture measured to a depth of 7 cm reveals a strong linear relationship which is the inverse of that of PC2 vs. DC (Figure 44). Higher DC values correspond to increased drying.

A



B

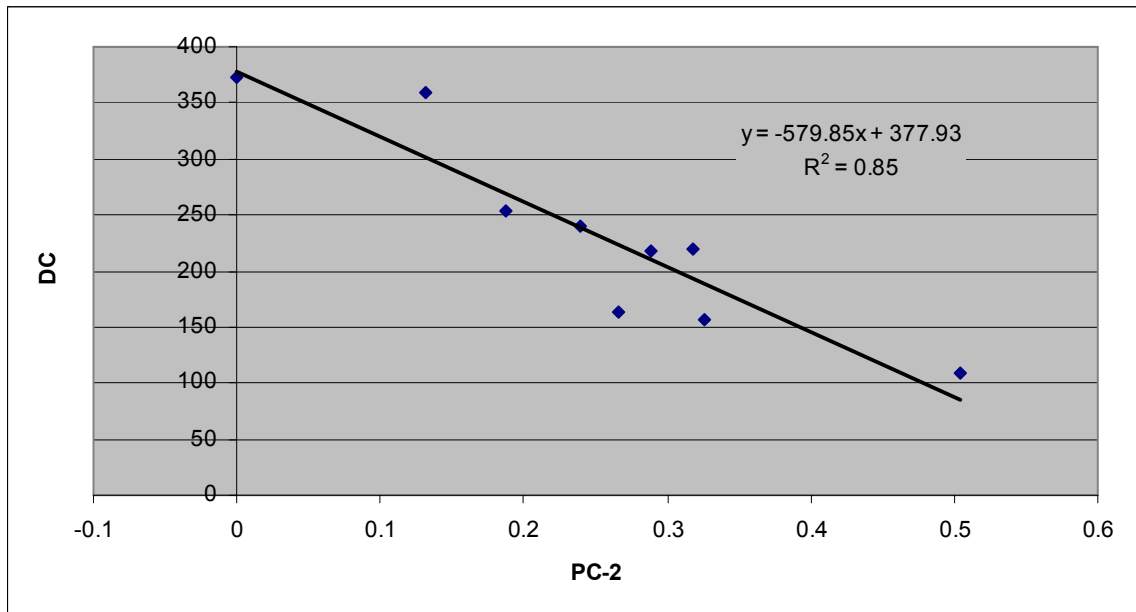


Figure 44. A) plot of PC2 vs 7 cm depth in situ moisture; and B) PC2 vs. DC.

9.3.1 Summary of PCA Results at Survey Line Burned Site

The results of the PC analysis at Survey Line burned site shows even more promising results than those of Delta Junction (DF) because both the FWI code, DC, and *in situ* moisture show strong relationships to PC loadings. The next step would be to

observe multi-year PCA at Survey Line and similar non-permafrost sites. These are the types of sites where the PCA methods and procedures should be developed since the problems with FWI codes are minimized, and then application to permafrost sites can be conducted.

9.4 Principal Component Analysis (PCA) with Radarsat Imagery over Delta Junction

An initial Radarsat PCA was conducted with the 2003 to 2004 data collected over Delta Junction. The data were separated into ascending and descending layer stacks, since the time of collection (8 am versus 8 pm local time) seems to have an affect on the backscatter (Bourgeau-Chavez *et al.* 2001, Abbott *et al.* 2006). Problems with consistent data acquisition and the need to separate ascending from descending passes delayed this analysis. By combining years 2003 and 2004 we now have enough data to run a PCA.

The results of the PCA were compared to Fine Fuel Moisture Code (FFMC), Duff Moisture Code (DMC), and Drought Code (DC) calculated at the Fort Greely (just north of Donnelly Flats) weather station for the days of interest.

The initial comparison suggests that a first order correlation exists between the second resultant of the PCA (the second PC-loading) and the FFMC (figure 45) or DC (figures 46&47). DC has an inverse relationship with PC-2 in the Gerstle River (figure 46) case while FFMC has a positive linear relationship (Figure 45). A regression of PC2 loading vs. DC for Radarsat had a coefficient of determination of 0.70 (Figure 47). No relationships were found between DMC and PC-loadings.

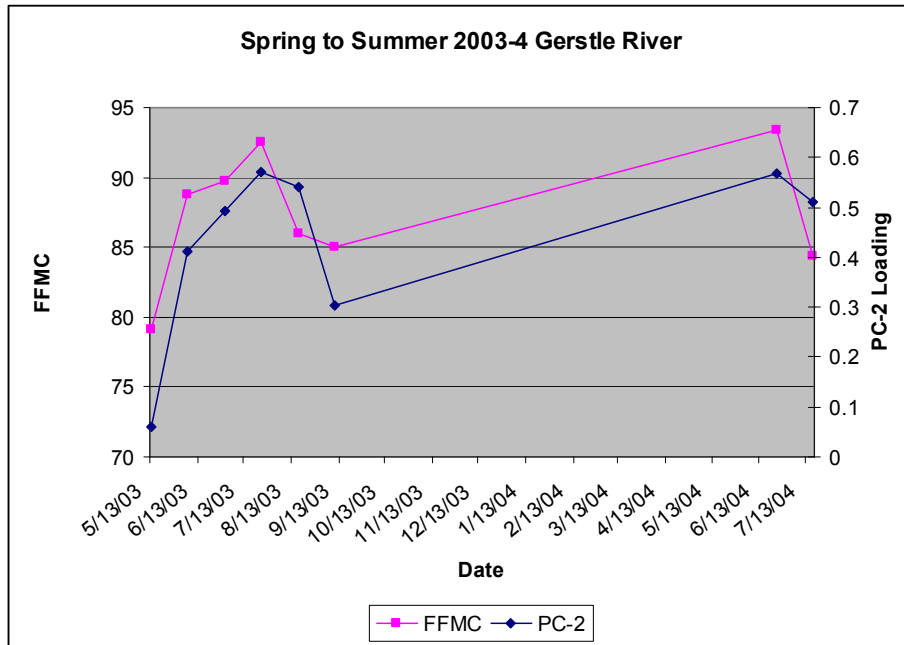


Figure 45. Plot of PC-2 loading versus FFMC for Radarsat ascending PCA spring to late summer 2003-4 data of Gerstle River. Coefficient of determination = 0.65 on a simple linear regression.

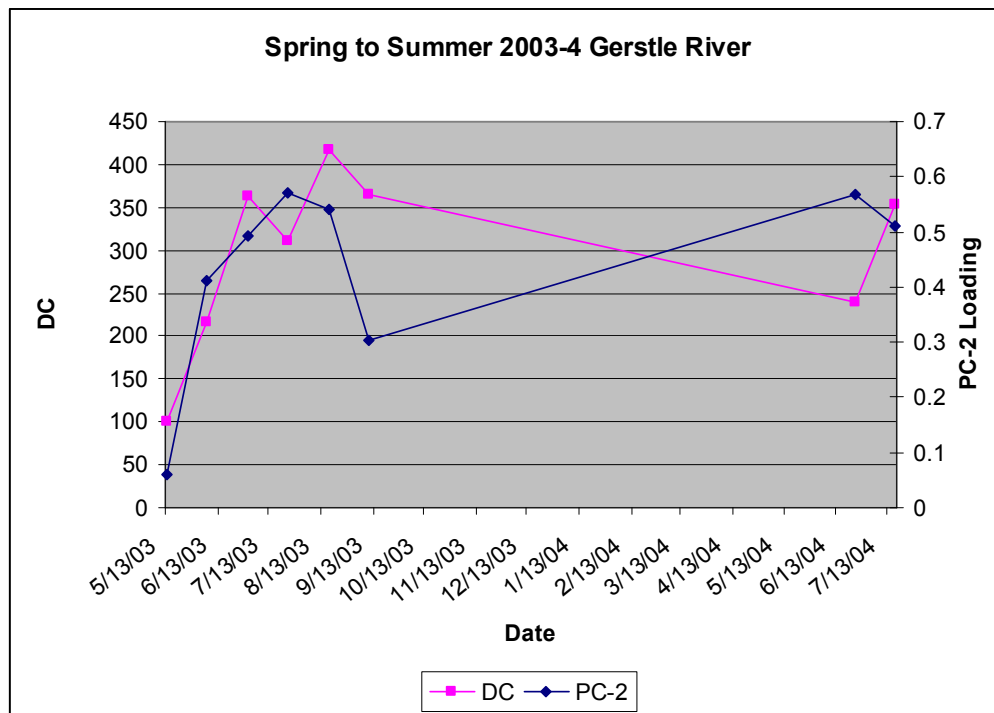


Figure 46. Plot of PC-2 loading versus DC for Radarsat ascending PCA spring to late summer 2003-4 data of Gerstle River. Coefficient of determination = 0.55 on a simple linear regression.

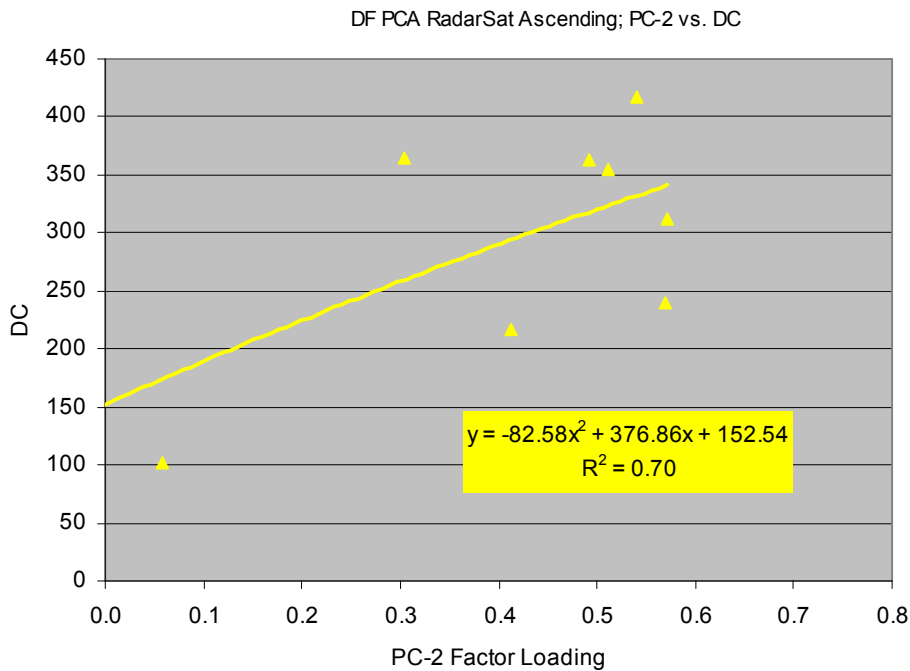


Figure 47. Plot of PC-2 loading versus DC for Radarsat ascending PCA spring to summer 2003-4 data of Donnelly Flats.

It should be noted that since the ascending and descending modes for Radarsat were compared separately, the number of data points for the descending PCA was limited and is therefore not presented. Further images need to be examined in order to verify the initial results. However, this initial analysis shows that C-HH data at a steep incidence angle (standard beam 1) are useful for fuel moisture monitoring.

9.5 PCA of Unburned Sites at Survey Line

Using the SAR data set presented in Figure 42 but from areas of the images that were unburned, we evaluated the utility of PCA in unburned non-permafrost forests. Previous analysis at Delta Junction had shown promising results (section 9.2). Analyses of two large unburned areas and the small area (200 x 200 m) of *in situ* measurements were conducted. For the unburned sites the relationships of PC2 to *in situ* were consistently high (Tables 7 , 8 and 9), however, the relationships to FWI codes were highly variable. Note that the Pearson correlation becomes slightly stronger as the moisture measurement depth increases at these sites (0.73 to 0.79 to 0.82 from 10, 18 and 30 cm depths, respectively for unburn area-1). This is in contrast to the burned site where

the shallowest depth had the strongest correlation (0.93) with PC-2 and the increasing depths had low correlations (0.39, 0.27). This pattern was not seen at Delta Junction, and likely has much to do with site conditions.

Table 7. Large Unburn Area-1 of Survey Line Region

	<i>pc1</i>	<i>pc2</i>	<i>pc3</i>
ATF	-0.58	-0.74	-0.04
PREC	0.01	0.29	0.45
WSM	-0.03	0.24	0.84
RHP	0.62	0.66	0.07
FFMC	-0.39	-0.64	-0.35
DMC	0.12	-0.28	-0.78
DC	-0.46	-0.36	0.37
ISI	-0.39	-0.80	-0.47
BUI	-0.10	-0.38	-0.57
FWI	-0.37	-0.76	-0.48
DSR	-0.32	-0.78	-0.51
10 cm	0.54	0.73	0.69
18 cm	0.60	0.79	0.68
30 cm	0.63	0.82	0.69

Table 8. Large Unburn Area-2 of Survey Line Region

	<i>pc1</i>	<i>pc2</i>	<i>pc3</i>
ATF	0.18	-0.44	0.21
PREC	0.37	0.52	-0.25
WSM	0.28	0.23	0.28
RHP	-0.01	0.26	0.05
FFMC	-0.18	-0.56	0.19
DMC	-0.23	-0.37	0.03
DC	0.39	-0.48	0.39
ISI	0.06	-0.50	-0.02
BUI	-0.03	-0.48	0.18
FWI	0.08	-0.54	0.06
DSR	0.19	-0.56	0.01
10 cm	0.12	0.76	-0.20
18 cm	0.10	0.83	-0.06
30 cm	0.09	0.85	-0.05

Table 9. Small Unburn Area of Survey Line Region

	<i>pc1</i>	<i>pc2</i>	<i>pc3</i>
DAY	0.41	-0.46	-0.35
ATF	0.05	-0.46	-0.51
PREC	0.28	-0.02	0.04
WSM	0.62	-0.22	-0.06
RHP	0.18	0.01	0.58
FFMC	-0.10	-0.27	-0.36
DMC	-0.39	-0.07	0.09
DC	0.29	-0.44	-0.36
ISI	-0.06	-0.47	-0.40
BUI	-0.34	-0.16	-0.09
FWI	-0.10	-0.46	-0.37
DSR	-0.07	-0.45	-0.34
10 cm	0.18	0.83	0.78
18 cm	0.05	0.90	0.80
30 cm	0.02	0.90	0.80

Figure 48 shows the relationship of each measured moisture depth (moisture probes were inserted from the surface down to the various depths) to PC2 loadings. At this site there are strong correlations to each depth, but there are also strong correlations between depths. In contrast to this, at unburned site DF2, moisture measured at 10 and 18 cm had similar patterns but 30 cm moisture was as dry or drier than the 10 cm surface. While at unburned GR site, GMS, a similar pattern was observed in the first two depths with the 30 cm moisture being much wetter and of a different seasonal moisture pattern. Thus, it is highly site dependent.

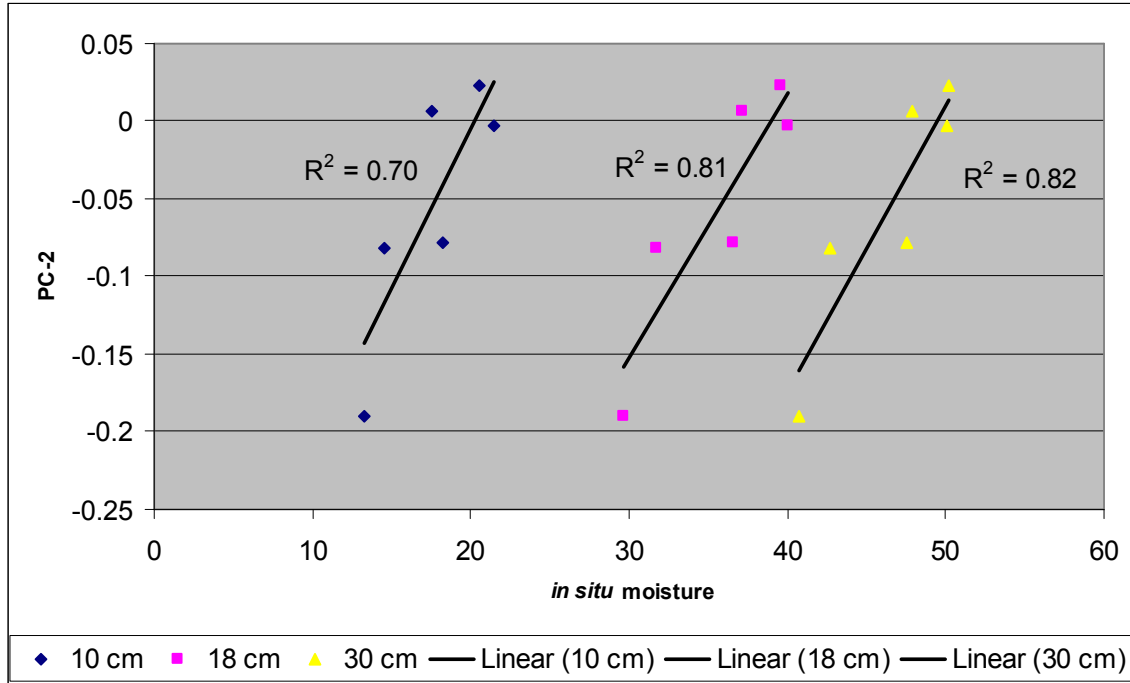


Figure 48. Small unburned area PC-2 loading versus in situ at various depths for SLU.

9.6 In Situ Versus FWI Codes at Unburned Sites

A comparison of continuous *in situ* moisture measured at 4 test sites over the 2005 growing season was made to FWI codes from neighboring weather stations at each site (Table 9) to determine if the *in situ* measurements that we collected were in fact related to the FWI codes. The sites GMS, DF2, and SLU are unburned sites while SLB was burned in 2002. The Pearson correlation coefficients (*r*) show that the *in situ* measurements are consistently strongly related to DMC and/or DC, depending on the site and depth of measurement. Also of strong correlation is the BUI variable which is a combination of DC and DMC. Thus the *in situ* measurements are capturing the fuel moisture variability at these sites. The correlations of Table 9 represent a sample size of about 80 dates per site, whereas the PCA represented a sample size of 6-8 dates per site. However, correlations from the smaller sample size PCA also show $r = 0.90$ or greater correlations between DC and all *in situ* moisture sample depths.

Table 9. Pearson correlation coefficients for four test sites sampled in 2005 using continuous monitoring soil moisture stations at three depths versus FWI codes. GMS is a Gerstle River Unburned site, DF2 is an unburned site near Donnelly Flats, SLU is a Survey Line unburned site and SLB is the sampling for the burned Survey Line site.

GMS	10 cm	18 cm	30 cm
FFMC	-0.42	-0.35	-0.11
DMC	-0.77	-0.78	-0.36
DC	-0.59	-0.52	-0.60
ISI	-0.31	-0.28	-0.16
BUI	-0.81	-0.79	-0.44
FWI	-0.44	-0.40	-0.19
SLU	10 cm	18 cm	30 cm
FFMC	-0.32	-0.25	-0.25
DMC	-0.94	-0.94	-0.94
DC	-0.93	-0.94	-0.95
ISI	-0.17	-0.09	-0.08
BUI	-0.95	-0.95	-0.95
FWI	-0.53	-0.47	-0.46
DF2	10 cm	18 cm	30 cm
FFMC	-0.33	-0.30	-0.32
DMC	-0.63	-0.56	-0.56
DC	-0.95	-0.98	-0.96
ISI	-0.28	-0.23	-0.22
BUI	-0.74	-0.67	-0.66
FWI	-0.36	-0.30	-0.30
SLB	7 cm	10 cm	18 cm
FFMC	-0.53	-0.20	-0.16
DMC	-0.76	-0.64	-0.50
DC	-0.71	-0.65	-0.52
ISI	-0.42	-0.17	-0.15
BUI	-0.77	-0.64	-0.50
FWI	-0.62	-0.38	-0.31

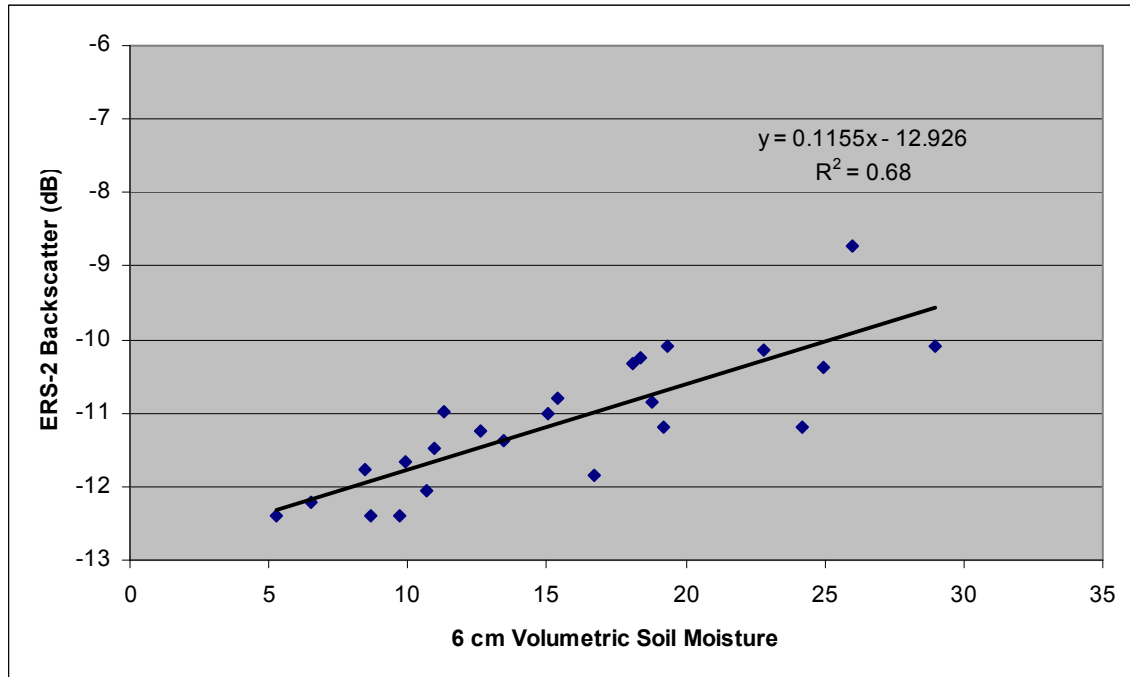


Figure 48.25 Plot of ERS-2 SAR backscatter versus 6 cm Percent Volumetric Soil Moisture from the Aspen test sites of Anderson and Delta Junction.

9.7 Modeling of Soil Moisture in Unburned Alaskan Forests

The relationships between SAR backscatter and moisture measured in the open (*Populus tremuloides*) test sites (GUA and AUA) is quite good (figure 48.25). These sites have soils with greater bulk densities and likely less microwave penetration than the airy moss covered spruce sites. A simple linear regression fits these data well with a coefficient of determination of 0.68.

The results from the spruce test sites were not as straight forward (figure 48.5). The spruce sites need to be evaluated on a per site basis. Only then do patterns of increasing backscatter with increasing ground moisture become apparent. Although our sample sizes are quite small when the sites are evaluated on an individual basis and the dynamic range for the forested sites is also small, our examples in figure 48.5 show that for the DF2 2004 dataset there is a strong linear relationship between moisture measured at that site and ERS-2 backscatter (0.75 R^2). This is also the case for GWS 2004 (0.78 R^2). The two Anderson unburned spruce sites (AUS-1 & 2) were evaluated together with a 0.33 coefficient of determination, and the GMS 2004 test site seems to fall within the

pattern of the AUS sites. When observed individually, AUS-1 has a coefficient of determination of 0.73 and AUS-2 of 0.44, while GWS2004 is 0.50. Of the two DF2 2003 measurements, only one falls near our trend line.

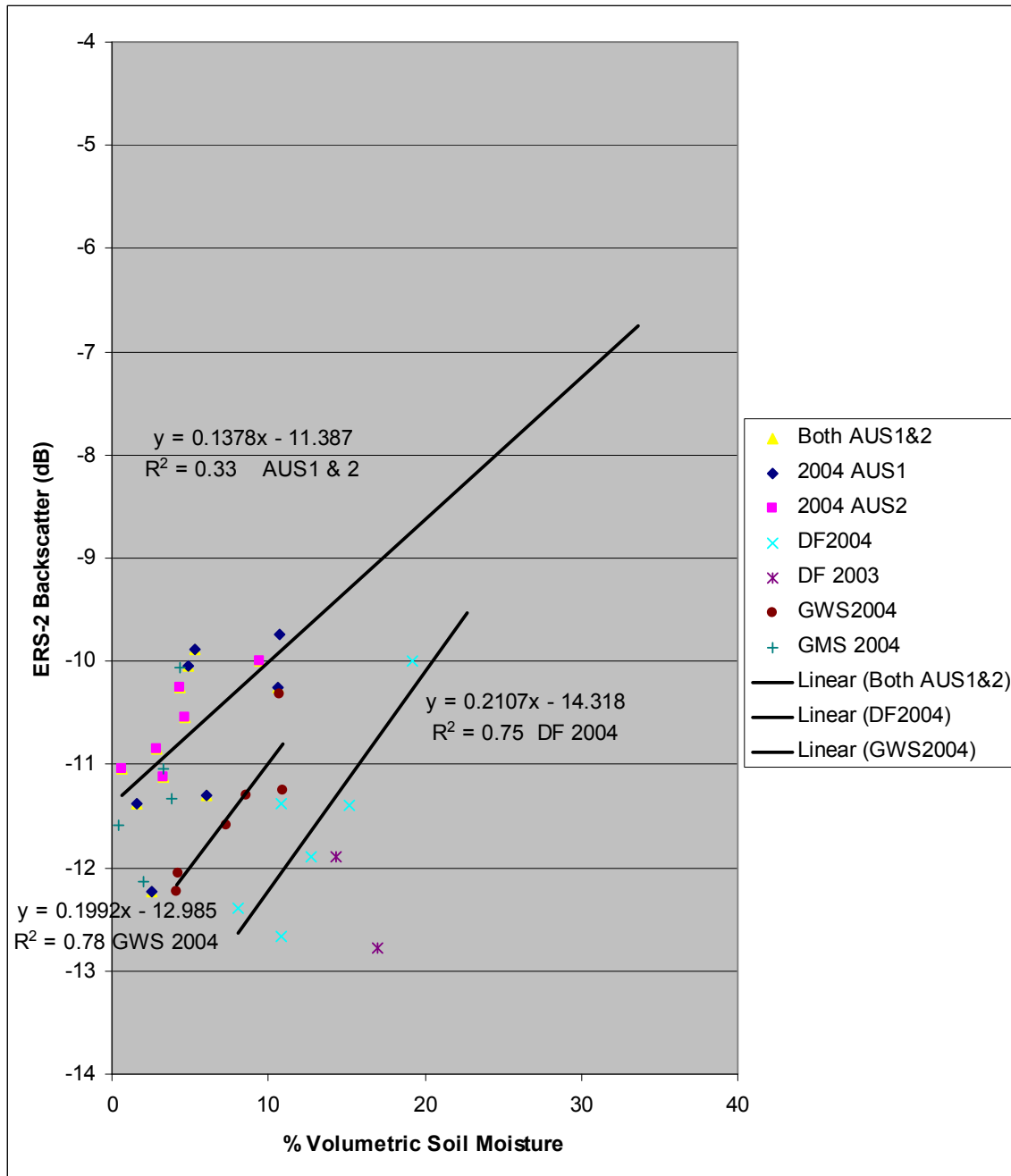


Figure 48.5. Plot of 6 cm volumetric soil moisture from the unburned spruce test sites versus ERS-2 backscatter. Rain dates were removed.

The moisture data collected at Delta and Survey Line Alaska in the summer 2005 were compared to coincident SAR backscatter for analysis of relationships at different soil depths, down to 30 cm. Unfortunately, the low range of soil moisture and coincident backscatter left the results for individual sites DF2 and GMS inconclusive. This is in contrast to the Survey Line unburned analysis, which showed backscatter to increase with soil moisture measured at all three depths, 10 cm, 18 cm and 30 cm. The strongest coefficient of determination was with the 30 cm moisture and ERS backscatter at Survey Line. When data from all three sites were combined, a relationship was found between 30 cm vertical soil moisture and ERS-2 backscatter (figure 48.75). If this relationship holds for additional data and test sites, such information could be used for a variety of ecological and hydrological applications.

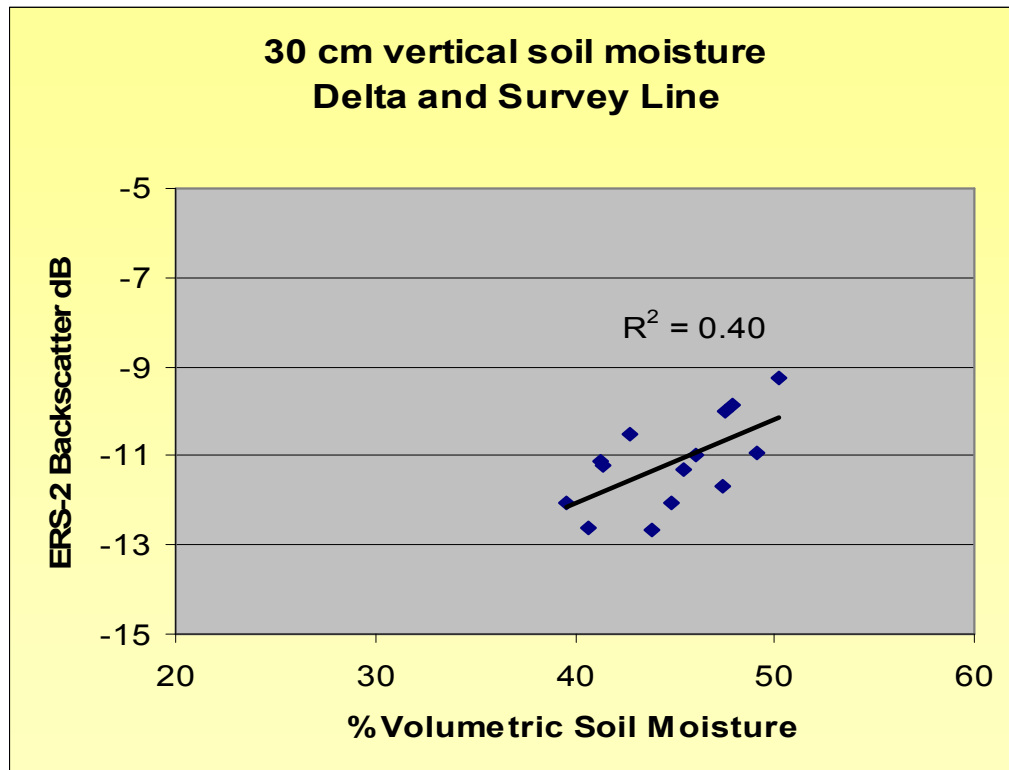


Figure 48.75. Plot of 30 cm soil moisture data sampled with the CS-625 water content reflectometers in the DF-2, GMS and Survey Line Unburned test sites in 2005. Data are from June to August.

9.7.1 Summary of Unburned Site PCA Results

At both the Delta and Survey Line unburned sites, a clear relationship between PC-loadings and *in situ* moisture in the top 10 to 30 cm is apparent. However, the facts that: A) our *in situ* measurements at 10, 18 and 30 cm depths were strongly correlated to DMC and DC; B) our *in situ* measurements were strongly correlated to PCA loadings; but C) our *in situ* measurements were sometimes strongly correlated to direct backscatter at unburned black spruce sites and sometimes not; and D) the PCA to DC or DMC were not well correlated, indicates that the C-band SAR wavelength may not be penetrating deep enough into these unburned black spruce moss forests with dense organic layers on the surface. Unburned sites are much more complex for radar scattering than the burned sites. Not only the effects of biomass but the greater degree of variability in surface soil densities and depths of horizons at different unburned sites are likely affecting backscatter results. It may be that a longer wavelength, such as L-band, would be better suited to fuel moisture retrieval at the unburned sites. The longer wavelength will be less influenced by the forest biomass of boreal Alaska, and will be able to penetrate deeper into the surface soil which may be needed to relate backscatter to the DC, which is representative of the lower duff layer. This layer is typically near the surface in burned forests making C-band (5.7 cm) a viable wavelength in that case. When one considers the fact that even a direct comparison between backscatter and *in situ* soil moisture at higher biomass but non-moss covered aspen test sites showed good results (figure 48.25) while black spruce feather moss site results were highly variable (figure 48.5), it is a likely conclusion that the feathermoss is what is confounding the analysis of unburned black spruce forests.

While more research is needed in this area, the results thus far, non-the-less, demonstrate that C-band data *can* be used with PC analyses to retrieve surface soil moisture information at *both* burned and unburned test sites. Although soil moisture extraction directly from SAR backscatter, even within a particular unburned site, often showed difficulty, results with PCA were good, thus PCA does seem to be a viable method for extracting soil moisture information while reducing effects from biomass and varying surface conditions at these unburned test sites. However, if it is the FWI code,

DC, that is needed for retrieval, then the C-band methodology only works in burned sites.

Using C-band data, methods may be developed at this point to predict surface soil moisture across a burned/unburned landscape. The surface soil moisture of the unburned sites will not always be representative of traditional fuel moisture codes as the SAR predicted surface soil moisture of a burned site is. Validation of the resulting product will be limited to *in situ* moisture measurements which will need to be scheduled, whereas for the burned areas, regularly collected weather data and FWI-codes may be used for validation. So limited validation of the results in unburned forests and a lack of relationship to fuel moisture FWI codes are really the only issues at this point for mapping surface soil moisture across the burned and unburned boreal landscape within a SAR scene using C-band. That does not mean that surface soil moisture information extracted using C-band in the unburned forests would not be useful for fuel moisture monitoring, it just does not consistently correspond to any one FWI code. The next step is development of the neural network or an alternative method to apply the PCA across the image. The first steps may be taken using existing datasets and existing *in situ*.

10. Initial Stages of Modeling for Time Series Analysis

Early in this project, we developed a diagram (Figure 49) depicting all possible remote sensors (current systems) and ancillary information useful for fuel moisture prediction. Having this overall view is helpful in development of the SAR fuel moisture monitoring methodology and in choosing ancillary data sources for integration into models, if necessary. This diagram also identifies all major parameters that may affect the relationship between remote sensing returns and soil moisture. Although our approach of time-series analysis virtually eliminates time-invariant parameters including surface roughness, biomass, and stand structure, leaving soil moisture variation as the main variable for extraction, we need to be mindful of the “big picture”.

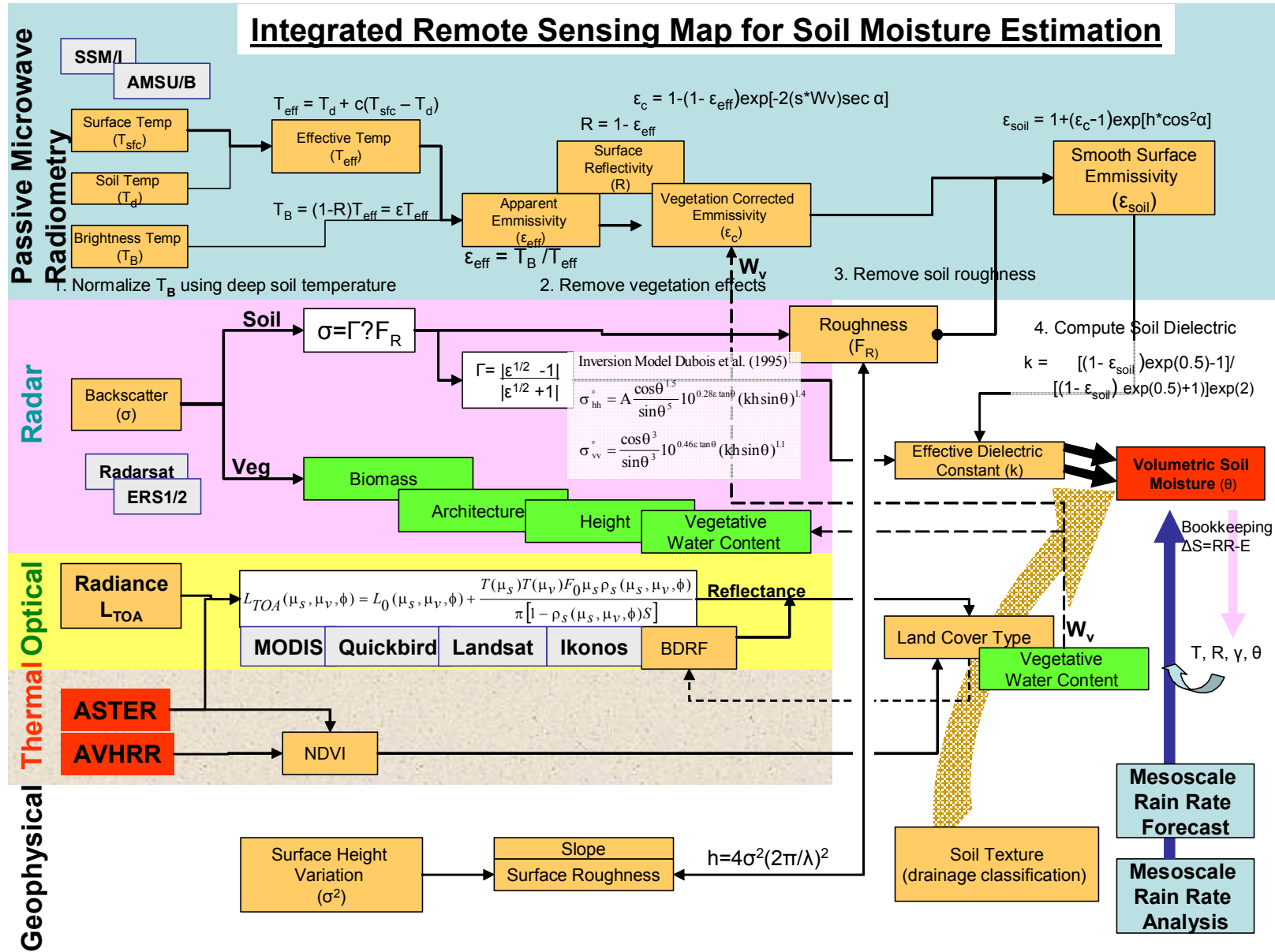


Figure 49. Diagram of all potentially useful remote sensors and ancillary information for fuel moisture prediction.

10.1 Image Segmentation

The issue of scale and how to segment our images was one of the first concerns and we decided that putting our imagery into regions would be the best way to approach the modeling. These regions should represent similar landscape features. We tried some internal software (called BLOB) which works great with Landsat, but the results were not as we had hoped with the radar. We then downloaded a trial version of e-Cognition and put a 1000x1000 sample of our data into that program to see how it worked (Figure 50). The results were much better than BLOB as this software segmented out the burn boundary and further segmented the burn scar into areas representing different levels of backscatter. An average backscatter value for that segment is calculated and given to the region. The unburned forest was separated from the burn and areas within the burn that are drier were separated from moister areas.

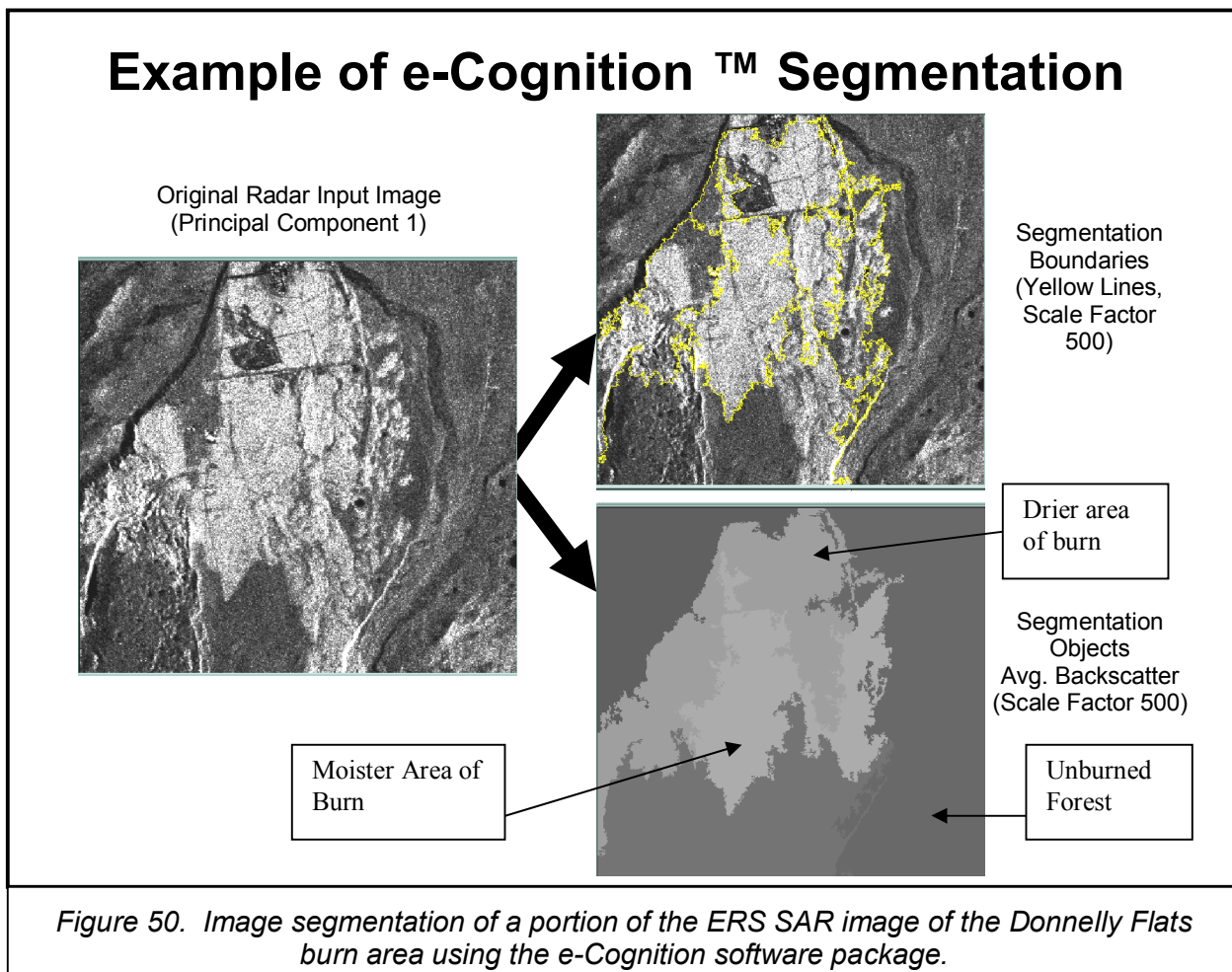


Figure 50. Image segmentation of a portion of the ERS SAR image of the Donnelly Flats burn area using the e-Cognition software package.

10.2 Summary of Initial Neural Network Analysis

An initial investigation into the use of neural networks as a fuel moisture prediction tool allowed us to experiment with the creation of neural networks and prove their potential as a prediction tool. It was thought that neural networks would be a benefit to this modeling due to the ability to incorporate many different data sets (including thematic and other non-numerical sets) and the possibility that the relationships can best be represented as non-linear. Although neural networks do not create an explicit mathematical relationship they have been proven through various past studies to improve a wide variety of complex prediction and classification problems.

A neural network software package (NeuroSolutions v.4 and NeuroSolutions for Excel) was downloaded as a demonstration version. This package allows for data to be formatted directly within Excel and then processed through the Neural Network. Through this demonstration version (60-day) a full set of results could be produced but the neural network weights could not be saved for future use.

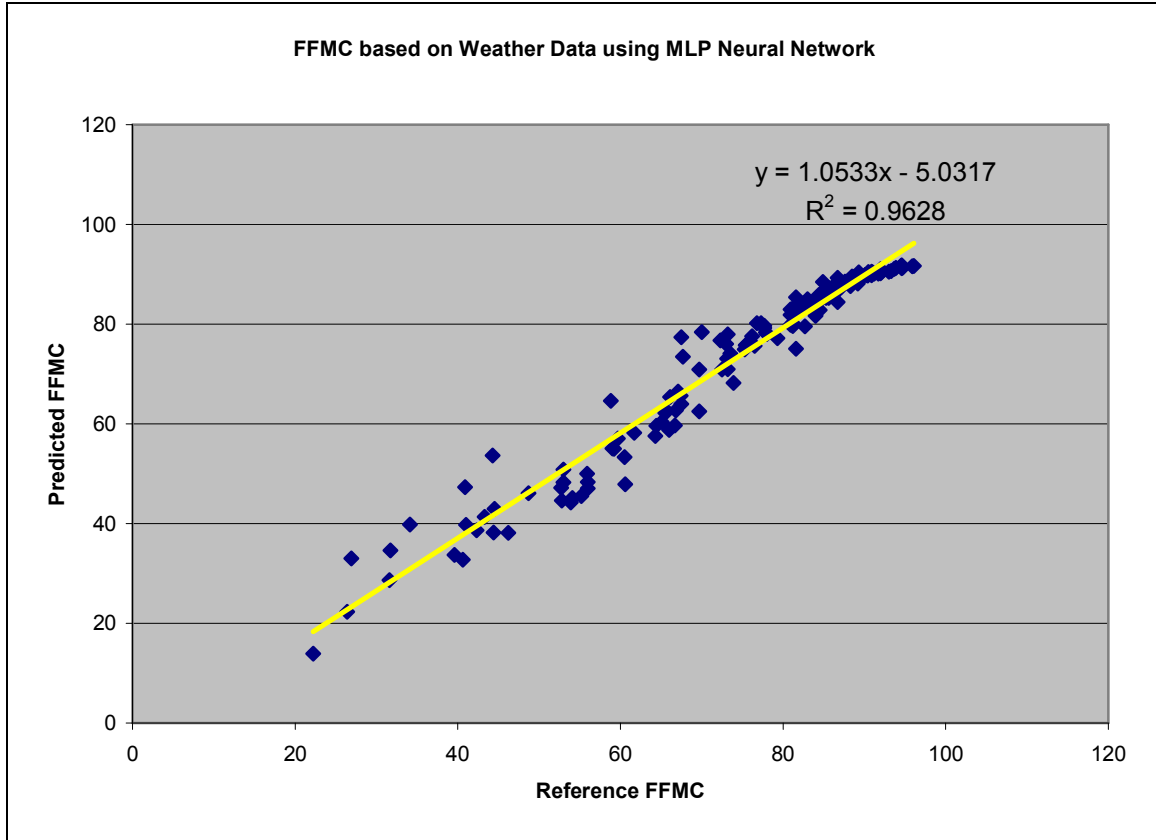


Figure 51. Plot of Reference vs. Predicted FFMC based on Weather Data Using MLP Neural Network.

One of the issues involving neural networks is the requirement for a large set of sample cases to be used to “train” the system. At the time of the analysis, soil moisture and backscatter measurements were relatively few, so a test was performed using weather data, fire danger codes, and principle component (PC) factor loadings for years 2000-2003 (30 bands). There is a known relationship between weather parameters and the fire danger codes. In testing the neural network, the input parameters of the previous day’s precipitation, wind speed, relative humidity, temperature, and the previous day’s Fine Fuels Moisture Code (FFMC) were used to predict the current day’s FFMC. The results

are shown in Figure 51 (*note: the resulting prediction was based on the same data used to train the system*).

The results show that the neural network does identify the relationship between the variables. The results show an agreement between the predicted FFMC value and the reference FFMC (R-squared) of 0.9628, with a regression line slope nearly perfect at 1 and just a slight offset (5.03).

There was a known relationship between the input parameters and the output for the example above. A second test was performed using the PC-2 and PC-3 factor loadings to predict FFMC for years 2000-2003. Passing this data through the neural network produced the results shown in Figure 52 (*note: again the same data used as input was used for the prediction*).

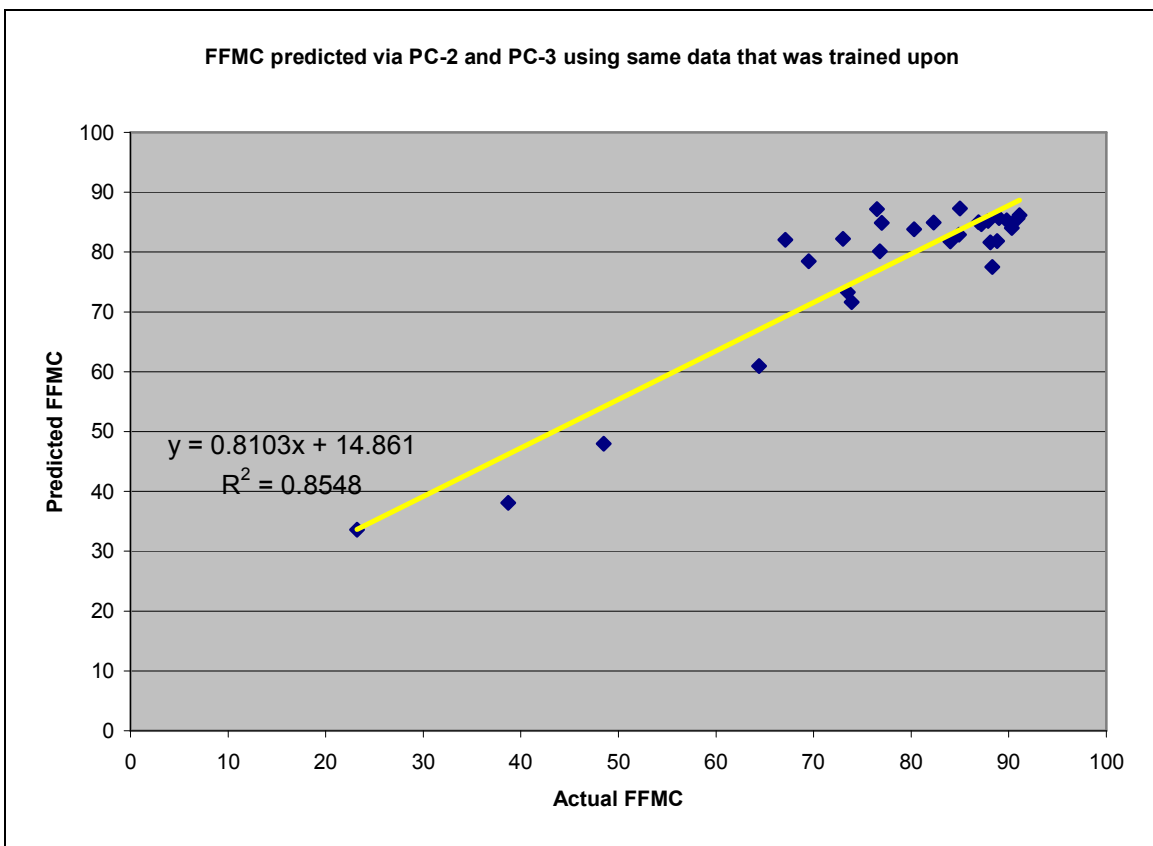


Figure 52. Plot of Actual versus Predicted FFMC using PC-2 and PC-3 to train a neural network.

The neural network results indicate that a strong relationship was found between the input variables (PC-2 and PC-3) and the FFMC. This relationship has an R-squared value of 0.85. These initial investigations demonstrated that there is a strong potential for neural networks to be used as a tool for the prediction of FFMC (and perhaps fuel moisture) from radar data.

The examples above show that the neural network can and does find patterns in the data, but the question is how well it works for predicting data which it has never been exposed. To test this, the PC-2 and PC-3 input parameters were used to predict FFMC (as above) by training on data from years 2000, 2001, and 2002. This trained network was then used to predict the FFMC values for data in years 2003. The results are shown in Figure 53 below.

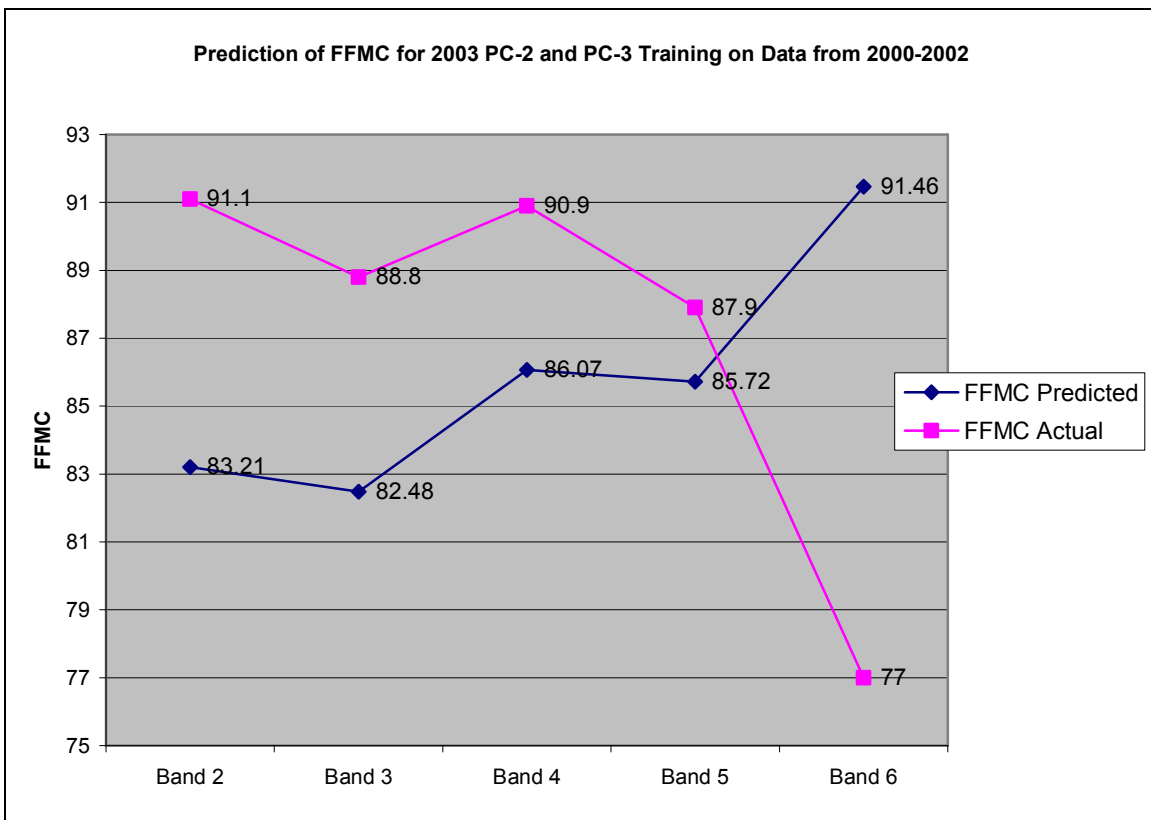


Figure 53. Predicted FFMC for 2003 based on training of PC-2 and PC-3 from 2000-2002.

The results from this prediction show that there is a clear relationship between the actual FFMC and predicted for the dates with the exception of Band 6 (July 30). It is not clear why this band is drastically different from the others, but may have to do with seasonal effects as described earlier. Images from dates starting around mid-summer and beyond have shown different trends than those from earlier in the season, likely at this DF site due to frozen ground thaw. Although there are too few data points to draw any absolute conclusion, this test further proves the potential for the use of neural networks to be used for fire danger predictions.

In addition to the demonstration software downloaded, neural networks are included in our in-house version of the GIS ENVI and in our version of the statistical software MatLab. Further investigation of these software packages revealed that the neural networks within ENVI may not be practical because of the inability to export the resulting model nor to integrate non-image based data. Neural networks within MatLab seems much more feasible, but has a larger learning curve.

Our initial investigation of neural networks presents an overview of the issues considered using neural networks. It also provides a firm footing for the continuation of the neural network investigation. However, there are concerns. One concern with neural networks is the lack of ability to predict situations for which they have not been trained. This may be an issue for us when applying an algorithm across a scene which has some conditions that are not captured in the training sets. Neural networks also require large training sets which we may not have in many cases. Despite these concerns neural networks provides a viable option.

11. Recommendations

The next steps are to test the methods demonstrated in sections 7 and 8 in an operational sense. The algorithms should be tested in other boreal forest types besides just black spruce to determine any limitations. The algorithms may need tweaking to meet the needs of the fire resource managers. Once this step has been taken, other sources of C-band data (Radarsat, Envisat) can be used to develop similar

algorithms. Existing SAR and *in situ* data can be used to develop these sensor specific algorithms.

For the time series analysis, L-band data should be evaluated for inclusion in the landscape scale mapping of fuel moisture in unburned forests. The ALOS PALSAR sensor will allow this analysis to be conducted. However, a limited analysis could also be conducted with JERS data from the mid- to late-1990s and FWI data. It may well be that a combination of L- and C-band data will provide enough information to map the FWI code DC across the landscape. For the C-band analysis, the mapping procedure for burned and unburned forests should proceed for direct mapping of surface soil moisture, with interaction from resource managers.

12. Presentations and Publications

This NASA SENH research was presented at three science conferences between 2004 and 2006, in addition to several small-group presentations to end-users in Alaska and Canada. These small group presentations were highly interactive and essential to the success of the project. Currently we remain in correspondence with the end-users including the more recent contact with a GIS expert (Parker Martyn) at the BLM's Alaska Fire Service (AFS) office near Fairbanks in Ft. Wainwright, concerning mapping fire scars in Alaska with SAR. This is a topic which we worked on under NASA grants in the late 1990s-2000 and published two journal articles (Bourgeau-Chavez et al. 1997, 2002). Martyn currently has a data grant from ASF to apply our developed SAR methods for mapping fire scars to their operations. They are testing it this fall "operationally". This is of great importance to this NASA SENH research because it breaks down the barrier of getting the end-user to integrate SAR into their operations, and because it provides multiple uses for the data, thus making the application more feasible.

Below are listed the main publications and presentations:

12.1.1 International Boreal Forest Research Association Conference

*May 2004
Fairbanks AK*

Riordan, K. L.L. Bourgeau-Chavez, J. Slawski, Orest Kwaka, M. Medvecz, S. Ames, and J. Allen. 2004. Improving Fire Danger Indices in Alaska through the Incorporation of Spatially Distributed Fuel Moisture Data from Satellite Radar Imagery. Proceedings of the International Boreal Forest Research Association Conference, May 2004, Fairbanks, AK.

12.1.2 Alaska Collaborator Meetings

We held meetings with our Alaska collaborators twice each year to get their input, help identify sites, provide updates on research conducted and obtain feedback. These meetings were critical to the success of this project. The dates and a list of Alaskan attendees are below.

Dates: June and August 2003, May & August 2004, March & August 2005

Alaskan Attendees (not every meeting was attended by each):

Brad Cella
National Park Service

Sharon Alden
National Park Service

Jennifer Allen
National Park Service

Mary Kwart
U.S. Fish and Wildlife Service

Karen Murphy
U.S. Fish and Wildlife Service

Jamie Hollingsworth, UAF

12.1.3 North American Boreal Forest Carbon Emissions Collaboration Meeting

May 2005

Altarum Ann Arbor MI

This meeting was designed to bring together researchers in the boreal forest, fire ecology, fire management, and post-fire remediation communities for collaboration and sharing of ideas and results. Attendees were from academic, private, and public institutions from both the US and Canada. A follow-up meeting was held in Spring 2006, in which we presented via teleconference in Edmonton, CA, see below.

Attendees

<u>Name</u>	<u>Affiliation</u>	<u>email</u>
Nancy French	Altarum Institute, Ann Arbor	nancy.french@altarum.org
Ron Hall	Canadian Forest Service, Edmonton	rhall@nrcan.gc.ca
Vern Peters	Canadian Forest Service, Edmonton	vpeters@nrcan.gc.ca
Bill DeGroot	Canadian Forest Service, Edmonton	
Janet Pritchard	Canadian Forest Service, Edmonton	jpritcha@nrcan.gc.ca
Tim Lynham	Canadian Forest Service, Sault Ste Marie	tlynham@nrcan.gc.ca
Eric Kasischke	University of Maryland	ekasisch@geog.umd.edu
Merritt Teretsky	Michigan State University	mrt@msu.edu

Teresa Hollingsworth University of Alaska, Fairbanks
Laura Bourgeau-Chavez General Dynamics, Ypsilanti

ftkn@uaf.edu
laura.chavez@gd-ais.com

12.1.4 Second North American Boreal Forest Carbon Emissions Collaboration Meeting

March 2006
Edmonton, Alberta, CA

Presentation of Initialization of Drought Code Results to the Boreal Carbon Consumption Working Group. This is the working group listed above. The meeting was held on 16 March and we presented via teleconference.

12.1.5 2005 Fall AGU Conference

December 2005
San Francisco, CA

An oral presentation was delivered at the American Geophysical Union in the Natural Hazards special session in early December in San Francisco.

Bourgeau-Chavez, L. L., K. Riordan, G. Garwood, J. Slawski, S. Alden, B. Cella, K. Murphy, and M. Kwart. 2005. Assessing Fuel Moisture With Satellite Imaging Radar for Improved Fire Danger Prediction in Boreal Alaska. Pages G13A-02 in: *Proc. AGU Fall Conference 2005*, San Francisco.

12.1.6 Alaska Satellite Facility (ASF) Newsletter Article

Bourgeau-Chavez, L.L., G. Garwood, K. Riordan, B. Cella, S. Alden, M. Kwart and K. Murphy. Assessing the Potential for Wildfire Using ERS SAR Imagery. Alaska Satellite Facility News & Notes, Spring 2006, Vol 3:1, pp. 2-4.

12.1.7 Circumpolar Remote Sensing Symposium

May 2006
Seward, Alaska

A poster was presented at the May 2006 meeting in Seward Alaska.

Bourgeau-Chavez, L.L., G. Garwood, K. Riordan, B. Cella, S. Alden, M. Kwart, K. Murphy and N. French. Improving the Prediction of Wildfire Potential in Boreal Alaska with Satellite Imaging Radar. Proceedings of the Ninth Circumpolar Remote Sensing Symposium, May 2006, Seward Alaska.

12.1.8 International Journal of Remote Sensing Manuscript

The revised manuscript submitted to International Journal of Remote Sensing was accepted for publication in August 2006. The manuscript is attached in Appendix E.

Bourgeau-Chavez, L.L., E.S. Kasischke, K. Riordan, S.M. Brunzell, M. Nolan, E. Hyer, J. Slawski, M. Medvecz, T. Walters and S. Ames. 2005. Remote monitoring of spatial and temporal surface soil moisture in fire disturbed boreal forest ecosystems with ERS SAR imagery. *International Journal of Remote Sensing*, (in press).

12.1.9 JGR Water Resources Research Manuscript

Critical to the success of this project was the calibration of the water content reflectometer probes used in the field for *in situ* measurements. These probes are designed and tested in mineral soils and needed calibration to the high organic content of the Alaska soils. This calibration was written in journal article format so that other researchers utilizing these probes in Alaska and other high organic soils can use our results and developed methods for calibration. See Appendix D.

Garwood, G., Riordan, K., Bourgeau-Chavez, L.L. and Slawski, J.. 2006. Calibration Algorithm Development for Selected Water Content Reflectometers to Organic Soils of Alaska JGR. Water Resources Research. *in submission*

12.1.10 Polar Record Manuscript

The presentation given in Seward Alaska in May 2006 was written in manuscript form and submitted to the Polar Record in August 2006 for publication (Appendix F).

Bourgeau-Chavez, L.L., G. Garwood, K. Riordan, B. Cella, S. Alden, M. Kwart, and K. Murphy. 2006. Improving the Prediction of Wildfire Potential in Boreal Alaska with Satellite Imaging Radar. Polar Record (in review).

13. Literature Cited

- Alexander, ME, Stocks BJ, and Lawson BD (1996) 'The Canadian Forest Fire Danger Rating System. Initial Attack.' Spring Issue.
- Alexander, M.E. 1983. Overwinter adjustment to spring starting values of the Drought Code. Can. Fore. Serv., North. For. Res. Cent, Edmonton, Alta, For. Rep. No. 28:5.
- Bourgeau-Chavez, L.L., G. Garwood, K.Riordan, B. Cella, S. Alden, M. Kwart, and K. Murphy. 2006a. Improving the Prediction of Wildfire Potential in Boreal Alaska with Satellite Imaging Radar. *Polar Record* (in review).
- Bourgeau-Chavez, L.L., E.S. Kasischke, K. Riordan, S.M. Brunzell, M. Nolan, E. Hyer, J. Slawski, M. Medvecz, T. Walters and S. Ames. 2006b. Remote monitoring of spatial and temporal surface soil moisture in fire disturbed boreal forest ecosystems with ERS SAR imagery. *International Journal of Remote Sensing* (accepted Aug. 2006).
- Bourgeau-Chavez, L.L., E.S. Kasischke, S.M. Brunzell, M. Tukman, and J.P. Mudd. 2002. Mapping fire scars in global boreal forests using imaging radar data. *Int. J. Rem. Sens.* Vol. 23(20):4211-4234.
- Bourgeau-Chavez, L.L., E. Hyer, M. Nolan, and S. Brunzell. 2000. Analysis of SAR Data for Fire Danger Prediction in Boreal Alaska, Final Report, ASF-IARC Grant NAS-98-129, 59 p. <http://www.gd-ais.com> (currently being transferred from <http://www.veridian.com/offering/subOffering.asp?offeringID=731&historyIDs=0,716,731,731,731>)
- Bourgeau-Chavez, L.L., E.S. Kasischke, and M.D. Rutherford. 1999. Evaluation of ERS SAR data for prediction of fire danger in a boreal region. *International Journal of Wildland Fire*.
- Bourgeau-Chavez LL, Harrell PA, Kasischke ES and French NHF (1997) The detection and mapping of Alaskan wildfires using a spaceborne imaging radar system. *International Journal of Remote Sensing* **18**(2),355-373.
- Dyrness, CT and Norum RA (1983) The effects of experimental fires on black spruce forest floors in interior Alaska. *Canadian Journal of Forest Research* **13**, 879-893.
- Garwood, G., Riordan, K., Bourgeau-Chavez, L.L. and Slawski, J.. 2006. Calibration Algorithm Development for Selected Water Content Reflectometers to Organic Soils of Alaska JGR. Water Resources Research. *in submission*
- French, NHF, Kasischke ES, Bourgeau-Chavez LL, and Harrell PH (1996) Sensitivity of ERS-1 SAR to variations in soil water in fire-disturbed boreal forest ecosystems. *International Journal of Remote Sensing* **17**(15),3037-3053.
- Lawson, B.D. and G.N. Dalrymple. 1996. Ground-truthing the Drought Code: field

verification of overwinter recharge of forest floor moisture. FRDA Report 268, Canada-British Columbia Partnership Agreement on Forest Resource Development: FRDA II. 21 pp.

Meadows, P.J., B. Rosich, and C. Santella. 2004. The ERS-2 SAR performance: the first 9 years. *Proceedings of the ENVISAT and ERS Symposium*, Salzburg, Austria, 6-10 September 2004.

Michalek, J.L., French, N.H.F., Kasischke, E.S., Johnson, R.D., and Colwell, J.E., 2000, Using Landsat TM data to estimate carbon release from burned biomass in an Alaskan spruce forest complex. *International Journal of Remote Sensing*, **21**, pp. 323-338.

Stocks, B.J. 1979. The 1976-1977 drought situation in Ontario. *For. Chron.* 55(3):91-94.

Stocks BJ, Lawson BD, Alexander ME, VanWagner CE, McAlpine RS, Lynham TJ, and Dube DE (1989) The Canadian forest fire danger rating system: an overview. *The Forestry Chronicle* **65**(6), 450-457.